



DOCTORAATSPROEFSCHRIFT
2017 Faculteit Geneeskunde

**Junctional Zone Thickness and Perfusion Characteristics
in Nulliparous, Primiparous and Infertile women
assessed by MRI,
as a Function of Menstrual Cycle and Hormonal
Contraception**

Proefschrift voorgelegd tot het behalen van de graad van Doctor in de Medische Wetenschappen aan de UHassel en de KUL

Te verdedigen door:

Liesbeth MEYLAERTS

Promotor: Vandersteen M, MD PhD (Hasselt University)
Copromotor: Ombelet W, MD PhD (Ziekenhuis Oost-Limburg)
Bazot M, MD PhD (Hôpital Tenon, Paris)

Met dank aan CENSTAT, Universiteit Hasselt en dienst Medische Beeldvorming van het Ziekenhuis Oost-Limburg

Chairman of the jury

Hendrix S, MD PhD
Hasselt University

Members of the Jury

Lambrichts I, MD PhD
Hasselt University

Oyen R, MD PhD
Leuven University Hospital

Palmers Y, MD PhD
Ziekenhuis Oost Limburg
Hasselt University

Peeters R, PhD
Leuven University Hospital

Vandekerckhove F, MD PhD
Gent University Hospital

Table of content

List of abbreviations

1. CHAPTER I: INTRODUCTION.....	13
1.1 In/Subfertility: Definitions - Diagnosis – Treatment	13
1.2 Definitions	14
1.2.1 Clinical definitions	14
1.2.2 Demographic definitions of infertility	14
1.2.3 Epidemiological definition of infertility	15
1.3 Diagnosis & Treatment	16
1.4 Anatomy of the uterus	17
1.4.1 The uterine wall	20
1.4.2 Vascularisation of the uterus.....	21
1.5 Pathophysiology Adenomyosis and Endometriosis	26
1.6 Aims of the study	29
1.7 Material and Methods.....	31
1.7.1 Study population	31
1.7.2 Blood laboratory tests	33
1.7.3 Magnetic Resonance Imaging.....	34
1.7.4 Image analysis.....	40
1.7.5 Statistical analysis	43
1.8 References	45
2. CHAPTER II: JUNCTIONAL ZONE THICKNESS IN NULLIPAROUS WOMEN BETWEEN 19 AND 35 YEARS OLD ASSESSED BY MRI, AS A FUNCTION OF MENSTRUAL CYCLE AND HORMONAL CONTRACEPTION. UTERINE JUNCTIONAL ZONE IN NULLIPAROUS WOMEN	55
2.1 Abstract	55
2.2 Introduction	56

2.3	Material and Methods.....	58
2.3.1	Study population	58
2.3.2	Blood laboratory tests	58
2.3.3	Magnetic Resonance Imaging.....	59
2.3.4	MR image analysis.....	60
2.3.5	Statistical analysis	63
2.3	Results	64
2.4	Discussion	69
2.4.1	Normal JZ thickness and ratio as a function of the menstrual cycle and uterine location	69
2.4.2	Normal JZ thickness and ratio as a function of the use hormonal contraception.....	70
2.4.3	The normal limits of JZ thickness in healthy women	71
2.5	Conclusion.....	73
2.6	References	74
3.	CHAPTER III: UTERINE JUNCTIONAL ZONE THICKNESS IN INFERTILE WOMEN EVALUATED BY MRI.....	81
3.1	Abstract	81
3.2	Introduction	82
3.3	Material and Methods.....	84
3.3.1	Study population	84
3.3.2	Blood laboratory tests	85
3.3.3	Magnetic Resonance Imaging.....	85
3.3.4	MR image analysis.....	87
3.3.5	Statistical analysis	89
3.4	Results	90
3.4.1	Junctional Zone Thickness.....	90
3.4.2	Outer Myometrial Thickness	92
3.4.3	Ratio Of Junctional Zone Versus Total Myometrial Thickness	95
3.5	Discussion	99

3.6	References	103
4.	CHAPTER IV: PERFUSION OF THE UTERINE JUNCTIONAL ZONE IN NULLIPAROUS AND PRIMIPAROUS WOMEN ASSESSED BY DCE-MRI, AS A FUNCTION OF MENSTRUAL CYCLE AND HORMONAL CONTRACEPTION	107
4.1	Abstract	107
4.2	Introduction	108
4.3	Material and Methods.....	110
4.3.1	Study population	110
4.3.2	Blood laboratory tests	111
4.3.3	Magnetic Resonance Imaging.....	111
4.3.4	MR image analysis.....	113
4.3.5	Statistical analysis	116
4.4	Results	116
4.4.1	Uterine volumes	117
4.4.2	Perfusion parameters throughout the menstrual cycle	118
4.4.3	Perfusion Parameters In Junctional Zone and Outer Myometrium.....	120
4.4.4	Perfusion Parameters in Nulliparous And Primiparous Non-users And Users Of Hormonal Contraception	126
4.5	Discussion	131
4.6	References	135
5.	CHAPTER V: PERFUSION OF THE UTERINE WALL IN INFERTILE WOMEN ASSESSED BY DCE-MRI: A PILOT STUDY	139
5.1	Abstract	139
5.2	Introduction	140
5.3	Material and Methods.....	141
5.3.1	Study population	141
5.3.2	Blood laboratory tests	142
5.3.3	Magnetic Resonance Imaging.....	142
5.3.4	MR image analysis.....	144
5.3.5	Statistical analysis	147

5.4	Results	148
5.4.1	Transfer Constant Of The Junctional Zone	148
5.4.2	Initial Blood Volume Of The Junctional Zone	150
5.4.3	Transfer Constant Of The Outer Myometrium	152
5.4.4	Initial Blood Volume Of The Outer Myometrium.....	154
5.4.5	Transfer constant and initial blood volume in the control group 156	
5.4.6	Discussion	156
5.5	References	159
6.	Discussion	163
6.1	JZ and Myometrial Thickness	164
6.2	Perfusion characteristics and fertility	165
7.	Conclusion	171
8.	References	173
9.	Samenvatting.....	179
10.	Summary	182
11.	Curriculum Vitae	186

List of abbreviations

AF	anterior wall at the fundus uteri
AI	anterior wall at the isthmus
Aka	also known as
AM	anterior wall at the midcorpus
AP	anteroposterior
AT	arrival time
BBB	blood brain barrier
BBT	basal body temperature
BW	bandwidth
Ca	arterial contrast agent concentration in function of time
Ce	cervix of the uterus
CENSTAT	Center for Statistics
CSF	central spinal fluid
Ct	tissue contrast agent concentration in function of time
2D	2-dimensional
3D	3-dimensional
4D	4-dimensional
DCE-MRI	dynamic contrast enhanced – magnetic resonance imaging
DHS	demographic and health surveys
EES	extravascular extracellular space
e.g.	exempli gratia – for example
EMA	European Medicines Agency
ESUR	European Society of Urogenital Radiology
EUROSTAT	European Statistics – Statistical Office of the European Communities
F	fundus of the uterus / follicular phase
F	blood flow
FDA	US (United States) Food and Drug Administration
FLASH	fast low angle shot
FSH	follicle-stimulating hormone
GBCA	Gadolinium-based contrast agents
Gd	Gadolinium
GDD	Gadolinium deposition disease
Gd DOTA	Gadolinium-tetra-azacyclo-dodecaetra-acetic acid
GIFT	gamete intra fallopian transfer
GnRH	Gonadotropin releasing hormone

hCG	human chorionic Gonadotrophin
HEPA	hamster egg penetration assay
hMG	human menopausal Gonadotropin
HSG	hysterosalpingogram
Hz/Px	Herz per pixel
I	isthmus of the uterus
iAUC	initial area under the curve
IBM	International Business Machines
ICMART	International Committee for Monitoring Assisted Reproductive Technology
ISMRM	International Society for Magnetic Resonance in Medicine
IUI	intra-uterinary insemination
IVF	in vitro fertilisation
J Magn Reson Imaging	Journal of Magnetic Resonance Imaging
JZ	junctional zone
JZ/TM ratio	junctional zone / total myometrium ratio
K trans	transfer constant
K ep	reflux constant
L	luteal phase
LH	luteinizing hormone
LL	laterolateral
M	midcorpus of the uterus
Magn Reson Imaging	Magnetic Resonance Imaging
MEDRAD	Inc - technology for contrast media delivery
min.sec	minute second
mm	millimeter
MMWP	multi-modality workplace
MRI	Magnetic Resonance Imaging
msec	millisecond
MT	myometrial thickness
n	number
NS	non specified
NSF	nephrogenic systemic fibrosis
O	ovulatory phase
OM	outer myometrium
P	probability
PCT	post coital test
PF	posterior wall at the fundus
PI	posterior wall at the isthmus

PLos Med	Public Library of Science in Medicine
PM	posterior wall at the midcorpus
PS	permeability-surface area product
RE	reproductive endocrinologist
Reprod Biomed Online	reproductive biomedicine online
ROI	region of interest
SAS	statistical analysis system
SD	standard deviation
SPSS	statistical package for the social science
1.5T	1.5 Tesla
T1 WI	T1 weighted image
T2 WI	T2 weighted image
TESA	testicular sperm aspiration
TIAR	tissue injury and repair
TIM 4G-Dot	total imaging matrix fourth generation day optimizing throughput
TSE	turbo spin echo
TTP	time to peak
V b	whole blood volume per unit of tissue/blood volume fraction
V e	total EES volume / interstitial volume fraction
WHO	World Health Organization

1. CHAPTER I: INTRODUCTION

1.1 In/Subfertility: Definitions - Diagnosis – Treatment

Pre-pregnancy counselling, recommendation and guidance documents often neglect to recognize that many women, men and couples who want to have a child have difficulties becoming pregnant. Infertility/subfertility or the inability to have a healthy born child can be defined as either a disease of the reproductive tract (no reproductive success after 1 year of actively attempting for a pregnancy) or a disability that results in an impairment of the normal function. Infertility can be attributed to any abnormality in the female or male reproductive system. Female infertility can have different causes, among others ovulation disorders, tubal factors and uterine problems (Jose-Miller et al., 2007). It has become a growing problem during the last decade with a prevalence of 14% in Europe (EUROSTAT 2008a).

According to the World Health Organisation, there is a high global health burden of childlessness. Based on the Demographic Health Survey (1994-2000), 186 million women in developing countries have been estimated by the WHO to experience childlessness, despite 5 years of attempting for pregnancy or live birth. This equals one in every four couples of reproductive age in developing countries presenting with an unfulfilled desire for a wanted pregnancy (WHO meeting to Develop a Global Consensus on Preconception Care to Reduce Maternal and Childhood Mortality and Morbidity, Demographic health survey. Geneva, World Health Organisation). Estimates generated for the First WHO/World Bank Report on Disability (2011) depict 35 million women with primary or secondary infertility (maternal morbidity) as a result of either maternal sepsis or infection due to unsafe abortions. It represents the fifth largest global burden of all disabilities evaluated within women of reproductive age (15-49 years) predominantly in developing and transitional countries.

In a large systematic analysis of 277 health surveys, Mascarenhas et al (PLoS Med, 2012) suggested that among women 20-44y of age who were exposed to the risk of pregnancy, 1,9% were unable to attain a live birth (primary infertility). In addition, 10,5% were unable to have another child (secondary

infertility) out of women who had had at least one live birth and were exposed to the risk of pregnancy (Mascarenhas, PLoS Med, 2012).

The unrecognized status ad hoc and highly stigmatized disease or disability as infertility is today, needs more care and recognition in our 21th century society. The fear of diagnosis inhibits individuals from seeking care. Infertile women and men are highly isolated; for example, in developing countries, women diagnosed with infertility have been abandoned by their husbands, have been victims of intimate partner and family violence, may not be buried on fertile agricultural ground, and risk complete alienation from their community and social functions due to fear of these women conferring infertility to other family or community members.

Another important evolution worldwide, in both developing and developed countries, occurs, namely the level of women's education is increasing and women are having children later in life.

Counselling and fertility awareness are key components of pre-pregnancy planning globally.

1.2 Definitions

1.2.1 Clinical definitions

- Infertility is "a disease of the reproductive system defined by the failure to achieve a clinical pregnancy after 12 months or more of regular unprotected sexual intercourse."... (WHO-ICMART glossary).
- "Infertility is the inability of a sexually active, non-contracepting couple to achieve pregnancy in one year. The male partner can be evaluated for infertility or subfertility using a variety of clinical interventions, and also from a laboratory evaluation of semen." (Semen manual, 5th Edition).

1.2.2 Demographic definitions of infertility

- An inability of those of reproductive age (15-49 years) to become or remain pregnant within five years of exposure to pregnancy. (DHS)

- An inability to become pregnant with a live birth, within five years of exposure based upon a consistent union status, lack of contraceptive use, non-lactating and maintaining a desire for a child. (Trends in prevalence).

1.2.3 Epidemiological definition of infertility

(for monitoring and surveillance) Women of reproductive age (15–49 years) at risk of becoming pregnant (not pregnant, sexually active, not using contraception and not lactating) who report trying unsuccessfully for a pregnancy for two years or more. (Reproductive Health Indicators).

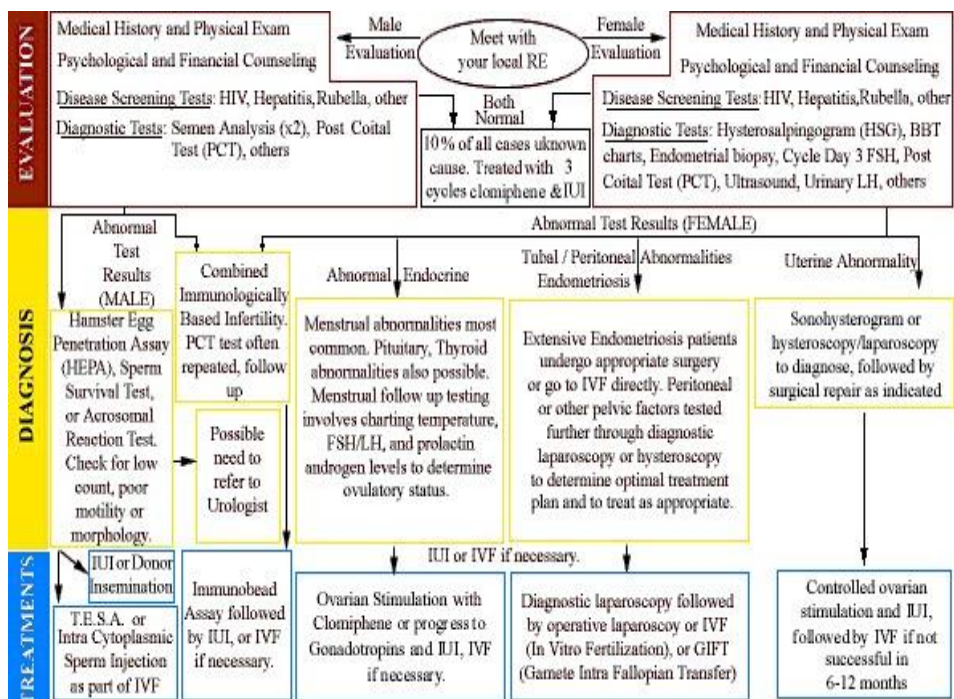
Primary infertility

When a woman is unable to ever bear a child, either due to the inability to become pregnant or the inability to carry a pregnancy to a live birth she would be classified as having primary infertility. Thus women whose pregnancy spontaneously miscarries, or whose pregnancy results in a stillborn child, without ever having had a live birth would present with primary infertility. (Trends in prevalence).

Sub-/Secondary infertility

When a woman is unable to bear a child, either due to the inability to become pregnant or the inability to carry a pregnancy to a live birth following either a previous pregnancy or a previous ability to carry a pregnancy to a live birth, she would be classified as having secondary infertility. Thus those who repeatedly spontaneously miscarry or whose pregnancy results in a stillbirth, or following a previous pregnancy or a previous ability to do so, are then not able to carry a pregnancy to a live birth would present with secondary infertility. (Trends in prevalence).

1.3 Diagnosis & Treatment



www.arcfertility.com

This algorithm gives an overview on the evaluation, diagnosis and treatment in both male and female in-/subfertility. Notice the absence of MRI examination in most algorithms used in daily practice in the diagnosis of the female infertility/subfertility work-up anno 2017.

1.4 Anatomy of the uterus

The uterus, located in the female pelvis in between the urinary bladder and rectum, is subdivided in two main segments: corpus uteri, which consists of a fundus and middle body, and the cervix uteri. The isthmus is located between the middle body and the cervix (Fig. 1).

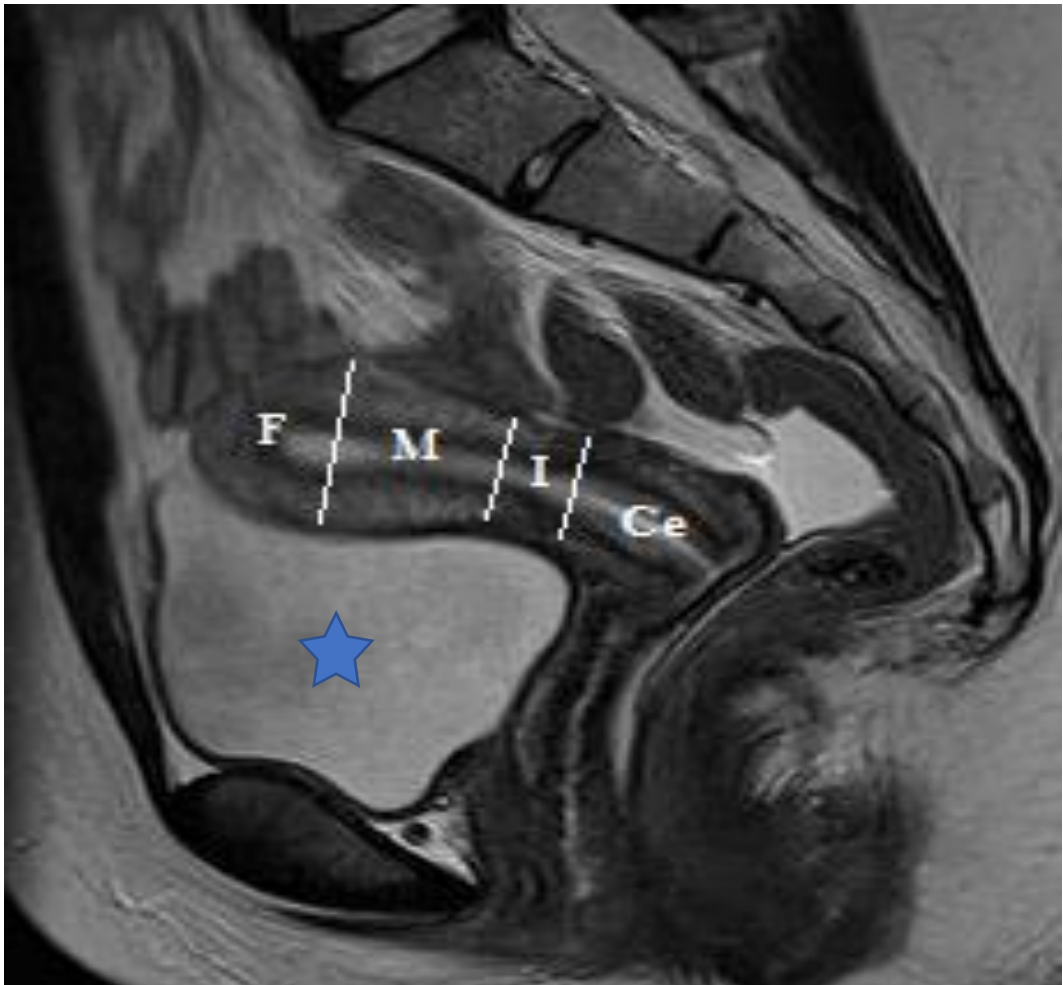


Fig. 1
Pelvic MRI image of a women in the midsagittal plane through the uterus, a T2 weighted image. F = Fundus, M= middle corpus, I= Isthmus, Ce= cervix uteri. The blue asterix is located in the urinary bladder (content is bright on T2 weighted image (a.k.a water weighted image)).

During reproductive age (15-46 years), three distinct layers can be recognized in the uterine wall. The inner layer known as the endometrium, the middle layer or the junctional zone (JZ), and the outer layer or the outer myometrium. This uterine zonal anatomy was first demonstrated in 1983 by means of Magnetic Resonance Imaging or MRI (Hricak et al., 1983).

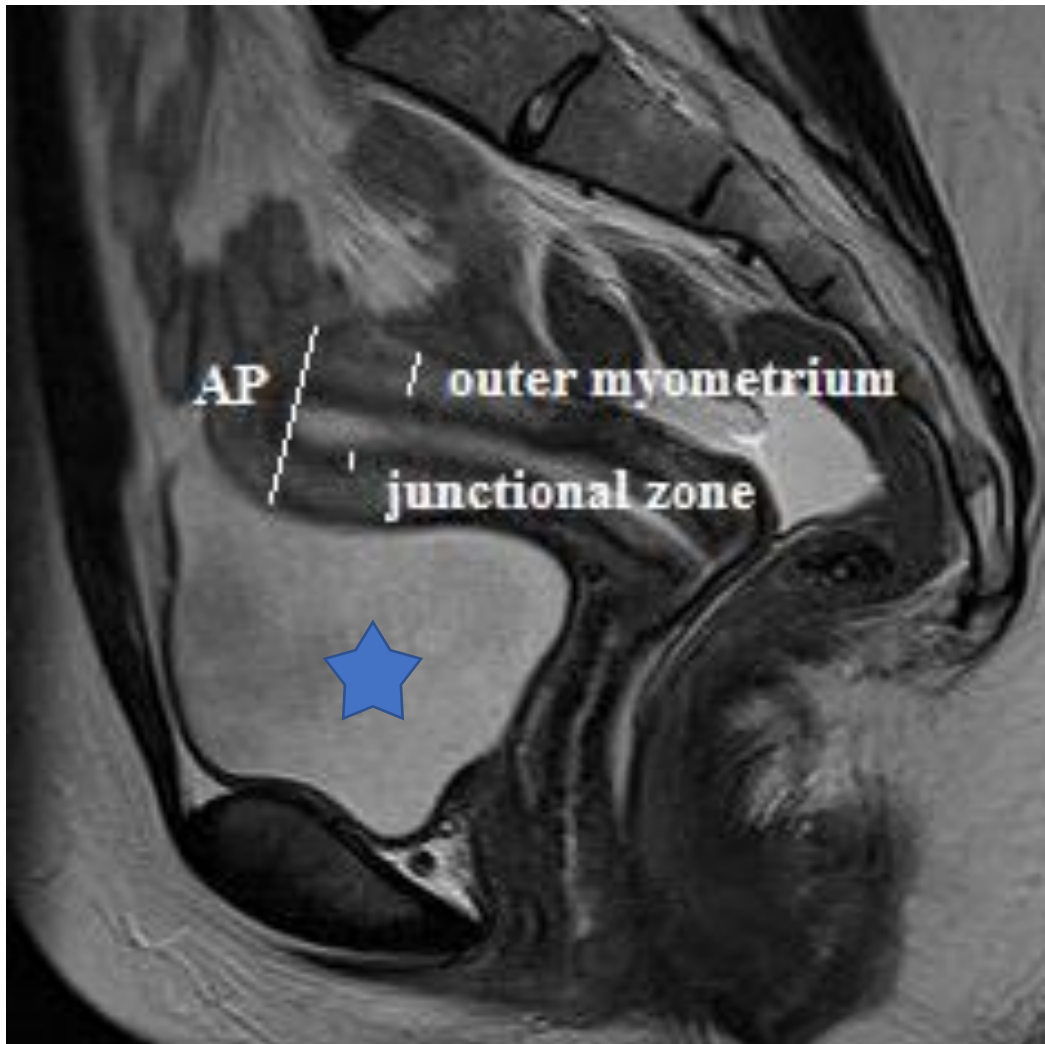


Fig.2

A pelvic MRI image, in the midsagittal plane through the uterus showing the inner or junctional zone (inner dark layer of the uterine wall) and the outer myometrium (brighter thicker layer of the uterine wall), on a T2 weighted image. AP = anteroposterior. The blue asterisk is located in the urinary bladder (content is bright on T2 weighted image (a.k.a water-weighted image)).

On T₂-weighted MRI images, the endometrium is presented as a high signal-intensity zone (bright), the JZ as a low signal-intensity zone (dark) and the outer myometrium as a medium signal-intensity zone (Fig. 2). These differences in signal intensity are mainly related to cell density in which the junctional zone has the highest cell density compared to the outer myometrium and endometrium. This means less intra- intercellular fluid and thus lower signal intensity (darker) on T2 and T1 weighted images (Hricak et al, 1983).

The uterine JZ plays a role in (in)fertility. First, the zone is a hormone-dependent structure that governs uterine peristalsis, which are involved in reproductive processes such as sperm transport and embryo implantation (Kunz et al., 1996; Ijland et al., 1996). Secondly, studies have shown that disorders of the JZ, such as uterine leiomyomas and adenomyosis, are linked with infertility (Woodward et al., 1993; Fusi et al., 2006). Third, it is assumed that the characteristics of the blood vessels and the JZ thickness affect the success rate of implantation of the embryo in the uterus (Fusi et al., 2006; Brosens et al., 2002; Lesny et al., 1999).

In literature, there is no consensus about normal values of junctional zone (JZ) and important variations are proposed. Initially, Brosens et al suggested that a normal JZ is equal or less than 5 mm in thickness (Brosens et al., 1998). Using MRI, Hauth et al. (2007) defines the JZ thickness as a function of age in 100 healthy women, between 21 and 73 years old. The thickness shows a significant increase until the age between 41-50 years and decrease thereafter. MRI findings in 21 women in different phases of the menstrual cycle, nine women using oral contraceptives and twelve not, demonstrates that the zone is significantly thinner in the pill using group compared to the non -pill group (McCarthy et al., 1986). Both studies show that there are no significant differences between the follicular and secretory phase of the menstrual cycle. Mitchell et al. (1990) also finds no differences in JZ thickness between these two menstrual phases when examining 12 female volunteers (20-33 years). This is in contrast with the results of Haynor et al. (1986), who evaluates the changes in appearance of the uterus on MR images obtained during the menstrual cycle in 6 healthy women. The thickness of the myometrium is shown to increase rapidly during the follicular phase and to increase at a slower rate during the

luteal phase. Wiczuk et al. (1988) reveals equal findings when evaluating 5 women between 22-40 years of age with normal ovulatory cycles.

It is clear that there is no consensus so far about the influence of the menstrual cycle on the JZ thickness.

1.4.1 The uterine wall

The uterine functions of protection, nidation and evacuation are located in the myometrium and endometrium (Fig. 3). The protective and expulsive function of the myometrium is accomplished by the large amount and pattern of arrangement of the smooth muscles. The muscle concentration is the highest in the fundus, with smaller amounts in the lateral walls than in the anterior and posterior areas. The concentration at the myometrial-endometrial surface, known as the junctional zone or inner myometrium, is higher than at the junction of myometrium and serosa.

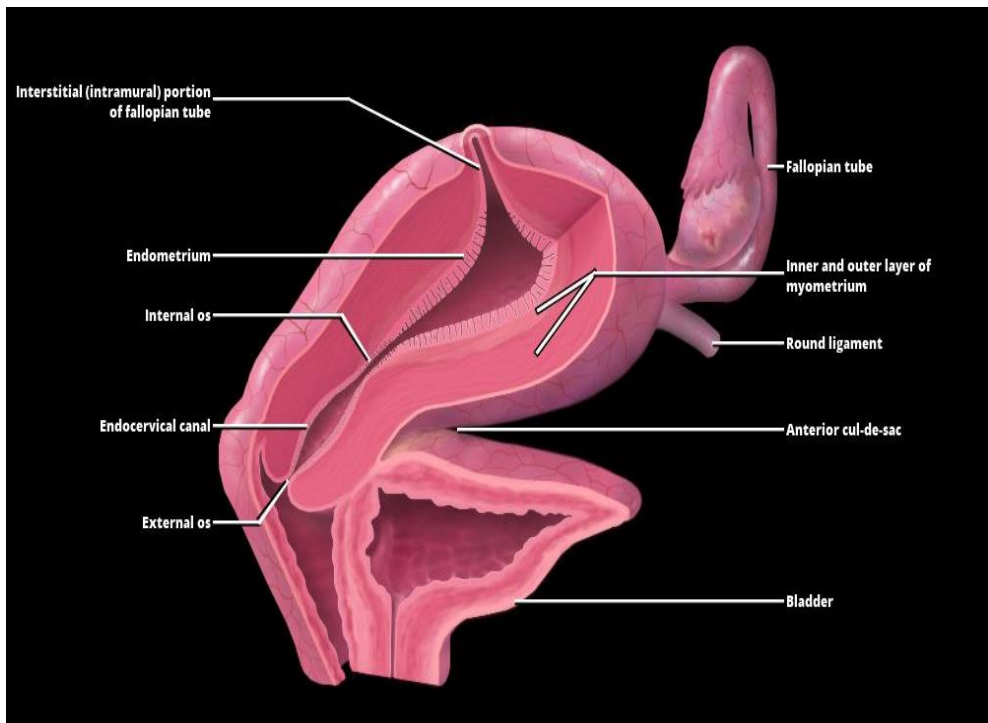


Fig. 3

The amount of uterine wall muscles decreases towards the cervix, with only 10 % of muscle present in the cervix, the remainder being fibrous connective tissue (Goerttler 1930, Haines and Taylor 1987). The muscular arrangement throughout the uterus is highly effective, especially for evacuation of contents. In the fundus, there is an outer covering of muscle, which is extended into the ligaments plus an internal muscular layer from which fibres enclose the orifices of the tubes and the internal cervical os, acting as sphincters in those regions. In both layers, there is an elaborate network of muscle cells. The individual muscle bundles are surrounded by connective tissue sheaths containing a small amount of elastic tissue. Blood vessels, lymphatics and nerves course in the sheaths. Between these layers, both of which are relatively narrow, lies the main portion of the musculature. This, again, is a dense network of interlacing fibres penetrated by blood vessels. The constituents are arranged in order to promote evacuation, constrict adjacent blood vessels and assist haemostasis at delivery. During pregnancy, an enlarged uterus consists mainly of myometrium. During the first trimester, myometrial growth is accomplished by an increase in number of muscle cells (hyperplasia) accompanied to a lesser degree by increase in the size of the cells (hypertrophy). The latter process takes over in the remainder of the first half of pregnancy. A mid-gestation uterine enlargement is accomplished by stretching alone by the increase in fetal size and volume of the amniotic fluid.

1.4.2 Vascularisation of the uterus

The uterine blood supply is largely derived from the aorta abdominalis, via the uterine and iliac arteries (Brosens I. et al, 1967; Robertson W.B. et al, 1975). Minor or variable contributions are made by the inferior mesenteric, middle sacral, inferior epigastric, internal pudendal and ovarian arteries. The collateral circulation is often through the ovarian arteries (White A et al 2007, Abbara S et al 2007, Smoger D et al 2010, Nikolic B et al 1999, Barth M et al 2003). Rarer but increasingly reported is extra-uterine, extra-gonadal arterial collateral circulation (McLucas B et al 2009, Pelage JP et al 2005, Dixon S et al 2013, Chang S et al 2013).

Razavi et al (2002) categorized ovarian artery-to-uterine artery anastomoses in three types (Fig. 4): (A) Type I ovarian artery-to-uterine artery anastomosis. The ovarian artery (OA) connects to the intramural uterine artery (UA) before the fibroid supply through the tubo-ovarian segment (arrow). (B) Type II ovarian artery-to-uterine artery anastomosis. The ovarian artery supplies the fibroid directly, without prior connection to the uterine artery. (C) Type III ovarian artery-to-uterine artery anastomosis. The ovarian supply is at least in part from the uterine artery, with flow in the tubo-ovarian segment toward the ovary. Arrow indicates the direction of flow.

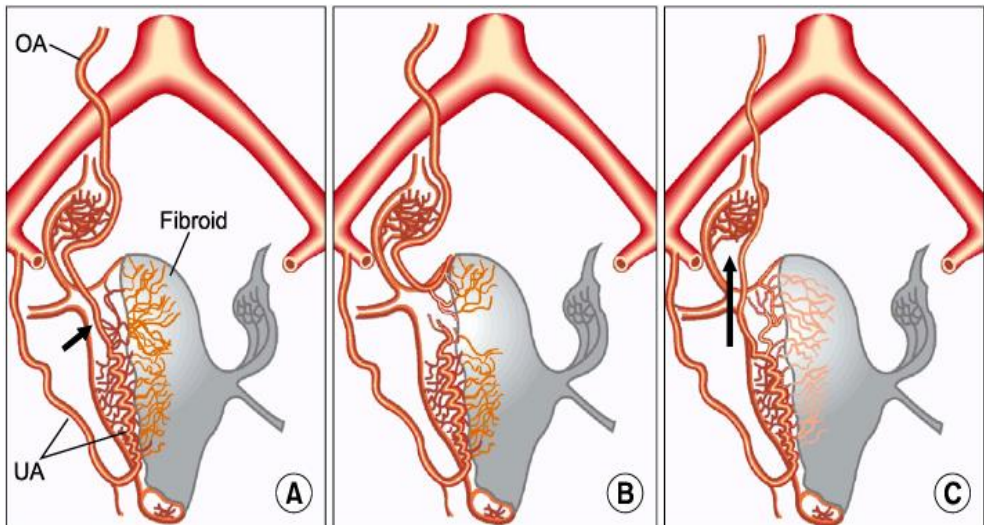


Fig. 4

Branches of the uterine artery enter the wall at a sharp angle and proceed through the myometrium to the middle third without significant branching. In the middle third, they form an arcuate garland to which branches of both right and left halves contribute. From the garland small branches are distributed throughout the myometrium.

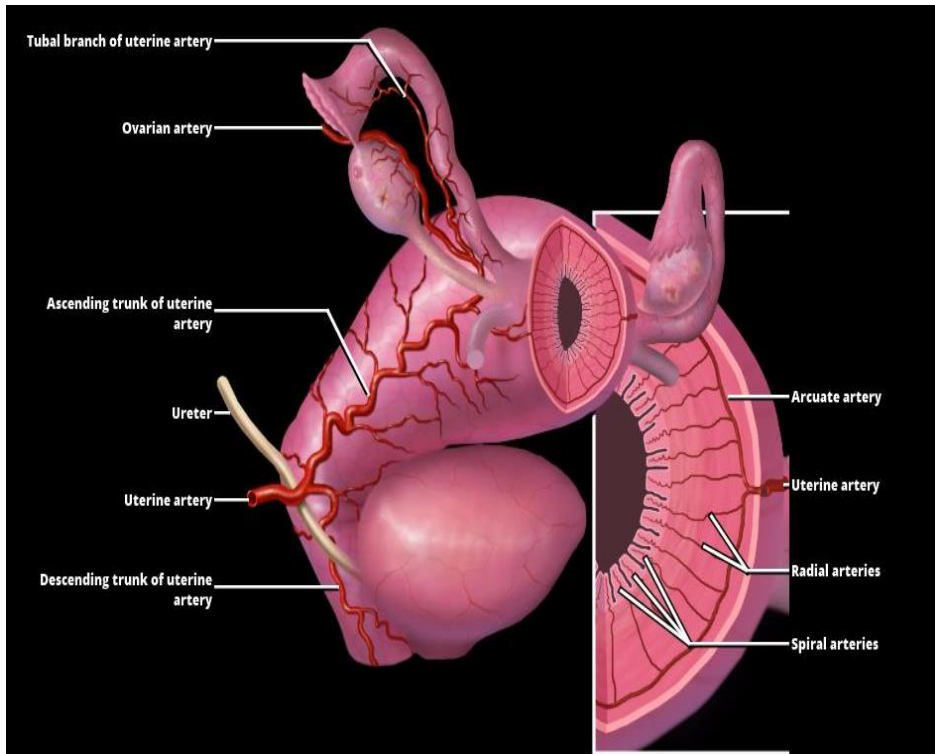


Fig. 5

The radial arteries are large stems, which come off the arcuate at right angles and travel toward the uterine lumen. As they pass the junctional zone they are known as the endometrial spiral arteries. The term is descriptive of both the course and the configuration of the endometrial segments of the vessels. Just after entering the endometrium, the spiral arteries split in off small branches, the basal arteries, which ramify in the deepest layer of the endometrium (Fig. 5). The composition of the walls of these two types of vessel is strikingly different. The spiral arteries, carrying forward the basic structure of the parent radial and arcuate arteries, contain extensive elastic and fibrous tissues and some muscle. They are surrounded by a sheath of dense connective tissue constituting the so-called Columns of Streeter. The basal arteries, on the other hand, are essentially muscular with little elastic and fibrous tissue and they have no fibrous sheath.

The venous drainage of the uterus is particularly noteworthy in the endometrium, where an extensive network of vessels of all sizes is distributed throughout. Many of the smaller veins coalesce to form prominent, dilated sinuses. These vessels of increasing size converge upon major stems, which enter the uterine vein bilaterally. These, in turn, lead to the hypogastric and common iliac veins (Fig. 6).

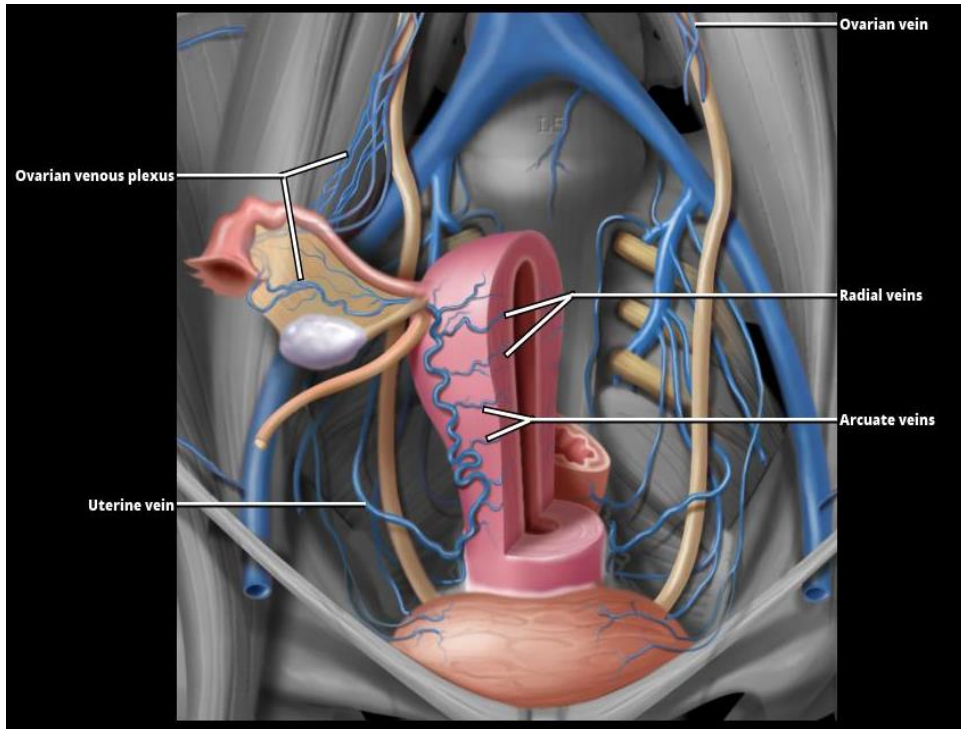


Fig. 6

This graphic shows the venous drainage from of the uterus, which follows the arterial system. There is venous drainage via both the uterine and ovarian veins (STATDX).

Following the menstrual cycle there is a period of repair in all parts of the uterine wall. Regeneration of the torn blood vessels is accomplished while the ovarian follicle is growing and elaborating oestrogen (More I.A.R. 1987, Bartelmez G.W. 1957a). As the thickness of the endometrial layer slowly increases, the spiral arteries grow towards the uterine lumen. The arterial stumps give rise to capillary sprouts, which proliferate towards the surface of the endometrium. Muscle and elastic tissues are gradually formed around them, converting them into arterioles and arteries, though a capillary bed persists in

the immediately subepithelial layer of the endometrium. As they grow, the arteries become increasingly convoluted. This is related to a greater arterial growth than thickening of the endometrial and thus these arteries become compressed (bedspring).

The deepest portions of the spiral arteries, together with the adjacent segments of radial arteries, reveal an activity, which has an important influence upon the course of menstrual and reproductive cycles. Localized ischemia resulting from temporary shutdown of blood supply is now regarded as the basis of the necrosis, bleeding and menstruation.

The peristalsis continues to occur throughout pregnancy, and are an important factor in regulating volume and pressure of maternal blood supply to the placenta.

The basal arteries are unresponsive to hormonal stimuli and take no part in the changes noted in the spiral arteries. They are not damaged in the menstrual cycle and remain unchanged throughout the whole cycle, maintaining their sole function of nourishing the basal (outermost) layer of the endometrium and preserving it as a seed bed for reconstruction of the destroyed superficial layers after menstruation or pregnancy.

Ultrasonographic studies have demonstrated that inner myometrium or junctional zone perfusion is impaired in women with unexplained infertility (Raine-Fenning et al, 2004). Other conditions of the reproductive system such as tumoral lesions, endometriosis, adenomyosis, abnormal severe menstrual bleeding and breakthrough bleeding are also associated with disturbances of the uterine angiogenic process and the vascular network (Raine-Fenning et al , 2004; Girling et al, 2005; Benagiano et al, 2009; Schreinemacher et al, 2012; Sala et al, 2010; Steer et al , 1994; Reynolds et al 2002). Microvascular parameter assessment could potentially be used to detect pathogenic conditions or in assisted reproductive therapy. This requires profound knowledge of the normal myometrial vasculature.

1.5 Pathophysiology Adenomyosis and Endometriosis

Investigating the junctional zone without mentioning anything on adenomyosis or endometriosis would be incomplete (cfr. algorithm 2.1.2). Both entities occur frequently and have serious impact on symptomatology and fertility. Adenomyosis is defined as the presence of endometrial glands and stroma within the myometrium, whereas endometriosis is the presence of endometrial tissue outside the uterus. Both are steroid hormone dependent conditions and, as the normal endometrium, their development is regulated by the levels of estrogen and progesterone. Bleeding is one of the responses of endometrial tissue to hormonal stimulation. This can lead to inflammation and scarring, and consequently to complications such as infertility, chronic pelvic pain,... Around the age of 50, the level of estrogen rapidly decreases. Therefore, adenomyosis and endometriosis are considered to be a problem mainly before the menopause. However, new cases are found beyond reproductive age (up to 83 year of age) since, if iatrogenic or endogenous hormones are present the disease can still be active (Acien P et Al 2013).

Incidence of endometriosis and adenomyosis in women aged 15-50 years is 0.14% (Morassuto et al, 2016). Adenomyosis representing 28% of all diagnoses, becomes increasingly prevalent after the age of 50 years, especially in the fourth and fifth decades (Morassutto et al, 2016). Sensibilisation of women and health professionals can identify possible undiagnosed cases.

Leyendecker et al (2009) integrated endometriosis and adenomyosis into the physiological mechanism of 'Tissue Injury And Repair (TIAR)'. It represents the extreme of a basically physiological, estrogen-related mechanism that is pathologically exaggerated in an extremely estrogen-sensitive, reproductive organ. They are caused by trauma as circumstantial evidence suggests. In the spontaneously developing disease, chronic uterine peristaltic activity or phases of hyperperistalsis induce, at the junctional zone of endometrial-myometrial interface near the fundo corneal raphe, microtraumatizations with the activation of the TIAR mechanism. This results in local production of estrogen. The etiology of this increased estrogen-producing "glandular" potential of these tissues is still unclear. The production of estrogen results in hyperperistalsis. This results in an increased desquamation of fragments of the basal endometrium and in

combination with an increased retrograde uterine transport capacity, in enhanced transtubal dissemination of these fragments. Hyperperistalsis and increased intra-uterine pressure would gradually result in myometrial disruptions that are infiltrated by basal endometrium with the secondary development of peristomal muscular tissue. Adenomyotic foci are usually localized in the anterior and/or posterior wall with preference of the posterior. Rarely they present in lateral walls. Early lesions usually present close to the 'fundo-cornual raphe' of the archimyometrium or junctional zone. The fundo-cornual raphe is a site of predilection of mechanical strain. In more advanced cases of adenomyosis the expansion of the junctional zone in MRI often shows predominance at the sagittal midline of the mid-corporal and fundal uterine part (Fig. 7).

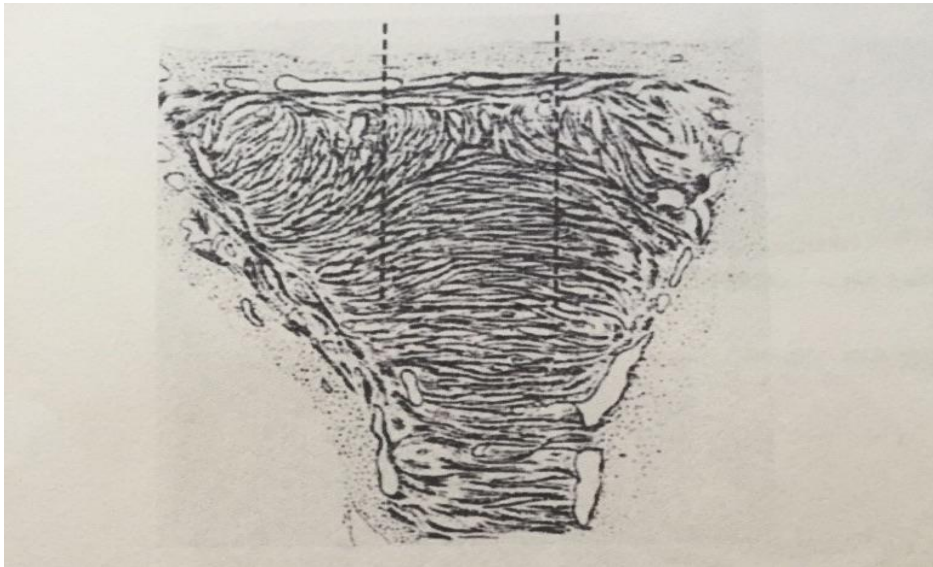


Fig. 7

Modified original drawing from Werth and Grusdew(1898). It presents the architecture of the subendometrial myometrium namely junctional zone or archimyometrium in the human fetal uterus. The specific circular orientation of the fibers of the junctional zone results from the fusion of the two paramesonephric ducts forming a fundo-cornual raphe in the midline (dashed rectangle). The peristaltic pump of the uterus, which is continuously active during the menstrual cycle, is driven by coordinated contractions of these fibers. Directed sperm transport into the dominant tube is made possible by differential activation of these fibers. The fundo-cornual raphe constitutes a region of increased mechanical strain and tissue injury followed by local estrogen production. By the time muscular distensions at the fundo-cornual raphe result in the formation of gaps that result in endometrial proliferation into these dehiscences.

With ongoing peristaltic activity, such sites of microtraumatization might increase and increasingly produce estrogens, which would interfere with the ovarian control over uterine peristaltic activity. This results in a permanent hyperperistalsis and a self-perpetuation of the disease process. In most cases of endometriosis/adenomyosis, a causal event early in the reproductive period of life must be postulated leading rapidly to uterine hyperperistalsis. In late premenopausal adenomyosis, such an event might not have occurred. However, chronic normoperistalsis throughout the reproductive period of life may lead to the same kind of microtraumatization. Activation of the TIAR mechanism, followed by chronic inflammation and infiltrative growth, endometriosis/adenomyosis of the younger woman and premenopausal adenomyosis seems to share the same pathophysiology.

On Transvaginal Ultrasound and MRI examination, thickening of uterine JZ is the criterion for the diagnosis of adenomyosis, with equivocal data about the value of abnormal JZ thickness. According to Mark et al. (1987), a JZ of more than 5 mm in thickness is abnormal and allows a confident diagnosis of adenomyosis. Kang et al. (1995), however, suggest that a uterus with a maximum JZ thickness of 8 mm or less can easily be normal, while Reinhold et al. (1996) propose an optimal JZ value of 12 mm or more for the diagnosis of adenomyosis. Several studies suggest that adenomyosis is strongly suspected when the JZ measures at least 12 mm in thickness on MR images (Novellas et al, 2011; Reinhold et al 1998, 1999; Kang et al, 1996; Kissler et al, 2008; Reinhold et al, 2001), whereas others conclude that a maximal thickness of 10 mm is considered the cut-off value beyond which JZ adenomyosis is assumed (Kunz et al, 2005 ; Bazot et al, 2001).

A thickened JZ is considered a negative predictive factor for IVF implantation (Maubon et al, 2010; Piver et al, 2005). And animal experiments and human studies suggest that adenomyosis is associated with infertility (Barrier et al, 2004; Zangos et al, 2004).

The results mentioned above indicate that there is no overall agreement about the thickness of an abnormal JZ.

Reinhold et al. (1996) and Bazot et al. (2001) introduces the JZ to total myometrial thickness ratio. This ratio gives additional information about the JZ

thickness, more specifically about the relationship between JZ and the total myometrial zone. The ratio of these two parameters can also be considered in the diagnosis of adenomyosis, as a ratio higher than 40% is one of the specific MRI criteria for diagnosing the condition. Reinhold et al. finds a significant difference between patients with adenomyosis (69%) and a control group (44%) (Reinhold et al, 1996). Bazot et al. conclude that a ratio higher than 40% allows a diagnosis of adenomyosis with a sensitivity of 65% and a specificity of 92% (Bazot et al, 2001). The results obtained for the ratio in our study also fit this criteria. A maximum ratio of 33% was observed, which is clearly below the defined threshold of 40%.

The underlying association between adenomyosis and infertility is still not fully understood. It can be postulated that a thickened or an altered morphology of the JZ reduces uterine peristaltic activity and decreases endometrial receptivity which affects respectively sperm transport and embryo implantation (Kido et al, 2007). Furthermore, Maubon et al. (2010) finds a significantly lower rate of embryo implantation when the maximum JZ thickness was 10 mm or higher. The incidence of a thickened JZ (defined as an average JZ in anterior, posterior and fundal wall of at least 7 mm or a maximal JZ thickness of at least 10 mm) is significantly higher in the group of women with unexplained infertility in comparison with the incidence in other subtypes of infertility (male infertility, endometriosis, dysovulation or tubal abnormalities) (Maubon et al, 2010). In addition, Youm et al. (2011) concludes that a thickened myometrium (>2.5 cm) in infertile women assessed by transvaginal ultrasonography also exerts overall adverse effects on IVF and embryo transfer outcomes.

1.6 Aims of the study

The first aim of this study is to determine the normal value of junctional zone thickness, the best phase in the menstrual cycle to perform the MRI examination and the best location within the wall of the uterus to measure the junctional zone thickness. As proven in literature (e.g. Hricak et al, 1983; Hauth et al, 2007 ...) MRI is the best method to evaluate the junctional zone. Examinations are executed in nullipara and primipara women between the age of 18 and 35years, both non-using or using contraception. The non-using participants are

evaluated in the follicular, ovulatory and luteal phase. The JZ thickness is measured in 6 locations of the uterine wall in every MRI examination.

The second aim is to detect a statistical significant difference in JZ thickness between fertile and infertile women between the age of 18-35 years, using the same method as mentioned above.

The third aim is to characterise the perfusion features of the junctional zone. The female reproductive system is characterized by rapid cyclic changes in blood flow throughout the menstrual cycle. During the female reproductive period, arteries present in the junctional zone supply the endometrium with oxygen and nutrients to contribute to endometrial growth. These arteries subsequently constrict in order to cause ischemia resulting in endometrial shedding during menstruation (Chard et al, 1994).

The purpose of this prospective study is to investigate perfusion characteristics of normal JZ and outer myometrium throughout the menstrual cycle in a population of healthy nulliparous and primiparous women between 18 and 35 years old, by means of DCE-MRI. In addition, to detect whether or not the perfusion parameters are influenced by the menstrual cycle phase, the use of hormonal contraceptives and the location in the uterine wall. Generally, it is accepted that an adequate uterine blood supply is required for successful embryo implantation as part of assisted reproductive therapy. However, contrary to this hypothesis, it is also believed that a period of relative ischemia and hypoxia during the peri-ovulatory period is beneficial for embryo implantation to occur (Brosens I et al, 2010). The second hypothesis is supported by evidence of a beneficial role for hypoxia during implantation in humans. It is demonstrated that relative low oxygen levels are present at the time the blastocyst implants (Brosens I et al, 2010). Less is known about the perfusion in the myometrium in the context of embryo implantation.

The fourth aim is evaluate perfusion characteristics of the JZ in infertile patients. If an impaired perfusion will be identified in an infertile woman by DCE-MRI in future examinations by using the achieved features found of the MRI vascularity parameters (iAUC, K trans, ...). These women may be offered treatments in

order to normalize the uterine perfusion as an attempt to increase natural fertility before continuing to other, more invasive treatments in the context of assisted reproductive therapy. Doppler ultrasound differences in internal myometrial perfusion during the menstrual cycle are well described and are believed to be involved in migration of spermatozoa (contraction) and in embryo implantation. Based on Doppler ultrasound findings, Raine-Fenning et al. characterized an increased vascularisation in the JZ during the proliferative (follicular) phase, peaking approximately three days prior to ovulation before decreasing to a nadir 5 days post-ovulation (Raine-Fenning et al, 2004).

The first description of healthy myometrial enhancement by 1.5T DCE-MRI was reported by Yamashita et al. in 1993, who investigated 27 healthy women (Yamashita et al, 1993). Another study assessed physiological microvascular perfusion of normal myometrium in 62 women of reproductive age using DCE-MRI, in which a 1.5T MRI scanner and a slice thickness of 5 mm was used (Thomassin-Naggara et al, 2010). However, this study made no distinction based on the parity or the use of hormonal contraception and the women were investigated only once during their menstrual cycle.

1.7 Material and Methods

1.7.1 Study population

48 volunteer nulliparous and 50 volunteer primiparous women at 6 to 12 months post-partum are included in this study (Table 1). Recruitment is achieved by emailing and writing co-workers in Ziekenhuis Oost Limburg, students and PhD students at the local university, personal contacts and cooperation with external physicians. Exclusion criteria are age less than 18 years or more than 35 years, non-Caucasian origin, pregnancy, medical history of infertility or a gynecological history such as heavy, prolonged or irregular menstrual periods, previous unknown uterine morphologic abnormality found on the first MRI examination, diminished renal function (assessed by creatinine levels collected prior to MRI investigation) and women with a pacemaker, clips or other MRI-incompatible implanted devices. Both the nulliparous and primiparous women are subdivided based on their use of hormonal contraception.

Table 1. Overview of the study population namely the control group and the menstrual phases during which MRI examination is performed.

			98 women			
48 nulliparous				50 primiparous (6-12 months post-partum)		
18 non-users of hormonal contraception		30 users sampled randomly		12 non-users of hormonal contraception	38 users sampled randomly	
16 women during follicular phase	17 women during ovulatory phase	17 women during luteal phase		7 women during follicular phase	5 women during luteal phase	

Subsequently 28 infertile patients are subdivided into three groups based on the underlying cause of their infertility and whether or not they were on ovarian stimulating therapy: 5 women with unexplained infertility (mean age 28.5 years), 12 anovulating women (mean age 30.8 years) and 11 women on ovarian stimulation therapy (mean age 29.3 years).

5 of these infertile patients underwent the DCE-MRI examination.

All women provided a written informed consent and filled out an epidemiological questionnaire in order to obtain information concerning their birth date, height, weight, age at menarche, whether or not they currently smoke and current menstrual status.

1.7.2 Blood laboratory tests

Blood samples are taken prior to each MRI examination in order to assess human chorionic gonadotrophin (hCG), creatinine, follicle-stimulating hormone (FSH), luteinizing hormone (LH), estradiol and progesterone levels. The follicular phase is considered around day 6-13 of the menstrual cycle, the ovulatory phase around day 14-16 and the luteal phase around day 17-28 (Fig. 8). The exact phase of the menstrual cycle is determined based on the hormone levels in all participants who did not use hormonal contraception.

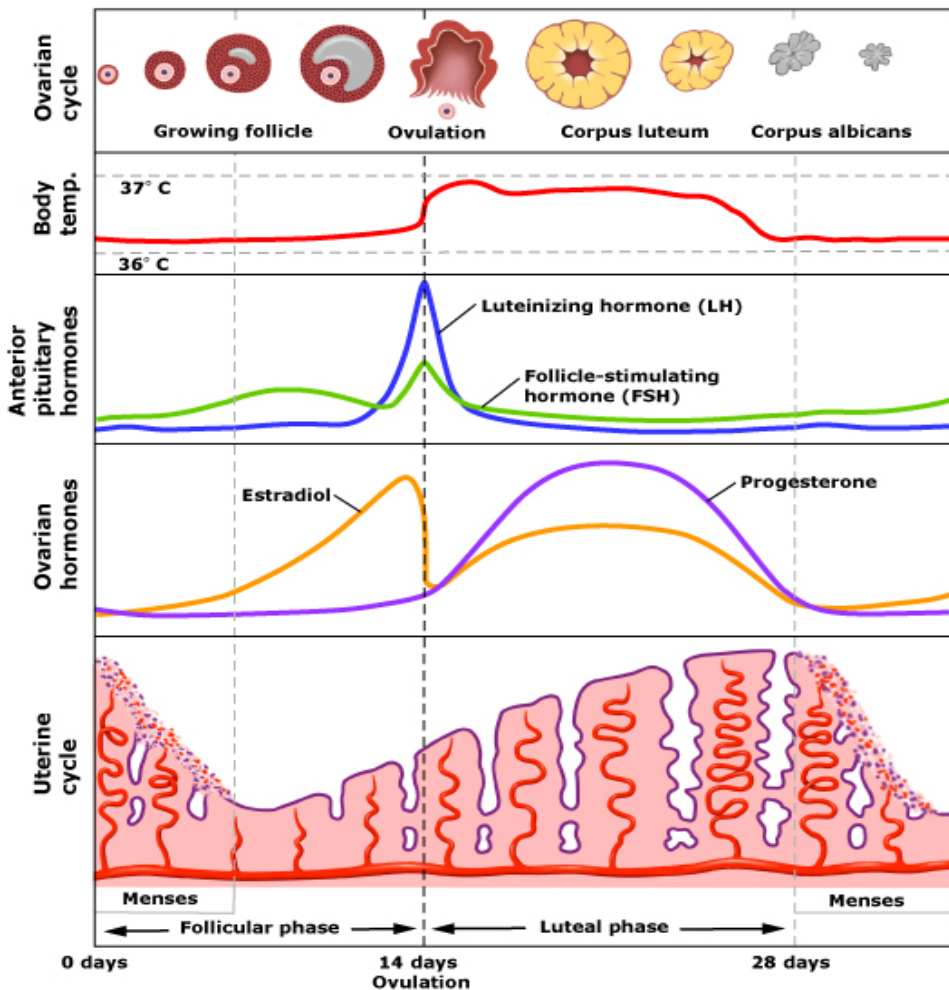


Fig. 8
Schematic overview of the menstrual cycle (*)

1.7.3 Magnetic Resonance Imaging

MRI examinations are obtained with a 1.5T magnet unit (Siemens Magnetom Symphony Tim (4G-Dot upgraded), Siemens, Erlangen, Germany; Software Syngo MR B15). An intravenous catheter is inserted in the elbow crease (in order to take a blood sample and) before they are positioned in head first - supine position. An eight channel receive only body array coil is placed on the pelvis (Fig. 9).



Fig. 9

Presentation of a patient in head first, supine position on a MRI table and a body array coil is placed on the pelvis.

During MRI, tissues are pulsed with radio-frequency in the presence of a magnetic field. This induces excitation of protons within water molecules. The release of energy when the protons relax back to their ground state is recorded, producing an MR image. Varying tissue signal intensity is determined by the relaxation time (T1 and T2) and proton density.

T2-weighted turbo spin echo (T2 TSE) sequences in three different planes are acquired in a transversal (Fig. 11), coronal (Fig. 12) and sagittal plane (Fig. 10).

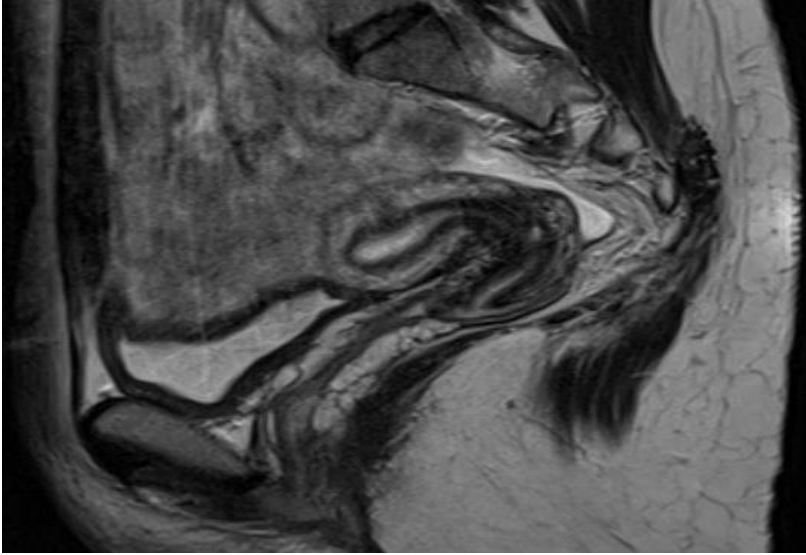


Fig. 10
MRI T2 weighted image in the sagittal plane of the pelvis.

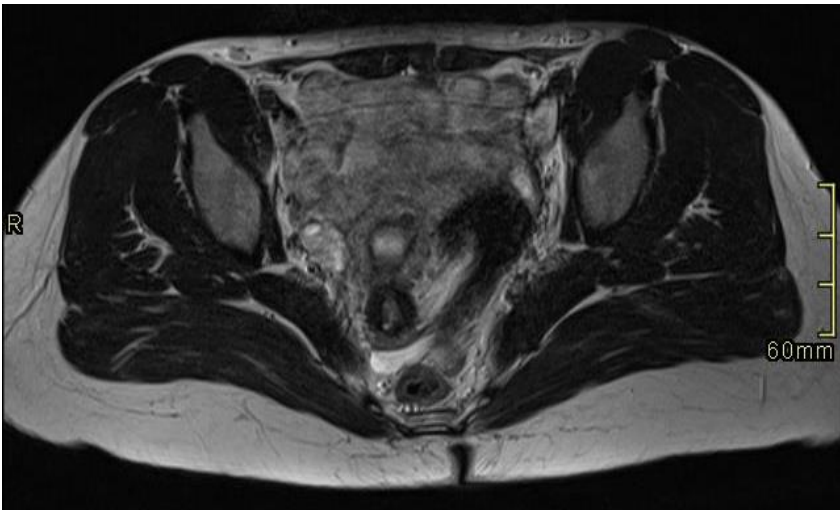


Fig. 11
MRI T2 weighted image in the transversal plane of the pelvis.

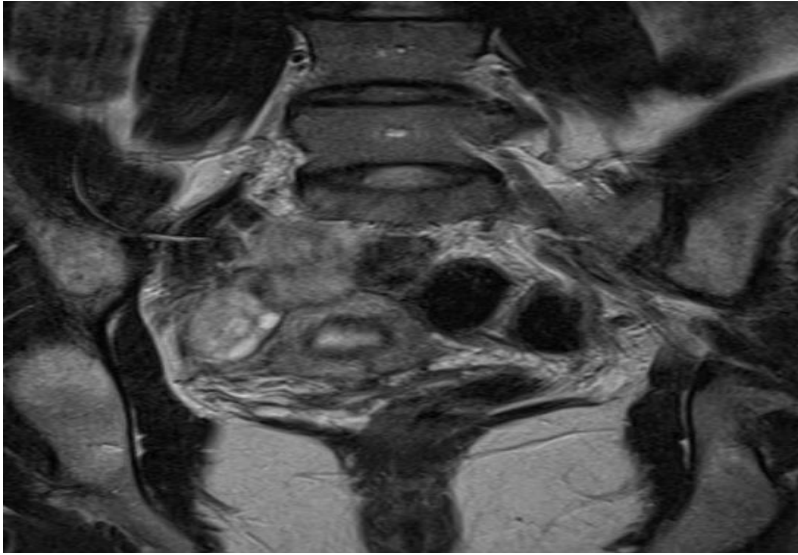


Fig. 12
MRI T2 weighted image in the coronal plane of the pelvis.

Then, in agreement with the woman (only 3 women refused – 2 primipara and 1 nullipara all users), the abdominal-specific antispasmodic Hyoscine Butylbromide (buscopan, 1 ml, 20 mg/ml, Boehringer Ingelheim, Germany), diluted in sodium chloride (10 ml, 0.09%, Baxter, Lessines, Belgium) is manually injected in order to reduce bowel peristalsis (Fig. 13). Afterwards, sagittal T2 TSE images without fat suppression are obtained.

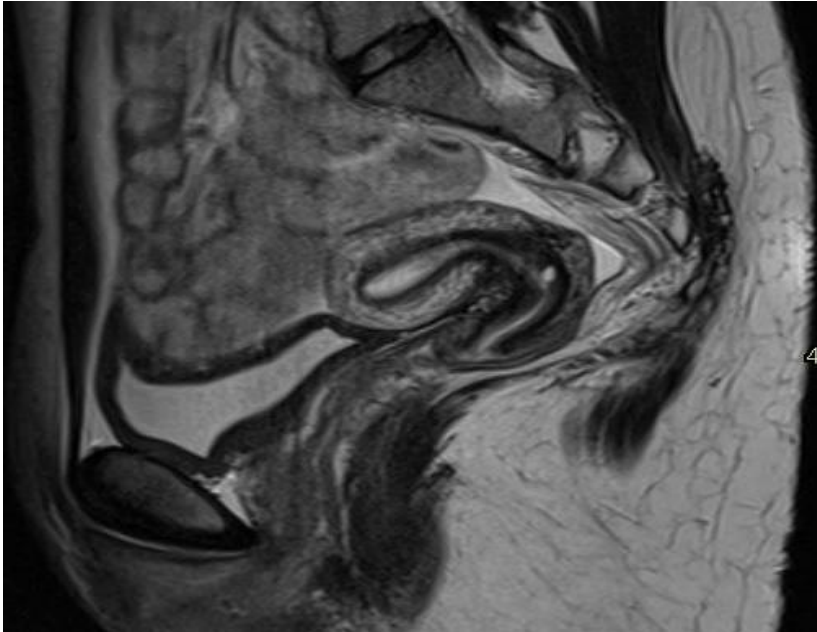


Fig. 13

MRI T2 weighted image of the pelvis in the sagittal plane after IV administration of antispasmodic agent. Notice the better delineation of the different layers of the uterine wall.

Dynamic contrast-enhanced magnetic resonance imaging (DCE-MRI) provides semi-quantitative assessment of perfusion kinetics, including perfusion assessment in myometrium (Thomassin-Nagara et al, 2010). This non-invasive technique obtains repeated T1-weighted MR images before, during and after a bolus injection of a contrast agent. Analysis of these images requires post-imaging processing with specialized software and physiological models. The software evaluates the signal enhancement resulting in the conversion of a signal intensity-time curve (Heye et al, 2014). Analysis of this curve, based on the model of Tofts (Tofts et al, 1997)(Fig. 14), provides quantitative information about the perfusion parameters of the organ of interest.

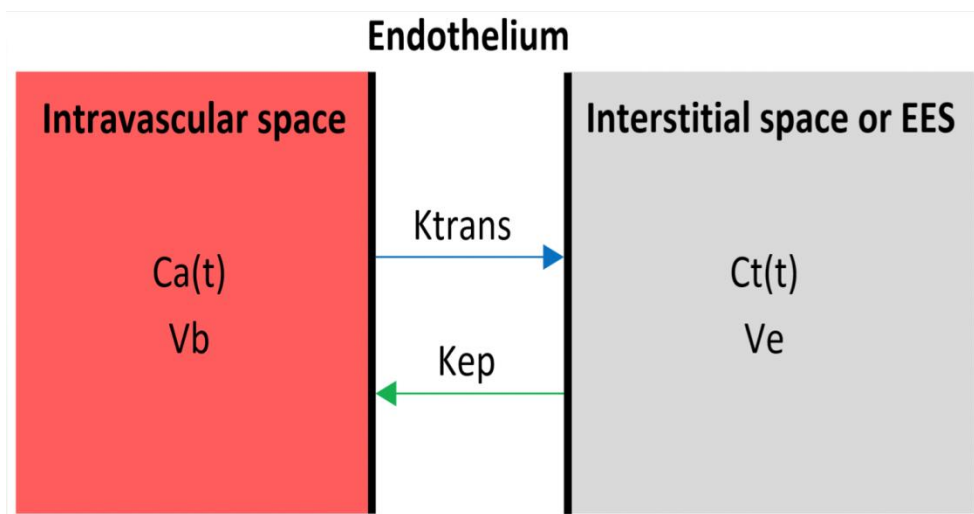


Fig. 14

The assumptions used by dynamic contrast-enhanced magnetic resonance imaging (DCE-MRI) are based on the two compartment model of Tofts.

Two compartments are assumed in this model: the intravascular space and the extracellular extravascular space (EES or interstitial space). The model provides information about the distribution of contrast agent across these compartments. C_a : arterial contrast agent concentration in function of time; C_t : tissue contrast agent concentration in function of time; V_b : whole blood volume per unit of tissue; V_e : total EES volume; K^{trans} : transfer constant; K_{ep} : reflux constant.

For DCE-MRI, perfusion acquisition consists of a pre-contrast T_1 mapping at different flip angle (three acquisitions pre-contrast). Subsequently, intravenous-contrast macrocyclic ionic Gadoterate acid (Gd-DOTA, Dotarem) is administered at a rate of 3 ml/sec followed by a flush of 10 ml sodium chloride at an equal rate with an automatic injector (MEDRAD) (6). Then, dynamic series are acquired in the mid- sagittal plane of the uterus (in 2D FLASH- only the 5 first participants receives a 2D FLASH examination – 3 nullipara users, 1 primipara user and 1 primipara non-user) or 3D FLASH) (Fig. 15). All images are sent to a dedicated workstation.

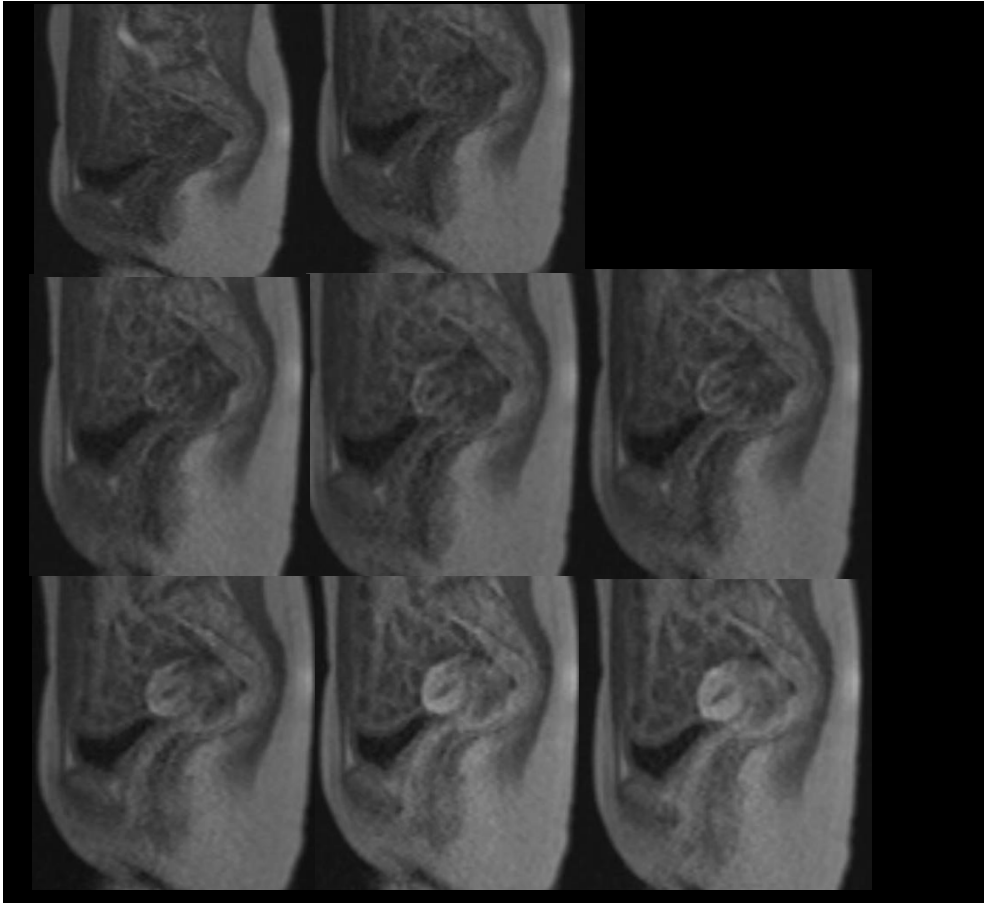


Fig. 15

Dynamic Contrast Enhanced sequence of MRI images in the midsagittal plane of the pelvis, T1 weighted images. Notice the filling-in of the uterine wall, starting with the serosa, followed by the junctional zone and finally the residual outer myometrium.

1.7.4 Image analysis

The measurements are performed on a specialized workstation (MMWP, Syngo MMWP VE36A) using the measuring cursor included in the workstation's software. All measurements are completed by two independent readers (expert pelvic imaging radiologist and fellow). Examinations are evaluated consecutively and both readers are blinded for the clinical information of the women.

The T2 TSE images in transversal, coronal and sagittal plane before buscopan injection of the healthy nulliparous women are first analyzed by the expert reader to avoid possible suspicious findings of congenital or acquired uterine abnormalities. The corpus size latero-lateral (transverse or LL) is measured on the transversal T2 TSE image obtained before buscopan injection. The sagittal T2 TSE image after buscopan injection is used in order to measure the corpus length and the antero-posterior (AP) uterus size. The volume of the corpus uteri is calculated using the formula for an ellipsoid: length x height (AP) x width (LL) x 0.523 (16). The sagittal T2 TSE image after buscopan injection is used to measure the JZ and outer myometrial thickness at six different uterine wall locations. These are measured in the anterior and posterior wall at the level of the isthmus, the middle (midcorpus) and the fundus (Fig.16 C & D). According to this method, both the anterior and posterior uterine wall are divided into three parts equally in length. Subsequently, the JZ and outer myometrial thickness are measured at the central point in each part. The ratio of JZ thickness versus total myometrial thickness is calculated as well by dividing the thickness of the JZ by the corresponding thickness of the total myometrium at the same location (ratio = JZ thickness/ (JZ thickness + outer myometrial thickness)).

The average JZ thickness, outer myometrial thickness and ratio of JZ versus total myometrial thickness are calculated as the average of the six measurements of every woman in the group.

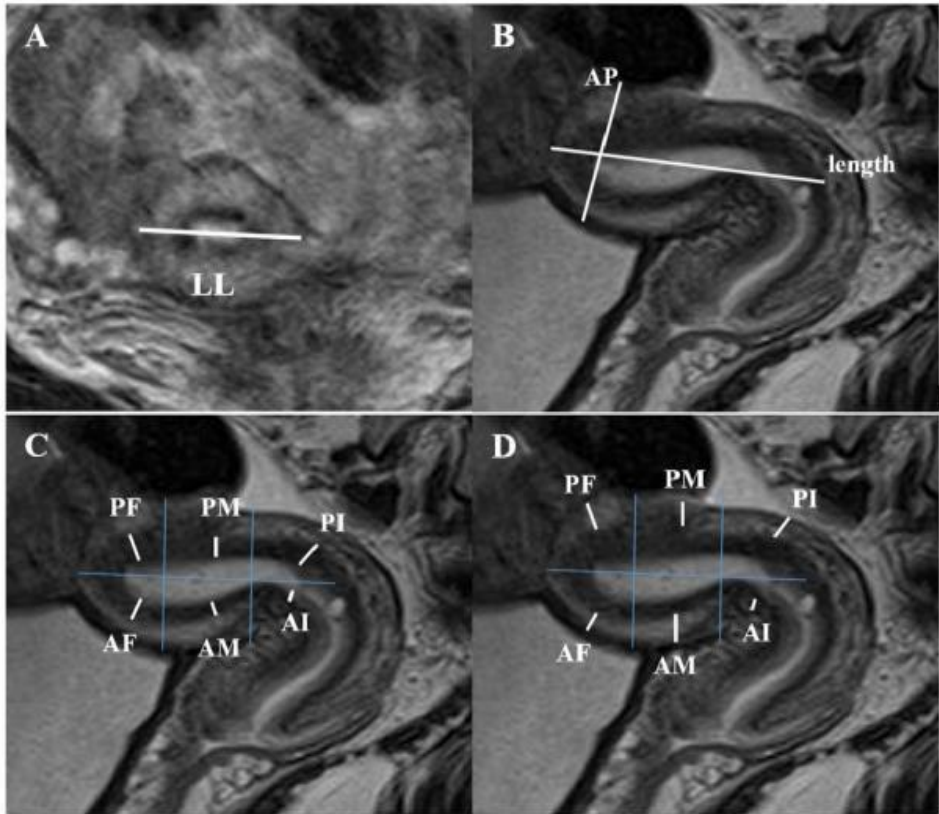


Fig. 16
Measurements of the corpus uteri volume, the junctional zone thickness and outer myometrium thickness, assessed on T₂-weighted turbo spin echo magnetic resonance images. A: The transversal image obtained before buscopan injection is used to measure the corpus size latero-lateral (LL). B: On the sagittal image after buscopan injection without fat suppression, the length and the antero-posterior (AP) uterus size are measured. C and D: The same sagittal image is also used to measure the junctional zone (C) and outer myometrium (D) thickness. According to the measuring method, the uterine walls are divided into three parts equally in length (blue lines), and the measurement is performed at a central point in each part. PF: posterior wall at the fundus; PM: posterior wall at the midcorpus; PI: posterior wall at the isthmus; AF: anterior wall at the fundus; AM: anterior wall at the midcorpus; AI: anterior wall at the isthmus.

The perfusion acquisitions are evaluated on Syngo Tissue 4D of Siemens. Two methods of evaluation are used: a quantitative method following the two compartment model of Tofts and a semi-quantitative evaluation method. The model of Tofts comprises the following parameters: transfer constant (k^{trans}), interstitial volume fraction (V_e) and reflux constant (K_{ep}).

The semi-quantitative evaluation method retrieves the following parameters: Time-to-Peak (TTP), Arrival Time (AT) and initial Area Under the Curve in 60 seconds (iAUC). The perfusion parameters analyzed in this study are: iAUC (in correlation with the uterus/cervix volume), K^{trans} , K_{ep} and V_e (Table 2).

Table 2. Description of the assessed perfusion parameters. EES: extravascular extracellular space.

Parameter	Description	Unit
iAUC/volume	Initial (first 60 seconds) area under the contrast agent concentration - time curve after contrast administration. It is an indicator for the amount of blood volume during the initial minute after the contrast agent enters the blood per unit mass of tissue. IAUC is evaluated in correlation with the volume of respectively the corpus or cervix uteri.	
K^{trans}	Transfer constant, the influx of contrast agent from the blood plasma into the EES, depends on capillary permeability, surface area and blood flow per unit mass of tissue.	min^{-1}
K_{ep}	Reflux constant, the efflux of contrast agent from the EES back into the blood plasma.	min^{-1}
V_e	EES volume fraction (K^{trans}/K_{ep}).	

In order to measure these parameters, Regions Of Interest (ROIs), with a diameter of 1 mm were placed in post-processing software at different places: the anterior and posterior wall of the JZ and outer myometrium (fundal and corpus region) (Fig. 17).

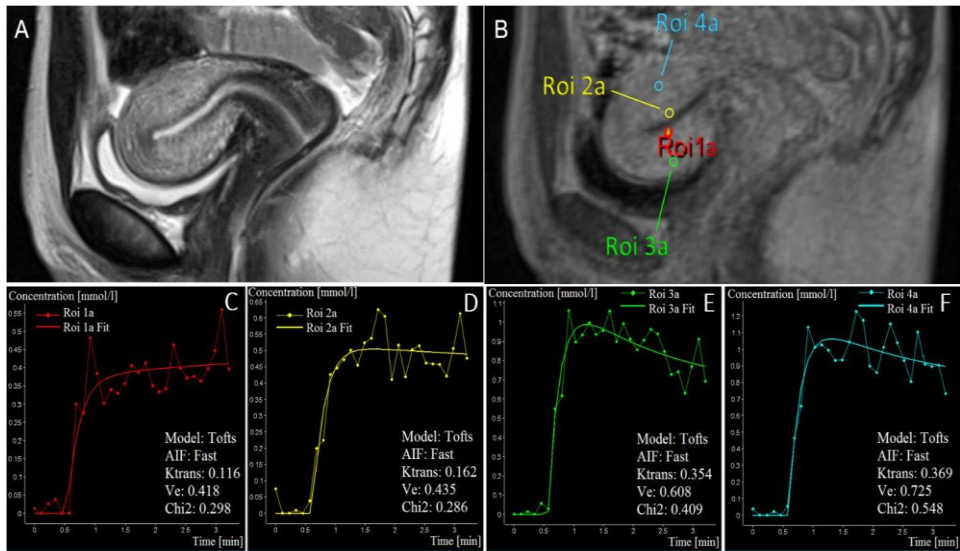


Fig. 17

Example of perfusion assessment by dynamic contrast-enhanced magnetic resonance imaging (DCE-MRI) in the corpus and cervix uteri. A: Sagittal T₂-weighted pelvic MRI-scan. B: Dynamic MRI-scan in order to assess perfusion Tissue 4D Calculations in different locations. The Regions of Interest (ROI) are placed at the anterior wall of the junctional zone (JZ) (ROI 1a), at the posterior wall of the JZ (ROI 2a), at the anterior wall of the outer myometrium (ROI 3a), at the posterior wall of the outer myometrium (ROI 4a), at the anterior wall of the inner third of the cervical stroma (ROI 1b), at the posterior wall of the inner third of the cervical stroma (ROI 2b), at the anterior wall of the outer two-thirds of the cervical stroma (ROI 3b) and at the posterior wall of the outer two-thirds of the cervical stroma (ROI 4b). C-J: Examples of concentration-time curves for respectively each ROI.

1.7.5 Statistical analysis

All statistical analyses are performed by means of the computer program SAS version 9.4. A 5% level of significance is used. No correction for multiple testing is applied. Inter-observer statistics are performed for the consistency in measurements by means of the informal Bland-Altman test (Bland JM and Altman, 1986; Altman DG, 1991) in chapter 2 and Cohen's kappa coefficient in chapter 3-5 (according to the preference of the journal reviewers respectively). Mann-Whitney U-tests are performed in order to compare the uterine volumes between groups by means of IBM SPSS Statistics (version 23.0) in chapter 4&5. In chapter 2&3 linear mixed models are used in order to investigate the effect of hormonal contraception, the effect of menstrual phase (for woman not using hormonal contraception) and the effect of the location in the uterine wall on the

JZ thickness, on the outer myometrial thickness, and on the ratio of JZ versus total myometrial thickness. The statistical model includes two main fixed effects and their interaction. The first fixed effect combines the use of hormonal contraception and the menstrual phase. This fixed effects analyses has four levels, i.e. phase 1 for non-users, phase 2 for non- users, phase 3 for non-users, and users of hormonal contraception. This effect allows the comparison of (1) users and non-users (per menstrual phase for the non-users or averaged over the three menstrual phases for the non-users) and (2) the different menstrual phases for the non- users of hormonal contraception. The second fixed effect is the location in the uterine wall. The association between measurements of the same woman (e.g. JZ thickness measured in the three menstrual phases) is incorporated by means of a random intercept at woman level. A parsimonious model is obtained by backward elimination of the fixed effects terms not statistically significant at a 5% level of significance. In order to normalize the data, statistical analyses are performed on the natural log transformed outcome data.

Chapter 4 & 5 linear mixed models are used in order to investigate the effect of menstrual phase (for women not using hormonal contraception), the effect of parity and the effect of the location in uterine wall on the perfusion parameters $iAUC/volume$, K^{trans} , K_{ep} and Ve . The statistical model investigating the effect of phase in the nulliparous and primiparous non-users of hormonal contraception, includes two main fixed effects and their interaction. The fixed effects are menstrual phase and the uterine location. In order to detect differences between groups, separate statistical models are constructed for nulliparous and primiparous women for each location including the fixed effect of hormonal contraception. The statistical models investigating the effect of uterine location, constructed for each group, contains the fixed effect of uterine location. The association between measurements of the same woman (e.g. measurements in different menstrual phases) is incorporated by means of a random intercept at woman level. A parsimonious model is obtained by backward elimination of interaction terms not statistically significant at a 5% level of significance. In order to normalize the data, statistical analyses are performed on the natural log transformed outcome data.

1.8 References

1. Abbara S, Nikolic B, Pelage JP, Spies JP (2007) Frequency and extent of uterine perfusion via ovarian arteries observed during uterine artery embolization for leiomyomas. *Am J Roentgenol* 188:1558-1563.
2. Acién P, Velasco I (2013) Endometriosis: a disease that remains enigmatic. *ISNR Obstet Gynecol Jul 17*:242149.
3. Altman D (1991) *Practical statistics for medical research*. London: Chapman and Hall. In.
4. Barrier BF, Malinowski MJ, Dick EJ, Hubbard GB, Bates GW. Adenomyosis in the baboon is associated with primary infertility. *Fertil Steril* 2004;82 Suppl 3:1091-1094.
5. Bartelmez GW (1957a). The phases of the menstrual cycle and their interpretation in terms of the pregnancy cycle. *American Journal of Obstetrics and Gynecology*, 74, 931-55.
6. Barth M, Spies J (2003) Ovarian artery embolization supplementing uterine embolization for leiomyomata. *J Vasc Interv Radiol* 14:1177-1182.
7. Bazot M, Cortez A, Darai E, et al. Ultrasonography compared with magnetic resonance imaging for the diagnosis of adenomyosis: correlation with histopathology. *Hum Reprod* 2001;16(11):2427-2433.
8. Benagiano G, Brosens I, Carrara S. Adenomyosis: new knowledge is generating new treatment strategies. *Womens Health (Lond Engl)* 2009;5(3):297-311.
9. Bland JM, Altman DG (1986) Statistical methods for assessing agreement between two methods of clinical measurement. *Lancet* 1:307-310.

10. Brosens I, Roberston WB, Dixon HG (1967). The physiological response of the vessels of the placental bed to normal pregnancy. *Journal of Pathology and Bacteriology*, 93, 569.
11. Brosens I, Derwig I, Brosens J, Fusi L, Benagiano G, Pijnenborg R.(2010) The enigmatic uterine junctional zone: the missing link between reproductive disorders and major obstetrical disorders? *Hum Reprod* 25(3):569-574.
12. Brosens JJ, de Souza NM, Barker FG (1998) Steroid hormone-dependent myometrial zonal differentiation in the non-pregnant human uterus. *Eur J Obstet Gynecol Reprod Biol Dec*;81(2):247-51.Review.
13. Brosens JJ, Pijnenborg R, Brosens IA (2002) The myometrial junctional zone spiral arteries in normal and abnormal pregnancies: a review of the literature. *Am J Obstet Gynecol* 187:1416-1423.
14. Brosens I, Derwig I, Brosens J, Fusi L, Benagiano G, Pijnenborg R. The enigmatic uterine junctional zone: the missing link between reproductive disorders and major obstetrical disorders? *Hum Reprod* 2010;25(3):569-574.
15. Chang S, Lee MS, Kim MD, Yoon CJ, Jung DC, Lee M, Park S, Won JY, Lee do Y (2013) Inferior mesenteric artery collaterals to the uterus during uterine artery embolization: prevalence, risk factors, and clinical outcomes. *J Vasc Interv Radiol* 24:1353-1360.
16. Chard T, Grudzinskas JG. *The Uterus - Anatomy of the Uterus - Nutrition*; p. 29-39: 1994.
17. Dixon S, Tapping CR, Chuah PS, Bratby M, Uberoi R, Anthony S (2013) Successful fibroid embolization of pelvic and inferior mesenteric artery collaterals after previous uterine artery embolization. *Acta Radiol* 53:292-295.

18. Fusi L, Cloke B, Brosens JJ. The uterine junctional zone. *Best Pract Res Clin Obstet Gynaecol* 2006;20(4):479-491.
19. Goerttler (1930). Die Architektur der Muskelwand des menschlichen Uterus und ihre funktionelle Bedeutung. *Morphologische Jahrbuch* 65,45. Also in *American Journal of Obstetrics and Gynecology*, 44, 952.
20. Girling JE, Rogers PA. Recent advances in endometrial angiogenesis research. *Angiogenesis* 2005;8(2):89-99.
21. Haines and Taylor *Obstetrical and Gynaecological Pathology* (1987). Ed. By H.Fox, 3rd edn, Churchill Livingstone, Edingburgh,UK.
22. Hauth EA, Jaeger HJ, Libera H, Lange S, Forsting M. MR imaging of the uterus and cervix in healthy women: determination of normal values. *Eur Radiol* 2007;17(3):734-742.
23. Haynor DR, Mack LA, Soules MR, Shuman WP, Montana MA, Moss AA. Changing appearance of the normal uterus during the menstrual cycle: MR studies. *Radiology* 1986;161(2):459-462.
24. Heye T, Boll DT, Reiner CS, Bashir MR, Dale BM, Merkle EM (2014) Impact of precontrast T1 relaxation times on dynamic contrast-enhanced MRI pharmacokinetic parameters: T1 mapping versus a fixed T10 reference value. *J Magn Reson Imaging* 39:1136-1145.
25. Hricak H, Alpers C, Crooks LE, Sheldon PE. Magnetic resonance imaging of the female pelvis: initial experience. *AJR Am J Roentgenol* 1983;141(6):1119-1128.
26. Ijland MM, Evers JL, Dunselman GA, van Katwijk C, Lo CR, Hoogland HJ. Endometrial wavelike movements during the menstrual cycle. *Fertil Steril* 1996;65(4):746-749.

27. Jose-Miller AB, Boyden JW, Frey KA. Infertility. *Am Fam Physician* 2007; 75(6):849-56.
28. Kang S, Turner DA, Foster GS, Rapoport MI, Spencer SA, Wang JZ. Adenomyosis: specificity of 5 mm as the maximum normal uterine junctional zone thickness in MR images. *AJR Am J Roentgenol* 1996;166(5):1145-1150.
29. Kissler S, Zangos S, Kohl J, et al. Duration of dysmenorrhoea and extent of adenomyosis visualised by magnetic resonance imaging. *Eur J Obstet Gynecol Reprod Biol* 2008;137(2):204-209.
30. Kido A, Togashi K, Nishino M, et al. Cine MR imaging of uterine peristalsis in patients with endometriosis. *Eur Radiol* 2007;17(7):1813-1819.
31. Kunz G, Beil D, Deininger H, Wildt L, Leyendecker G. The dynamics of rapid sperm transport through the female genital tract: evidence from vaginal sonography of uterine peristalsis and hysterosalpingoscintigraphy. *Hum Reprod* 1996;11(3):627-632.
32. Kunz G, Beil D, Huppert P, Noe M, Kissler S, Leyendecker G. Adenomyosis in endometriosis--prevalence and impact on fertility. Evidence from magnetic resonance imaging. *Hum Reprod* 2005;20(8):2309-2316.
33. Lesny P, Killick SR, Tetlow RL, Manton DJ, Robinson J, Maguiness SD. Ultrasound evaluation of the Uterine zonal anatomy during in-vitro fertilization and embryo transfer. *Hum Reprod*.1999; 14(6):1593-8.
34. Leyendecker G, Wildt L, Mall G. The pathophysiology of endometriosis and adenomyosis: tissue injury and repair. *Arch Gynecol Obstet* 2009; 280: 529-538.

35. Mark AS, Hricak H, Heinrichs LW, Hendrickson MR, Winkler ML, Bachica JA, Stickler JE. Adenomyosis and leiomyoma: differential diagnosis with MR imaging. *1987 Radiology* 1987; 163 (2): 527-9.
36. Mascarenhas MN, Flaxman SR, Boerma T, Vanderpoel S, Stevens GA. National, Regional, and Global Trends in Infertility Prevalence Since 1990: A Systematic Analysis of 277 Health Surveys. *PLoS Med* 9(12):e1001356.
37. Maubon A, Faury A, Kapella M, Pouquet M, Piver P. Uterine junctional zone at magnetic resonance imaging: a predictor of in vitro fertilization implantation failure. *J Obstet Gynaecol Res* 2010;36(3):611-618.
38. McCarthy S, Tauber C, Gore J (1986) Female pelvic anatomy: MR assessment of variations during the menstrual cycle and with use of oral contraceptives. *Radiology* 160:119-123.
39. McLucas B (2009) Collateral supply to uterine leiomyomata from an unnamed vessel: a case report. *Minim Invasive Ther Allied Technol* 18(1):106-108.
40. McLucas B (2009) Extra-gonadal collateral supply to uterine leiomyomata: a case report. *Minim Invasive Ther Allied Technol* 18(2):103-105.
41. Mitchell DG, Schonholz L, Hilpert PL, Pennell RG, Blum L, Rifkin MD. Zones of the uterus: discrepancy between US and MRI images. *Radiology* 1990; 174(3Pt1): 827-31.
42. Morassutto C, Monasta L, Ricci G, Barbone F, Ronfani L. Incidence and Estimated Prevalence of Endometriosis and Adenomyosis in Northeast Italy: A Data Linkage Study. *PLOS One*. 2016; 11(4):e0154227.

43. More IAR (1987). The normal human endometrium. In Haines and Taylor *Obstetrical and Gynecological Pathology*, ed. H. Fox., vol. I, Churchill Livingstone, Edingburgh, UK.
44. Nikolic B, Spies JP, Abbara S, Goodwin S (1999) Ovarian artery supply of uterine fibroids as a cause of treatment failure after uterine artery embolization: a case report. *J Vasc Interv Radiol* 10:1167-1170.
45. Novellas S, Chassang M, Delotte J, et al. MRI characteristics of the uterine junctional zone: from normal to the diagnosis of adenomyosis. *AJR Am J Roentgenol* 2011;196(5):1206-1213.
46. Pelage JP, Gazejust J, Pluot E, Le Dref O, Laurent A, Spies J, Chagnon S, Lacome P (2005) Uterine fibroid vascularization and clinical relevance to uterine fibroid embolization. *Radiographics* 25:S99-S117.
47. Piver P. Uterine factors limiting ART coverage. *J Gynecol Obstet Biol Reprod (Paris)* 2005;34(7 Pt 2):5S30-35S33.
48. Raine-Fenning NJ, Campbell BK, Kendall NR, Clewes JS, Johnson IR. Endometrial and subendometrial perfusion are impaired in women with unexplained subfertility. *Hum Reprod* 2004;19(11):2605-2614.
49. Razavi MK, Wolanske KA, Hwang GL, Sze DY, Kee ST, Dake MD (2002) Angiographic Classification of Ovarian Artery-to-Uterine Artery Anastomoses: Initial Observations in Uterine Fibroid Embolization. *Radiology*.
50. Reinhold C, McCarthy S, Bret PM, Mehio A, Atri M, Zakarian R, Glaude Y, Liang L, Seymour RJ (1996) Diffuse adenomyosis: comparison of endovaginal US and MR imaging with histopathologic correlation. *Radiology* 199:151-158.

51. Reinhold C, Tafazoli F, Wang L. Imaging features of adenomyosis. *Hum Reprod Update* 1998;4(4):337-349.
52. Reinhold C, Tafazoli F, Mehio A, et al. Uterine adenomyosis: endovaginal US and MR imaging features with histopathologic correlation. *Radiographics* 1999;19 Spec No:S147-160.
53. Reynolds LP, Grazul-Bilska AT, Redmer DA. Angiogenesis in the female reproductive organs: pathological implications. *Int J Exp Pathol* 2002;83(4):151-163.
54. Robertson WB, Brosens I, Dixon G (1975). Uteroplacental vascular pathology. *European Journal of Obstetrics, Gynecology and Reproductive Biology*, 5, 47-65.
55. Sala E, Rockall A, Rangarajan D, Kubik-Huch RA. The role of dynamic contrast-enhanced and diffusion weighted magnetic resonance imaging in the female pelvis. *Eur J Radiol* 2010;76(3):367-385.
56. Schreinemacher MH, Backes WH, Slenter JM, et al. Towards endometriosis diagnosis by gadofosvesetrisodium enhanced magnetic resonance imaging. *PLoS One* 2012;7(3):e33241.
57. Smoger D, Kancherla V, Shlansky-Goldberg R (2010) Uterine fundal blood supply from an aberrant left ovarian artery originating from the inferior mesenteric artery: implications for uterine artery embolization. *J Vasc Interv Radiol* 21(6):941-944.
58. Steer CV, Tan SL, Mason BA, Campbell S. Midluteal-phase vaginal color Doppler assessment of uterine artery impedance in a subfertile population. *Fertil Steril* 1994;61(1):53-58.

59. Thomassin-Naggara I, Balvay D, Cuenod CA, Daraï E, Marsault C, Bazot M (2010) Dynamic contrast-enhanced MR imaging to assess physiologic variations of myometrial perfusion. *Eur Radiol* 20:984-994.
60. Tofts PS (1997) Modeling tracer kinetics in dynamic Gd-DTPA MR imaging. *J Magn Reson Imaging* 7:91-101.
61. Werth R, Grusdew W. Untersuchungen über die Entwicklung und Morphologie der menschlichen Uterusmuskulatur. *Arch Gynëkol* 1898; 55: 325-409.
62. White A, Banovac F, Yousefi S, Slack RS, Spies JB. (2007) Uterine fibroid embolization: the utility of aortography in detecting ovarian artery collateral supply. *Radiology* 244(1):291-298.
63. Wiczuk HP, Janus CL, Richards CJ, Graf MJ, Gendal ES, Rabinowitz JG, Laufer N (1988) Comparison of magnetic resonance imaging and ultrasound in evaluating follicular and endometrial development throughout the normal cycle. *Fertil Steril* 49:969-972.
64. Yamashita Y, Harada M, Sawada T, Takahashi M, Miyazaki K, Okamura H. Normal uterus and FIGO stage I endometrial carcinoma: dynamic gadolinium-enhanced MR imaging. *Radiology* 1993;186(2):495-501.
65. Youm HS, Choi YS, Han HD. In vitro fertilization and embryo transfer outcomes in relation to myometrial thickness. *J Assist Reprod Genet* 2011;28(11):1135-1140.
66. Zangos S, Kissler S, Mueller A, et al. Uterine adenomyosis in infertile patients: MR imaging findings and clinical conclusions. *Rofo* 2004;176(11):1641-1647.

- EUROSTAT 2008a
- WHO meeting to Develop a Global Consensus on Preconception Care to Reduce Maternal and Childhousd Mortality and Morbidity, Demographic health survey. Geneva, World Health Organisation-1994-2000.
- First WHO/World Bank Report on Disability (2011)
- WHO-ICMART revised
glossaryhttp://www.who.int/reproductivehealth/publications/infertility/art_terminology2/en/
- Infecundity, infertility, and childlessness in developing countries. Demographic and Health Surveys (DHS) Comparative reports No. 9
- WHO laboratory manual for the examination and processing of human semen
- Woodward PJ, Wagner BJ, Farley TE (1993) MR Imaging in the evaluation of female infertility. Radiographics Mar;13(2):293-310. Review.
- National, regional, and global trends in infertility: a systematic analysis of 277 health surveys
- <http://www.who.int/reproductivehealth/topics/infertility/definitions/en/>
- <https://www.arcfertility.com/patient-resources/infertility-tutorial/treatments/>
- * <http://sbi4u3.weebly.com/endocrine-hormones-basic-mechanisms-and-the-menstrual-cycle.html>

2. CHAPTER II: JUNCTIONAL ZONE THICKNESS IN NULLIPAROUS WOMEN BETWEEN 19 AND 35 YEARS OLD ASSESSED BY MRI, AS A FUNCTION OF MENSTRUAL CYCLE AND HORMONAL CONTRACEPTION. UTERINE JUNCTIONAL ZONE IN NULLIPAROUS WOMEN

Reprod Biomed Online. 2017 Feb;32(2):212-220

2.1 Abstract

This prospective study aims to determine the optimal menstrual phase and uterine location to detect the thickest junctional zone (JZ) by magnetic resonance imaging (MRI). This study is performed on volunteer healthy nulliparous women, subdivided according to their use of hormonal contraception. Each women was investigated three times during their menstrual cycle.

Eighteen nulliparous non-users and 29 nulliparous users of hormonal contraception (mean age 26.4 and 25.8 years, respectively) underwent a pelvic MRI (1.5T) examination during the follicular, ovulatory and luteal phase. The JZ thickness was measured at six locations in the uterine wall.

A significantly thinner JZ was observed at the anterior and posterior wall of the midcorpus and fundus, in the contraception users compared to the non-users. No differences in JZ thickness were noticed between the menstrual phases and the uterine wall locations. The ratio of JZ versus total myometrial thickness also demonstrated differences between both groups and between the assessed uterine locations.

To conclude, any phase in the menstrual cycle and location within the uterine wall was validated to determine the junctional zone thickness on MRI, although the fundal location is preferred.

KEYWORDS: Junctional Zone; Uterus; MRI; Thickness; Fertility

2.2 Introduction

One of the fundamental functions of the uterus in reproduction is directing sperm transport into the tube ipsilateral to the dominant follicle, which is provided by uterine peristalsis (Kunz et al., 1996, 2000a; Lyons et al., 1991; Wildt et al., 1998). This function is dependent upon the architecture of the myometrial wall, more particularly the junctional zone (JZ), also called archimyometrium or stratum subvasculare. This layer is characterized by predominantly circular arrangement of muscular fibers and bipartition at the level of the mid- and upper corporal region. Its origin is dedicated to the fusion of the paramesonephric ducts during early ontogeny (Fusi et al., 1996; Leyendecker et al., 1998; Leyendecker, 2000; Noe et al., 1999; Werth and Grusdew, 1898; Wetzstein, 1965).

During the reproductive period of women, three distinct layers can be recognized in the uterine wall: the endometrium, the JZ and the outer myometrium. This uterine zonal anatomy was first identified in 1983 by means of magnetic resonance imaging (MRI) (Hricak et al., 1983). On T₂-weighted MR images, the endometrium is presented as a high signal-intensity zone, the JZ as a low signal-intensity zone and the outer myometrium as a medium signal-intensity zone (Hricak et al., 1983; McCarthy et al., 1986, 1989; Scutt et al., 1991). The JZ is only clearly defined during the reproductive years, implying that it represents a hormone dependent differentiation process. This is reflected by the cyclic changes in immunoreactive estrogen and progesterone receptor expression in JZ myocytes which mimic those observed in the endometrium, whereas no cyclic changes are detectable in the outer myometrial smooth muscle cells (Hauth et al., 2001, Noe et al., 1999).

Adenomyosis is a gynecological disorder of the myometrium, characterized by a benign invasion of basal endometrial glands and stroma into the JZ and outer myometrium. Also growing evidence exists linking a thickened JZ in adenomyosis, as seen on a pelvic MRI scan, with primary/secondary infertility in young adults (Barrier et al., 2004; de Souza et al., 1995; Devlieger et al., 2003; Garavaglia et al., 2015). Inner myometrium adenomyosis is expressed by an abnormal thickening and disruption of the JZ, which is considered the MR

imaging criterion for diagnosing this condition, although myometrial hyperplasia as a normal variant could not be excluded (Reinhold et al., 1998, 1999.; Novellas et al., 2011). The diagnosis of JZ adenomyosis on the basis of MR images remains difficult because of the difficulty in determining a strict cut-off value for the JZ thickness from which adenomyosis is assumed. First of all, it is of importance to define normal limits of the JZ thickness in healthy women.

The purpose of this study was to define the optimal menstrual cycle phase and uterine wall location in order to measure the normal JZ thickness. This optimal menstrual phase and uterine wall location will be defined by the menstrual phase and location where the thickest JZ can be measured. To determine this, this study investigates whether there are cyclic or location dependent changes in JZ thickness, outer myometrial thickness and the ratio of JZ to the total myometrial thickness, by measuring this thickness in 47 healthy nulliparous women (18 non-users and 29 users of hormonal contraception), at six different uterine wall locations, in which each women is investigated three times during a menstrual cycle.

2.3 Material and Methods

The health insurance, study protocol and informed consent were approved by the local hospital ethics committee in order to perform this longitudinal study on volunteers.

2.3.1 Study population

Over a recruitment period of approximately 50 months (21/12/2007 – 12/01/2012), 47 voluntary nulliparous Caucasian women were included in this single center, prospective study divided in two groups: 18 non-users (group 1) and 29 users (group 2) of hormonal contraception. The different types of hormonal contraception were oral contraceptive pills and hormonal vaginal rings. The age of the participants ranged between 19 and 35 years (mean age for group 1 and 2 are respectively 26.4 and 25.8 years). Inclusion criteria comprises Caucasian, nulliparous women between 18-35 years old with no medical history of infertility and no gynecological history (no bleeding disorders, irregular menstrual cycle). The women were hence of unknown fertility status as they were nulliparous. Exclusion criteria were women with a pacemaker, clips or other MRI-incompatible implanted devices, pregnancy, diminished renal function and previous unknown uterine morphologic abnormality found on the first MRI examination. Recruitment was achieved by emailing and writing co-workers in our hospital, students and PhD students at the University of Hasselt (local university), personal contacts and cooperation with external physicians. All volunteers provided a written informed consent and filled out an epidemiological questionnaire.

2.3.2 Blood laboratory tests

Blood samples were collected from each subject prior to each MRI examination to assess human chorionic gonadotrophin (hCG), creatinine, follicle-stimulating hormone (FSH), luteinizing hormone (LH), estradiol and progesterone levels. The follicular phase was considered around day 6-13 of the menstrual cycle, the ovulatory phase around day 14-16 and the luteal phase around day 17-28. The exact phase of the menstrual cycle was determined based on the hormone

levels, for each MRI examination in all participants who did not use hormonal contraception.

2.3.3 Magnetic Resonance Imaging

Three MRI scans were performed during the menstrual cycle in the non-users of hormonal contraception: one in the follicular phase (n = 17), one in the ovulatory phase (n = 17) and one in the luteal phase (n = 16). Fifteen out of 18 women who did not use hormonal contraceptives underwent an MRI examination in the three phases, one only in the follicular phase, one in the follicular and ovulatory phase and one in the ovulatory and luteal phase. This resulted in a total of 50 MRI examinations for the non-users of contraception. The majority of the women in the group of the users of hormonal contraceptives also underwent three MRI scans during their cycle resulting in a total number of 83 MRI investigations for the 29 users of hormonal contraception. Two women underwent only two MRI investigations during their cycle, whereas one woman only underwent one MRI investigation.

All MRI scans were performed on a 1.5T MR imaging system (Siemens Magnetom Symphony Tim (4G-Dot upgraded), Siemens, Erlangen, Germany; Software Syngo MR B15). The study women were positioned on the table of the scanner in head first - supine position and an eight channel receive only body array was placed on the pelvis of the women. An intravenous catheter was inserted in the elbow crease. The MRI examination started with a localizer sequence followed by T₂-weighted turbo spin echo (T₂ TSE) sequences acquired in three different planes: transversal, coronal and sagittal. After manual injection of the abdominal-specific antispasmodic Hyoscine Butylbromide (buscopan, 1 ml, 20 mg/ml, Boehringer Ingelheim, Germany), diluted in sodium chloride (10 ml, 0.09%, Baxter, Lessines, Belgium), sagittal T₂ TSE images with and without fat suppression were acquired (table 1). The antispasmodic agent was used to reduce bowel movement artefacts and uterine peristalsis. All images were sent to a dedicated workstation.

Table 1: Overview of the performed MRI-scan parameters.

Parameters/Sequence	Localizer	T ₂ TSE	T ₂ TSE	T ₂ TSE	T ₂ TSE: buscopan	T ₂ TSE: buscopan
Orientation	Sagittal	Transversal	Coronal	Sagittal	Sagittal	Sagittal
Repetition time (msec)	20	5100	5000	5000	5610	4060
Time to echo (msec)	5	88	89	89	89	93
Field of view (mm)	400	370	320	340	360	360
Slice thickness (mm)	10	5	5	5	4	4
Flip angle (degree)	40	180	180	180	180	180
Voxel size (mm x mm x mm)	3.1 x 1.6 x 10	1.1 x 0.8 x 5	0.8 x 0.6 x 5	0.9 x 0.7 x 5	0.9 x 0.7 x 4	0.9 x 0.7 x 4
Acquisition time (min.sec)	0.14	1.03	2.52	2.02	2.22	3.12
Fat suppression	No	No	No	No	Yes	No

T2 TSE: T2-weighted turbo spin echo sequences; T2 TSE: T2-weighted turbo spin echo sequences after manual buscopan injection.

2.3.4 MR image analysis

All measurements were performed on a specialized workstation (MMWP, Syngo MMWP VE36A) by two independent observers, an experienced radiologist and an intern in radiology with 3 years of pelvic MRI experience, using the measuring cursor included in the workstation's software. Both observers were blinded for the hormonal contraception status of the women and examinations were evaluated consecutively. The T₂ TSE images obtained in the three anatomical planes before buscopan injection were used to localize the uterus in the pelvis and to ensure that the uterus was within normal limits (no congenital or acquired uterine abnormalities; assessed by a radiologist). The corpus and cervix sizes latero-lateral (transverse) (LL) were measured on the coronal image (figure 1C). The T₂ TSE sagittal images after buscopan injection with and without fat suppression were compared and used to measure the following parameters: corpus and cervix length, antero-posterior (AP) uterus size (figure 1A), JZ and outer myometrium thickness at six different locations in the uterine wall. The six locations at which the JZ and myometrium thickness were measured are the uterine anterior and posterior wall at the level of the isthmus,

the middle (midcorpus) and the fundus (figure 1B). According to this method, both the uterine anterior and posterior wall were divided into three parts equally in length. Subsequently, the JZ and outer myometrial thickness were measured at a central point in each part.

The ratio of the JZ thickness to total myometrial thickness was measured by dividing the thickness of the JZ and the corresponding thickness of the total myometrium at the same location (JZ thickness/ (JZ thickness + outer myometrial thickness)).

Fig. 1

Uterine measurement parameters.

A and B. On the T₂-weighted turbo spin echo (T₂ TSE) sagittal MR image after buscopan injection without fat suppression, the junctional zone (JZ) thickness and the thickness of the outer myometrium (OM) [A] were measured at the level of the isthmus (I), the midcorpus (M) and the fundus (F) of the uterine anterior and posterior wall [B]. On this image, the antero-posterior (AP) size of the corpus was also determined.

C. The latero-lateral (LL) size of the corpus was measured on the coronal T2-weighted MR image obtained before buscopan injection.

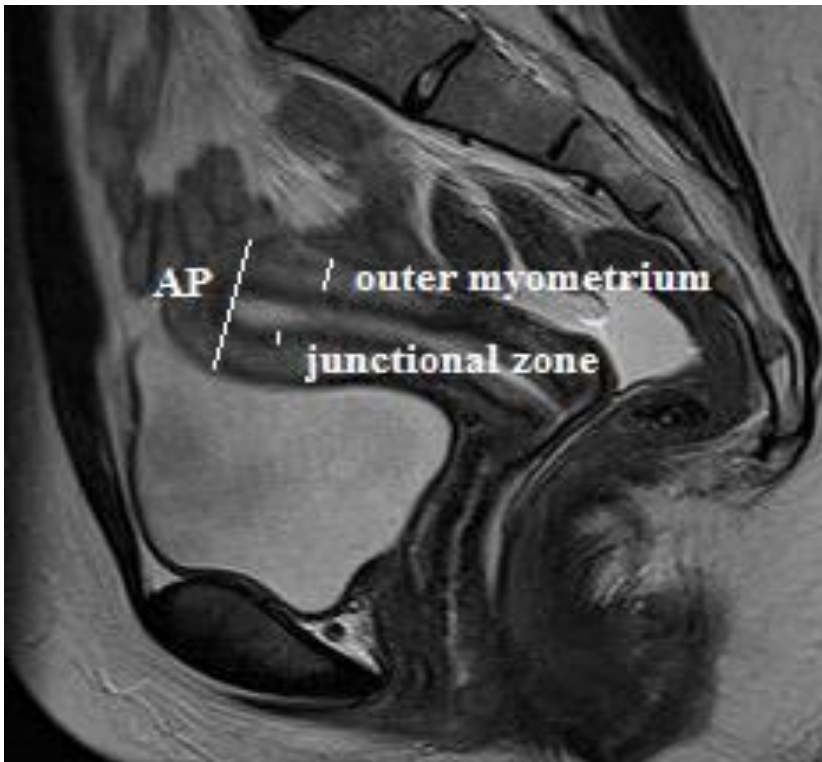


Fig. 1A

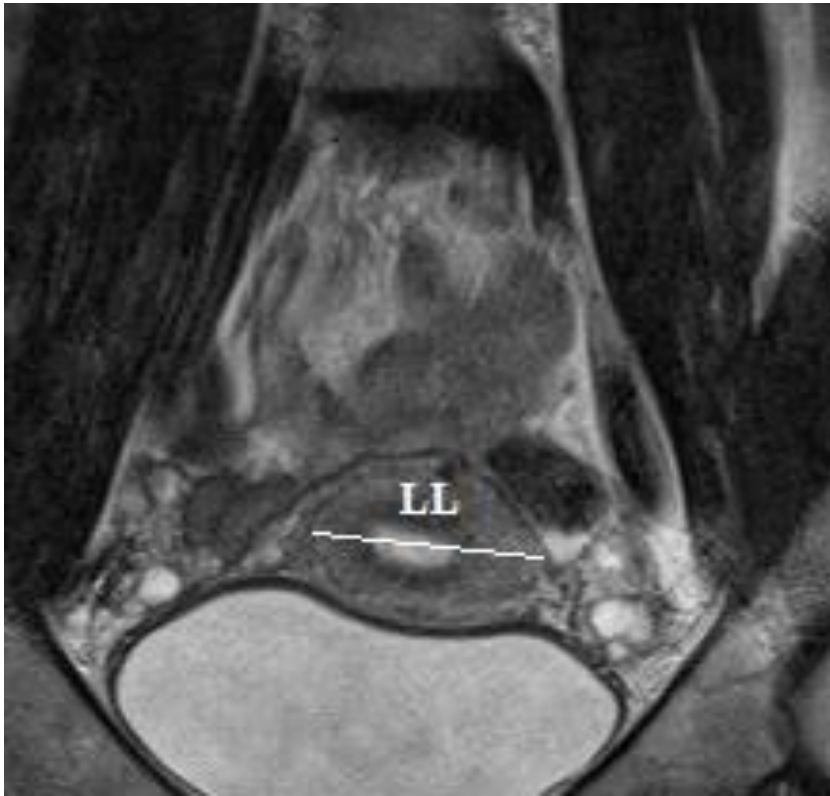


Fig. 1B

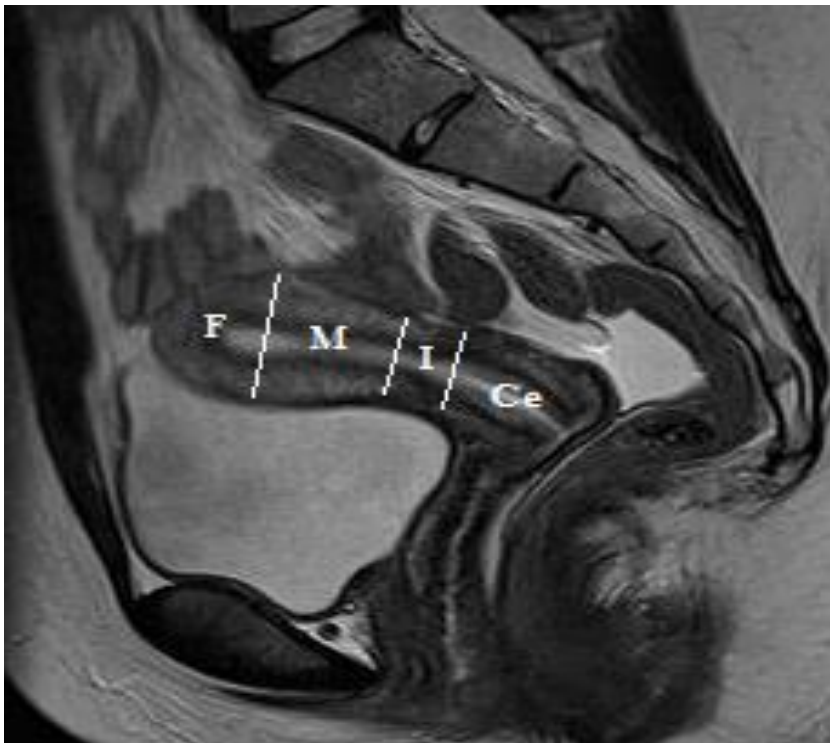


Fig. 1C

2.3.5 *Statistical analysis*

The volume of the corpus uteri (used to detect correlations with the JZ or outer myometrial thickness) was calculated using the formula: length x height (AP) x width (LL) x 0.523 (Goldstein et al., 1988).

All statistical analyses were performed by means of the computer program SAS version 9.4. A 5% level of significance is used. No correction for multiple testing was applied.

Inter-observer statistics was performed for the consistency in measurements by means of the informal Bland-Altman test (Bland JM and Altman, 1986; Altman DG, 1991).

Linear mixed models were used in order to investigate the effect of hormonal contraception, the effect of menstrual phase (for woman not using hormonal contraception) and the effect of the location in the uterine wall on the JZ thickness, on the outer myometrial thickness, and on the ratio of JZ versus total myometrial thickness. The statistical model includes two main fixed effects and their interaction. The first fixed effect combines the use of hormonal contraception and the menstrual phase. This fixed effects has four levels, i.e. phase 1 for non-users, phase 2 for non-users, phase 3 for non-users, and users of hormonal contraception. This effect allows the comparison of (1) users and non-users (per menstrual phase for the non-users or averaged over the three menstrual phases for the non-users) and (2) the different menstrual phases for the non-users of hormonal contraception. The second fixed effect is the location in the uterine wall. The association between measurements of the same woman (e.g. JZ thickness measured in the three menstrual phases) is incorporated by means of a random intercept at woman level. A parsimonious model is obtained by backward elimination of the fixed effects terms not statistically significant at a 5% level of significance. In order to normalize the data, statistical analyses were performed on the natural log transformed outcome data.

2.3 Results

The T₂ TSE sagittal MR images after buscopan injection without fat suppression provided the best delineation of the JZ compared to the images with fat suppression. Therefore, we used the MRI images without fat suppression to perform the thickness measurements at the different locations of the uterine wall.

The informal Bland-Altman test showed no significant differences between the measurements of the two investigators, as the kappa value equaled 0.87. The data of the JZ thickness, outer myometrium thickness and ratio of JZ to total myometrium thickness (mean, minimum and maximum) at the six different locations in the uterus are presented in figure 2, 3 and 4 respectively.

No statistical correlations were found between JZ thickness and other parameters such as uterus volume, height and weight of the women, age at menarche and smoker status.

The mean JZ thickness of the non-users of contraception, averaged over all locations, was 3.2 mm during the follicular phase, 3.0 mm during the ovulatory phase and 3.1 mm during the luteal phase. The users of contraception had a mean JZ thickness of 2.7 mm.

According to the linear mixed model analysis comparing the non-users and users of hormonal contraception, the effect of menstrual phase on the JZ thickness in the non-users was dependent upon the uterine wall location and vice versa. The JZ thickness in the users of hormonal contraception was significantly thinner compared to the JZ of the non-users at both the anterior and posterior wall of the midcorpus during each menstrual phase ($p = 0.0123$, $p = 0.0458$ and $p = 0.0356$, for respectively the follicular, ovulatory and luteal phase in the anterior wall of the midcorpus; and $p = 0.0108$, $p = 0.0089$ and $p = 0.0280$, for respectively the follicular, ovulatory and luteal phase in the posterior wall of the midcorpus). The JZ thickness was also thinner in the users at the fundus in the anterior wall during the follicular and luteal phase ($p = 0.0105$ and $p = 0.0261$, respectively) and at the fundus in the posterior wall during the follicular phase ($p = 0.0377$). Furthermore, a trend towards a thinner JZ was noticed in the

users of contraception compared to the non-users of hormonal contraception at the anterior wall of the fundus during the ovulatory phase ($p = 0.0613$) and at the posterior fundus wall during the ovulatory and luteal phase ($p = 0.0597$ and $p = 0.0823$, respectively).

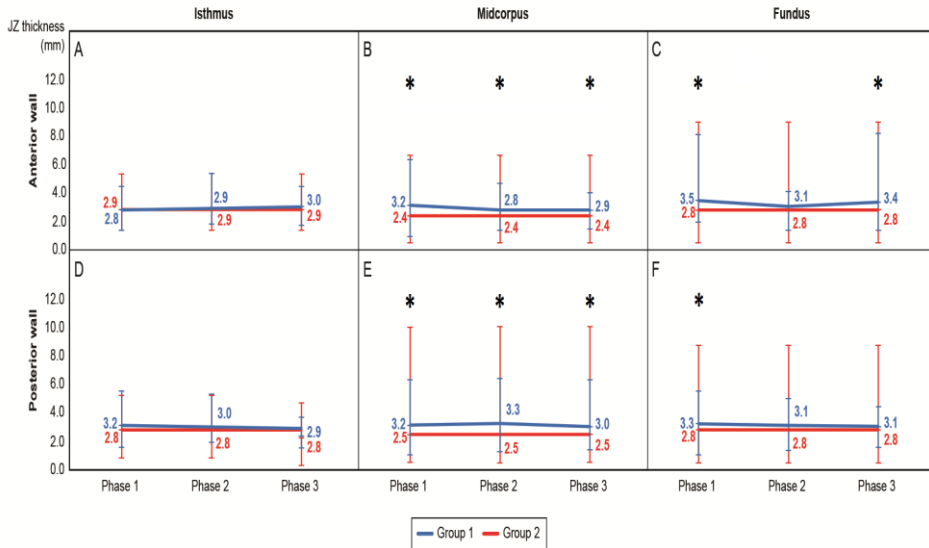


Fig. 2: Junctional Zone (JZ) thickness of healthy nulliparous non-users and users of hormonal contraception. The minimum, maximum and mean JZ thickness measurements are represented at 6 locations in the uterine wall, in the follicular phase (phase 1), ovulatory phase (phase 2) and luteal phase (phase 3) of non-users (group 1) and users (group 2) of hormonal contraception. * : $p < 0.05$ between the non-users and users of hormonal contraception, NS: $p < 0.1$ between the non-users and users of hormonal contraception.

In non-users, no differences were observed by comparing the JZ thickness during the different menstrual phases. In this group, the JZ thickness was also not significantly different between the anterior and posterior wall, nor between the isthmus, midcorpus and fundus.

In the non-users of contraception, the thickest mean JZ (3.5 mm) was measured in the anterior uterine wall at the level of the fundus during the follicular phase.

The mean outer myometrial thickness, averaged over all measured uterine locations, was 8.1 mm, 8.0 mm and 8.5 mm respectively during the follicular,

ovulatory and luteal phase in the non-users of hormonal contraception, whereas this thickness in the users of hormonal contraception equaled 8.4 mm. The thickness of the outer myometrium was not significantly different between both groups, nor between the menstrual phases in the non-users of hormonal contraception. However, the outer myometrial thickness differed depending on the location in the uterine wall. In the non-users of hormonal contraception, a significantly thicker outer myometrium was observed at the anterior and posterior wall of the midcorpus and fundus compared to the anterior and posterior wall of the isthmus ($p < 0.0001$, for all comparisons).

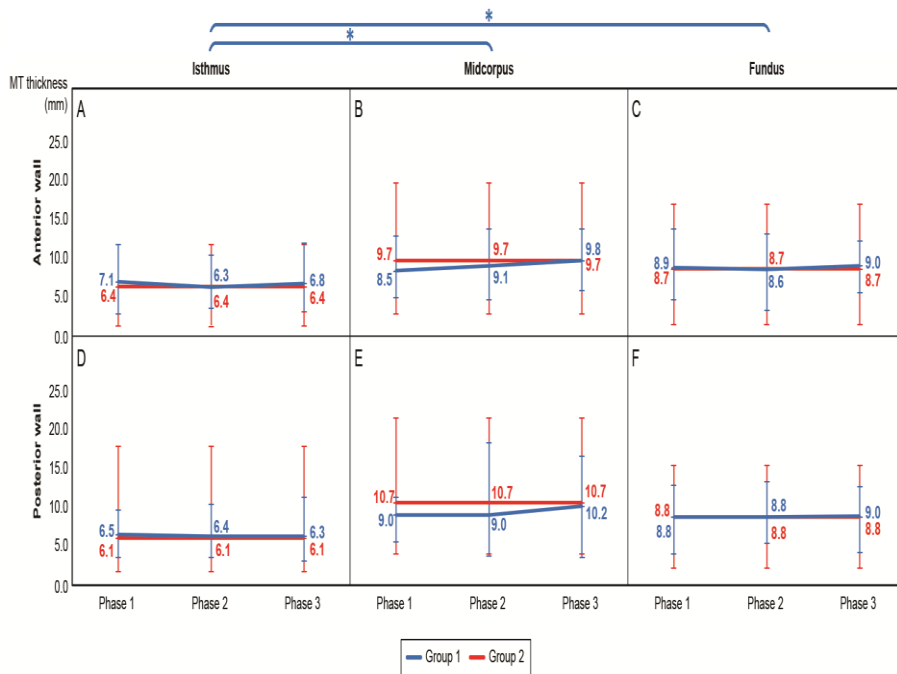


Fig. 3: Myometrial (MT) thickness of healthy nulliparous non-users and users of hormonal contraception. The minimum, maximum and mean MT thickness measurements are represented at 6 locations in the uterine wall, in the follicular phase (phase 1), ovulatory phase (phase 2) and luteal phase (phase 3) of non-users (group 1) and users (group 2) of hormonal contraception. * (blue): $p < 0.05$ between the locations in the uterine wall (both anterior and posterior wall) for the non-users of hormonal contraception.

The mean ratio of JZ versus total myometrial thickness averaged over all measured sites in the uterus was 29% during the follicular and ovulatory phase and 28% during the luteal phase of the non-users of contraception, whereas this mean ratio numbered 26% in the contraception using group. Similarly as with the JZ thickness, by comparing both groups, the effect of the menstrual phase of the non-users of hormonal contraception on the ratio varies according to the location in the uterine wall and vice versa. The ratio of JZ to total myometrial thickness was significantly lower in the users of hormonal contraception compared to the non-users of hormonal contraception at the anterior midcorpus during the follicular phase ($p = 0.0136$) and at the posterior midcorpus during the follicular ($p = 0.0052$), ovulatory ($p = 0.0032$) and luteal phase ($p = 0.0322$). A trend towards a lower ratio was observed in the users of hormonal contraception in comparison to the non-users at the anterior midcorpus during the ovulatory ($p = 0.0568$) and luteal ($p = 0.0996$) phase, at the anterior fundus during the follicular ($p = 0.0517$) and ovulatory ($p = 0.0900$) phase and at the posterior fundus during the follicular phase ($p = 0.0856$). This ratio was not significantly affected by the menstrual phase in the non-users of hormonal contraception.

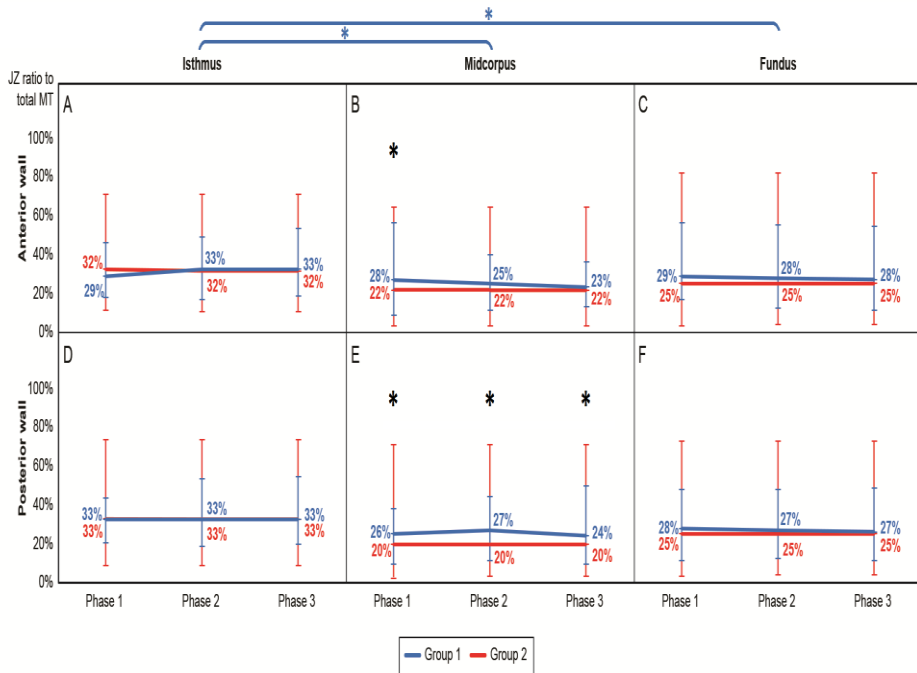


Fig. 4: The ratio of junctional zone thickness versus total myometrial thickness of healthy nulliparous non-users and users of hormonal contraception. The minimum, maximum and mean ratios are represented at 6 locations in the uterine wall, in the follicular phase (phase 1), ovulatory phase (phase 2) and luteal phase (phase 3) of non-users (group 1) and users (group 2) of hormonal contraception. * (black): $p < 0.05$ between the non-users and users of hormonal contraception, NS: $p < 0.1$ between the non-users and users of hormonal contraception, * (blue): $p < 0.05$ between the locations in the uterine wall (both anterior and posterior wall) for the non-users of hormonal contraception.

Furthermore, the ratio of JZ versus total myometrial thickness was dependent upon the site in the uterine wall where the thicknesses were measured. This ratio in the non-users of contraception at the anterior and posterior wall of the isthmus was significantly higher compared to the anterior and posterior wall of the midcorpus ($p = 0.0004$ and $p = 0.0011$, respectively for the anterior isthmus and $p < 0.0001$ and $p < 0.0001$ for the posterior isthmus) and the anterior and posterior wall of the fundus ($p = 0.0454$ and $p = 0.0210$, respectively for the anterior isthmus and $p = 0.0051$ and $p = 0.0021$, respectively for the posterior isthmus).

2.4 Discussion

In order to be able to diagnose JZ adenomyosis or to assess JZ thickness in infertility workup, one must know the normal values of the JZ thickness. As mentioned above, it is clear that age, the use of hormonal contraceptives, the exact location of the measurement in the uterine wall and the medical history of the women are all features which need to be considered in evaluating the thickness of the JZ (Devlieger et al., 2003; Garavaglia et al., 2015; Hauth et al., 2007; Noe et al., 1999). This study was designed and performed in order to determine the best menstrual phase and uterine wall location to measure the thickest JZ on MRI examinations. We prospectively investigated the JZ thickness, outer myometrial thickness and the ratio of JZ versus total myometrial thickness in 47 healthy nulliparous women between the age of 19 and 35 years on T₂ images acquired on a 1.5T MRI (a total of 133 MRI examinations). These women were subdivided based on the hormonal contraception status. To our knowledge, this study is the first in literature to perform MRI examinations during three menstrual phases in the same woman in a group of women between the age of 19 and 35 years.

2.4.1 Normal JZ thickness and ratio as a function of the menstrual cycle and uterine location

Our results revealed in non-users that the menstrual phase nor the uterine wall location affected the JZ thickness significantly. However, the outer myometrial thickness and the ratio of JZ versus total myometrial thickness were dependent on the location in the uterine wall, and not on the menstrual phase. This thickness and ratio were significantly lower at the midcorpus and fundus in both the anterior and posterior wall. The thickest mean JZ was measured at the anterior fundal wall during the follicular phase. The mean thickness in this phase and location equaled 3.5 mm, with a ratio of 29% to the total myometrial thickness. During the evaluation of the MR images, we noticed empirically that the JZ thickness measurements at the anterior wall of the fundus and midcorpus has the benefit of minimal bowel movement artefacts. Another advantage of the fundal site is its direct relation to fertility, namely the integral part in embryo implantation.

Our findings concerning the JZ thicknesses are consistent with previous studies which assume the normal JZ to be 5-8 mm in thickness (Hauth et al., 2007; Kunz et al., 2000a; Novellas et al., 2011). The group of Hauth et al. (2007) evaluated the normal thickness of different uterine wall layers (endometrium, JZ and outer myometrium) in 100 women (47 women with and 53 women without adenomyosis and/or myomas with age between 20 and 80 years) as a function of age and menstrual cycle phase. They noticed an increase in JZ thickness until the age of 41-50 years, followed by a decrease in thickness. The mean JZ thickness in a similar group as this study of 16 healthy women without adenomyosis and myomas between the age of 20 and 30 years was 5 mm and a mean thickness of the myometrium was 10 mm. They did also not observe a significant difference in the JZ thickness between the women who were in the follicular and those who were in the luteal phase. Different to our study was that they used MR images with 8 mm slice thickness (4 mm was used in our study) and they did not compare the JZ thickness within the menstrual cycle of each women.

The JZ thickness and the ratio in the non-users of hormonal contraception did not differ significantly between the three menstrual phases. This is consistent with previous studies, where also no significant changes in JZ thickness between the follicular phase and luteal phase have been reported (Hauth et al, 2007; McCarthy et al, 1986).

2.4.2 Normal JZ thickness and ratio as a function of the use hormonal contraception

The users of contraception revealed a statistically significant thinner JZ than the non-users at both the anterior and posterior wall of the midcorpus and fundus. Furthermore, in the non-users, the ratio of JZ to total myometrial thickness was significantly higher at the anterior and posterior wall of the midcorpus and fundus compared to the anterior and posterior wall of the isthmus. The use of hormonal contraception significantly lowered this ratio at the midcorpus in both the anterior and posterior wall and at the fundus in the anterior wall. The

significant lower ratio in the hormonal contraception users can be explained by the significantly thinner JZ measured at these locations in those women.

Our findings are in line with previous results including those by McCarthy et al. (1986) and Kido et al. (2005). McCarthy et al. also indicated that the JZ thickness was significantly smaller in the pill-using group (9 subjects) than in the non-pill-using group (12 subjects) ($p < 0.005$). Kido et al. reported a significantly thinner JZ in the posterior uterine wall in women who use oral contraceptives (23 women) in comparison to women who did not use oral contraceptives (15 women) at mid-cycle (day 11-15 in the non-users of oral contraceptives and day 11-13 in the users of oral contraceptives). He and his colleagues also observed a markedly suppressed uterine peristalsis in oral contraceptives users which could contribute to the prevention of conception by disturbing the upward sperm transport. This finding of a thinner JZ in the users of hormonal contraception suggests that the thickness of the JZ at the midcorpus and fundus can be involved in the prevention of conception.

Our findings concerning the JZ ratio to total myometrial thickness were in concordance with the findings of Kido et al. (2005), who also found a significantly lower ratio of JZ thickness versus myometrium thickness in the oral contraceptive users than in the non-users of oral contraceptives in both the anterior and posterior uterine wall.

2.4.3 The normal limits of JZ thickness in healthy women

In literature, disagreement exists in defining a clear threshold for the maximum JZ thickness in order to declare it within normal limits. Previous research revealed that JZ adenomyosis can be diagnosed by MRI when a JZ thickness of 12 mm or higher is measured, whereas a JZ thickness of lower than 8 mm excludes adenomyosis (Kang et al., 1996; Kissler et al., 2008; Novellas et al., 2011, Reinhold et al. 1996). When the measured thickness is within 8-12 mm, the diagnosis of adenomyosis requires specific secondary criteria such as relative thickening of the JZ in a localized area, poor definition of the borders of the JZ or high signal intensity foci (Reinhold et al., 1998, 1999). However, according to Bazot et al., the threshold of 12 mm carries a sensitivity of only 63% (2001).

Kunz et al. (2005) investigated the impact of adenomyosis associated with endometriosis on fertility and determined a maximal diameter of 10 mm in a healthy control group (age between 21-46 years) as a cut-off value beyond which adenomyosis was assumed. He and his colleagues showed a statistically significant difference in the posterior wall JZ thickness between healthy women and women with known endometriosis (as there is evidence of high association between adenomyosis and endometriosis).

Our study, performed in 47 young healthy women between 19 and 35 years old, measured a maximum JZ thickness of 10.1 mm in a total of 133 MRI examinations across different menstrual phases and contraception and non-contraception users.

Reinhold et al. (1996) and Bazot et al. (2001) introduced the JZ to total myometrial thickness ratio, measured at the same place in the uterine wall. This ratio gives additional information about the JZ thickness, more specifically about the relationship between JZ and the total myometrial zone. The ratio of these two parameters can also be considered in the diagnosis of adenomyosis, as a ratio higher than 40% is one of the specific MRI criteria for diagnosing the condition. Reinhold et al. found a significant difference in this ratio between patients with adenomyosis (69%) and a control group (44%) (Reinhold et al, 1996). Bazot et al. concluded that a ratio higher than 40% allows a diagnosis of adenomyosis with a sensitivity of 65% and a specificity of 92% (Bazot et al, 2001). The results obtained for the ratio in this study also fit this criteria. A maximum ratio of 33% was observed, which is clearly below the defined threshold of 40%.

The limitation of our study is the low number of participating nulliparous non-users of hormonal contraception. Despite the low number of subjects, these findings are useful to contribute to uniform future measurements of the JZ thickness.

2.5 Conclusion

To conclude, the present MRI study in nulliparous women demonstrated that JZ thickness is statistically significant affected by the use of hormonal contraception, not by the uterine wall location or the menstrual phase. A statistically significant thinner JZ was observed in users of contraception in comparison to non-users at the anterior and posterior uterine wall at the level of the fundus and midcorpus. However, in contrast to the junctional zone thickness, the outer myometrial thickness varied according to the location in the uterine wall. A thicker outer myometrium was noticed at the level of the fundus and midcorpus. These differences observed in thickness of the JZ and the outer myometrium were reflected in the ratio of JZ versus total myometrial thickness, as it demonstrated differences between both groups and between uterine wall locations. We do recommend to perform the measurements of JZ thickness at the level of the midcorpus and fundus.

2.6 References

1. Absenger Y, Hess-Stumpp H, Kreft B, Krätzschar J, Haendler B, Schütze N, Regidor PA, Winterhager E (2004) Cyr61, a deregulated gene in endometriosis. *Mol Hum Reprod* 10:399-407. doi: 10.1093/molehr/gah053.
2. Adamson GD, Pasta DJ (1994) Surgical treatment of endometriosis-associated infertility: meta-analysis compared with survival analysis. *Am J Obstet Gynecol* 171:1488-1504; discussion 1504-148.
3. Altman D (1991) *Practical statistics for medical research*. London: Chapman and Hall. In.
4. Barrier BF, Malinowski MJ, Dick EJ, Hubbard GB, Bates GW (2004) Adenomyosis in the baboon is associated with primary infertility. *Fertil Steril* 82 Suppl 3:1091-1094. doi: 10.1016/j.fertnstert.2003.11.065.
5. Bazot M, Cortez A, Darai E, Rouger J, Chopier J, Antoine JM, Uzan S (2001) Ultrasonography compared with magnetic resonance imaging for the diagnosis of adenomyosis: correlation with histopathology. *Hum Reprod* 16:2427-2433.
6. Bland JM, Altman DG (1986) Statistical methods for assessing agreement between two methods of clinical measurement. *Lancet* 1:307-310.
7. Cicinelli E, Einer-Jensen N, Cignarelli M, Mangiacotti L, Luisi D, Schonauer S (2004) Preferential transfer of endogenous ovarian steroid hormones to the uterus during both the follicular and luteal phases. *Hum Reprod* 19:2001-2004. doi: 10.1093/humrep/deh404.
8. de Souza NM, Brosens JJ, Schwieso JE, Paraschos T, Winston RM (1995) The potential value of magnetic resonance imaging in infertility. *Clin Radiol* 50:75-79.

9. Devlieger R, D'Hooghe T, Timmerman D (2003) Uterine adenomyosis in the infertility clinic. *Hum Reprod Update* 9:139-147.
10. Fujimoto K, Nakai A, Okada T, Ikeuchi T, Satogami N, Daido S, Yakami M, Togashi K (2010) Effect of hyoscine butylbromide (HBB) on the uterine corpus: quantitative assessment with T2-weighted (T2W) MRI in healthy volunteers. *J Magn Reson Imaging* 32:441-445. doi: 10.1002/jmri.22252.
11. Fusi L, Cloke B, Brosens JJ (2006) The uterine junctional zone. *Best Pract Res Clin Obstet Gynaecol* 20:479-491. doi: 10.1016/j.bpobgyn.2006.02.001.
12. Garavaglia E, Audrey S, Annalisa I, Stefano F, Iacopo T, Laura C, Massimo C (2015) Adenomyosis and its impact on women fertility. *Iran J Reprod Med* 13:327-336.
13. Goldstein SR, Horii SC, Snyder JR, Raghavendra BN, Subramanyam B (1988) Estimation of nongravid uterine volume based on a nomogram of gravid uterine volume: its value in gynecologic uterine abnormalities. *Obstet Gynecol* 72:86-90.
14. Hauth EA, Jaeger HJ, Libera H, Lange S, Forsting M (2007) MR imaging of the uterus and cervix in healthy women: determination of normal values. *Eur Radiol* 17:734-742. doi: 10.1007/s00330-006-0313-3.
15. Hricak H (1994) [Magnetic resonance imaging of the female pelvis]. *Lijec Vjesn* 116:149-154.
16. Kang S, Turner DA, Foster GS, Rapoport MI, Spencer SA, Wang JZ (1996) Adenomyosis: specificity of 5 mm as the maximum normal uterine junctional zone thickness in MR images. *AJR Am J Roentgenol* 166:1145-1150. doi: 10.2214/ajr.166.5.8615259.

17. Kido A, Togashi K, Nakai A, Kataoka ML, Koyama T, Fujii S (2005) Oral contraceptives and uterine peristalsis: evaluation with MRI. *J Magn Reson Imaging* 22:265-270. doi: 10.1002/jmri.20384.
18. Kissler S, Zangos S, Kohl J, Wiegratz I, Rody A, Gätje R, Vogl TJ, Kunz G, Leyendecker G, Kaufmann M (2008) Duration of dysmenorrhoea and extent of adenomyosis visualised by magnetic resonance imaging. *Eur J Obstet Gynecol Reprod Biol* 137:204-209. doi: 10.1016/j.ejogrb.2007.01.015.
19. Kunz G, Beil D, Deininger H, Wildt L, Leyendecker G (1996) The dynamics of rapid sperm transport through the female genital tract: evidence from vaginal sonography of uterine peristalsis and hysterosalpingoscintigraphy. *Hum Reprod* 11:627-632.
20. Kunz G, Beil D, Huppert P, Leyendecker G (2000) Structural abnormalities of the uterine wall in women with endometriosis and infertility visualized by vaginal sonography and magnetic resonance imaging. *Hum Reprod* 15:76-82.
21. Kunz G, Beil D, Huppert P, Noe M, Kissler S, Leyendecker G (2005) Adenomyosis in endometriosis--prevalence and impact on fertility. Evidence from magnetic resonance imaging. *Hum Reprod* 20:2309-2316. doi: 10.1093/humrep/dei021.
22. Kunz G, Kissler S, Wildt L (2000) Uterine peristalsis: directed sperm transport and fundal implantation of the blastocyst. In Felicori M (ed.) *Endocrine Basis of Reproductive Function*; Bologna, Italy; 409-422. In.
23. Leyendecker G (2000) Redefining endometriosis: endometriosis is an entity with extreme pleiomorphism. *Hum Reprod* 15:4-7.

24. Leyendecker G, Bilgicyildirim A, Inacker M, Stalf T, Huppert P, Mall G, Böttcher B, Wildt L (2015) Adenomyosis and endometriosis. Re-visiting their association and further insights into the mechanisms of auto-traumatisation. An MRI study. *Arch Gynecol Obstet* 291:917-932. doi: 10.1007/s00404-014-3437-8.
25. Leyendecker G, Herbertz M, Kunz G, Mall G (2002) Endometriosis results from the dislocation of basal endometrium. *Hum Reprod* 17:2725-2736.
26. Leyendecker G, Kunz G, Herbertz M, Beil D, Huppert P, Mall G, Kissler S, Noe M, Wildt L (2004) Uterine peristaltic activity and the development of endometriosis. *Ann N Y Acad Sci* 1034:338-355. doi: 10.1196/annals.1335.036.
27. Leyendecker G, Kunz G, Noe M, Herbertz M, Mall G (1998) Endometriosis: a dysfunction and disease of the archimetra. *Hum Reprod Update* 4:752-762.
28. Leyendecker G, Kunz G, Wildt L, Beil D, Deininger H (1996) Uterine hyperperistalsis and dysperistalsis as dysfunctions of the mechanism of rapid sperm transport in patients with endometriosis and infertility. *Hum Reprod* 11:1542-1551.
29. Lyons EA, Taylor PJ, Zheng XH, Ballard G, Levi CS, Kredentser JV (1991) Characterization of subendometrial myometrial contractions throughout the menstrual cycle in normal fertile women. *Fertil Steril* 55:771-774.
30. Maubon A, Faury A, Kapella M, Pouquet M, Piver P (2010) Uterine junctional zone at magnetic resonance imaging: a predictor of in vitro fertilization implantation failure. *J Obstet Gynaecol Res* 36:611-618. doi: 10.1111/j.1447-0756.2010.01189.
31. McCarthy S, Scott G, Majumdar S, Shapiro B, Thompson S, Lange R, Gore J (1989) Uterine junctional zone: MR study of water content and relaxation properties. *Radiology* 171:241-243. doi: 10.1148/radiology.171.1.2928531.

32. McCarthy S, Tauber C, Gore J (1986) Female pelvic anatomy: MR assessment of variations during the menstrual cycle and with use of oral contraceptives. *Radiology* 160:119-123. doi: 10.1148/radiology.160.1.3715022.
33. Noe M, Kunz G, Herbertz M, Mall G, Leyendecker G (1999) The cyclic pattern of the immunocytochemical expression of oestrogen and progesterone receptors in human myometrial and endometrial layers: characterization of the endometrial-subendometrial unit. *Hum Reprod* 14:190-197.
34. Novellas S, Chassang M, Delotte J, Toullalan O, Chevallier A, Bouaziz J, Chevallier P (2011) MRI characteristics of the uterine junctional zone: from normal to the diagnosis of adenomyosis. *AJR Am J Roentgenol* 196:1206-1213. doi: 10.2214/AJR.10.4877.
35. Piver P (2005) [Uterine factors limiting ART coverage]. *J Gynecol Obstet Biol Reprod (Paris)* 34:5S30-35S33.
36. Reinhold C, McCarthy S, Bret PM, Mehio A, Atri M, Zakarian R, Glaude Y, Liang L, Seymour RJ (1996) Diffuse adenomyosis: comparison of endovaginal US and MR imaging with histopathologic correlation. *Radiology* 199:151-158. doi: 10.1148/radiology.199.1.8633139.
37. Reinhold C, Tafazoli F, Mehio A, Wang L, Atri M, Siegelman ES, Rohoman L (1999) Uterine adenomyosis: endovaginal US and MR imaging features with histopathologic correlation. *Radiographics* 19 Spec No:S147-160. doi: 10.1148/radiographics.19.suppl_1.g99oc13s147.
38. Reinhold C, Tafazoli F, Wang L (1998) Imaging features of adenomyosis. *Hum Reprod Update* 4:337-349.

39. Scoult LM, Flynn SD, Luthringer DJ, McCauley TR, McCarthy SM (1991) Junctional zone of the uterus: correlation of MR imaging and histologic examination of hysterectomy specimens. *Radiology* 179:403-407. doi: 10.1148/radiology.179.2.2014282.
40. Takahashi K, Nagata H, Kitao M (1989) Clinical usefulness of determination of estradiol level in the menstrual blood for patients with endometriosis. *Nihon Sanka Fujinka Gakkai Zasshi* 41:1849-1850.
41. Werth R, Grudew W (1989) Untersuchungen über die Entwicklung und Morphologie der menschlichen Uterusmuskulatur. *Arch Gynakol* 55: 325-409. In.
42. Wetzstein R (1965) Der Uterusmuskel: Morphologie 202:1-13. In.
43. Wiczak HP, Janus CL, Richards CJ, Graf MJ, Gendal ES, Rabinowitz JG, Laufer N (1988) Comparison of magnetic resonance imaging and ultrasound in evaluating follicular and endometrial development throughout the normal cycle. *Fertil Steril* 49:969-972.
44. Wildt L, Kissler S, Licht P, Becker W (1998) Sperm transport in the human female genital tract and its modulation by oxytocin as assessed by hysterosalpingoscintigraphy, hysteronography, electrohysterography and Doppler sonography. *Hum Reprod Update* 4:655-666.

3. CHAPTER III: UTERINE JUNCTIONAL ZONE THICKNESS IN INFERTILE WOMEN EVALUATED BY MRI

J Magn Reson Imaging. 2017 Mar;45(3):926-936.

3.1 Abstract

Purpose: To prospectively evaluate and compare the junctional zone (JZ) and outer myometrial thickness in infertile and healthy nulliparous women at different locations in the uterine wall during the menstrual cycle by magnetic resonance imaging (MRI).

Material and methods: We performed pelvic 1.5T MRI (T_2 -weighted turbo spin echo sequences) on 28 infertile women: 5 with infertility of unknown origin, 12 anovulating and 11 on ovarian stimulation therapy (mean age 28.5, 30.8 and 29.3 years, respectively); and a control group consisting of 18 healthy nulliparous volunteers (mean age 26.4 years). The women with unknown infertility origin and the control group underwent MRI investigations during their follicular, ovulatory and luteal phase. The JZ and outer myometrial thicknesses were measured at six locations in the uterine wall: anterior and posterior wall of the isthmus, midcorpus and fundus.

Results: The JZ in the anovulating women at the posterior wall of the isthmus (4.2 mm) was significantly thicker compared to the control group (3.2, 3.0 and 2.9 mm, in respectively the three menstrual phases) ($p=0.027$).

The outer myometrium in the anovulating women was significantly thicker at all measured locations (average 11.5 mm) in comparison to the control group (8.1, 8.0 and 8.5 mm, in respectively the three menstrual phases) ($p<0.050$). The infertile women on ovarian stimulation therapy showed a significantly thicker outer myometrium at the anterior wall (isthmus, midcorpus and fundus) ($p<0.050$).

Conclusion: The results indicate that a thickened JZ, and especially a thickened outer myometrium might be associated with infertility.

KEYWORDS: Junctional Zone – Myometrium - Thickness - Infertility – Magnetic Resonance Imaging

3.2 Introduction

Infertility has a prevalence of 14% in the general population (1,2). A female underlying cause is involved in about two-thirds of cases. In 15-30% of infertile couples, the underlying cause of infertility is not identified after completion of standard fertility tests (e.g. tests to investigate ovulatory disorders, tubal damage, uterine or peritoneal problems and male factors) (2).

The uterine junctional zone (JZ) plays an integral part in many reproductive functions (3). The JZ, also called the archimyometrium or the stratum subvasculare, is the inner third of the myometrium and is hence located at the interface between endometrial mucosa and outer myometrium (3). It is a hormone dependent structure represented by the presence of cyclic changes in immunoreactive estrogen and progesterone receptor expression throughout the menstrual cycle comparable with the changes observed in the endometrium (3,4).

The major function of the JZ during the reproductive period of women is directing sperm transport into the tube ipsilateral to the dominant follicle, which is provided by JZ uterine peristalsis (5-7). Furthermore, it is proven that an optimal JZ thickness is important in embryo implantation. Maubon et al. (8) and Piver (9) showed that a thickened uterine JZ on magnetic resonance imaging (MRI) is a failure predictive factor for embryo implantation in *in vitro* fertilization (IVF) attempts. They both showed a pregnancy failure rate of more than 74% if the average JZ thickness was > 7 mm or if the maximal JZ thickness was > 10 mm.

Thus there might be an association between abnormalities of the JZ and sub- or infertility. Several studies have reported a link between infertility and various gynecological disorders involving the JZ, such as adenomyosis, endometriosis and leiomyomas (10-12). Despite these associations, the exact role of this zone in infertility is still unclear.

The standard imaging method to visualize the JZ and to discriminate it from the adjacent zones is pelvic MRI, as was first described by Hricak et al. (13). On T₂-

weighted MR images, the JZ is presented as a low signal-intensity zone sandwiched between the high signal-intensity endometrium and the medium signal-intensity outer myometrium (13-15).

The aim of the present study was to analyze and compare the JZ thickness, outer myometrial thickness and the ratio of JZ versus total myometrial thickness in healthy nulliparous women and in infertile women during their menstrual cycle and at different locations in the uterine wall by MRI. We hypothesized that the JZ is thicker in infertile women.

3.3 Material and Methods

The study protocol and informed consent were approved by the local hospital ethics committee (registration number 056).

3.3.1 Study population

In this prospective study, 18 healthy nulliparous volunteers and 28 infertile women were included over a recruitment period of 50 months (from December 2007 to January 2012). The healthy nulliparous volunteers had no history of infertility and were not taking hormonal contraception (control group, mean age 26.4 years). The healthy nulliparous women were recruited by contacting co-workers from our hospital, students and PhD students from the local university, personal contacts and by cooperation with external physicians. The infertile patients were referred for participation in this study by our hospital infertility center. Exclusion criteria were age less than 18 years or more than 35 years, non-Caucasian origin, women with a pacemaker, clips or other MRI-incompatible implanted devices, pregnancy, diminished renal function (assessed by creatinine levels collected prior to MRI investigation), medical history of infertility or a gynecological disorder such as a bleeding disorder or an irregular menstrual cycle (for the control group) and previous unknown uterine morphologic abnormality found on the first MRI examination. All women provided a written informed consent and filled out an epidemiological questionnaire in order to obtain information concerning their birth date, height, weight, age at menarche and whether or not they currently smoke.

The infertile patients were subdivided into three groups based on the underlying cause of their infertility and whether or not they were on ovarian stimulating therapy: 5 women with unexplained infertility (mean age 28.5 years), 12 anovulating women (mean age 30.8 years) and 11 women on ovarian stimulation therapy (table 1) (mean age 29.3 years).

Table 1: Types of ovarian stimulation therapy taken by the 11 infertile women at the time of MRI examination.

Patient	Ovarian stimulation therapy
1	clomiphene citrate
2	GnRH agonist (triptorelin), recombinant FSH (follitropin beta) and HCG
3	GnRH agonist (triptorelin), hMG and HCG
4	GnRH agonist (buserelin acetate) and recombinant FSH (follitropin beta)
5	clomiphene citrate, GnRH antagonist (ganirelix acetate) and recombinant FSH (follitropin alpha)
6 and 7	prostaglandin
8 and 9	GnRH antagonist (ganirelix acetate) and hMG
10 and 11	ethinylestradiol and gestodene

GnRH: gonadotropin releasing hormone; FSH: follicle stimulating hormone; HCG: human chorionic gonadotropin; hMG: human menopausal gonadotropin

3.3.2 Blood laboratory tests

Blood samples were collected prior to each MRI examination in order to assess the levels of human chorionic gonadotrophin (hCG), creatinine, follicle-stimulating hormone (FSH), luteinizing hormone (LH), estradiol and progesterone. The follicular phase was considered around day 6-13 of the menstrual cycle, the ovulatory phase around day 14-16 and the luteal phase around day 17-28. The exact phase of the menstrual cycle was determined based on the hormone levels.

3.3.3 Magnetic Resonance Imaging

The 18 healthy nulliparous women were scheduled to undergo MRI investigations during three phases of their menstrual cycle: follicular (n = 17), ovulatory (n = 17) and luteal (n = 16) phase. Due to practical considerations, one woman underwent MRI only during her follicular phase, one woman during her follicular and ovulatory phase and one woman during her ovulatory and luteal phase. This resulted in a total of 50 MRI examinations in the healthy nulliparous women. The five women with unexplained infertility were also subjected to MRI examinations during the follicular (n = 4), ovulatory (n = 3) and luteal (n = 5) phases. One woman underwent MRI only during her follicular and luteal phase and one woman only during her luteal phase, resulting in 12

MRI examinations in total. MRI was performed on a random day during the menstrual cycle for the anovulating women (n = 12) and for the infertile women who used ovarian stimulation therapy (n = 11) (figure 1).

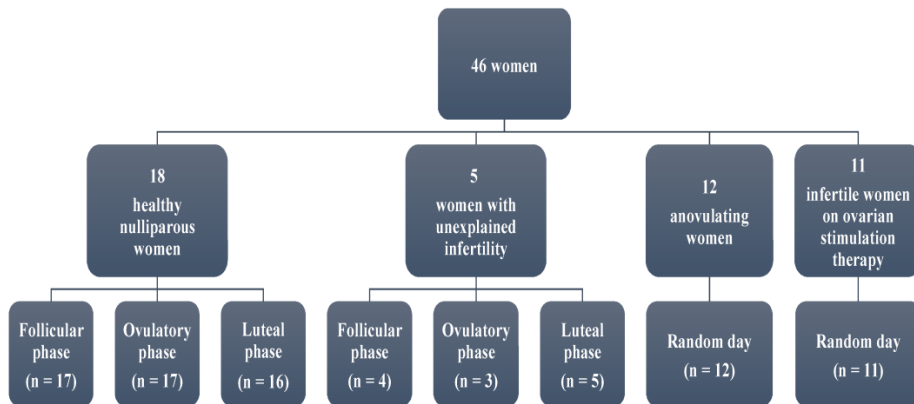


Figure 1: Overview of the study population and the menstrual phases during which MRI investigations were performed.

MRI investigations were obtained with a 1.5T magnet unit (Siemens Magnetom Symphony Tim (4G-Dot upgraded), Siemens, Erlangen, Germany; Software Syngo MR B15). An intravenous catheter was inserted in the elbow crease of the women before they were positioned in head first - supine position. An eight channel receive only body array was placed on the pelvis. T₂-weighted turbo spin echo (T₂ TSE) sequences in three different planes were acquired: transversal, coronal and sagittal plane (table 2). Then, in agreement with the woman, the abdominal-specific antispasmodic Hyoscine Butylbromide (buscopan, 1 ml, 20 mg/ml, Boehringer Ingelheim, Germany), diluted in sodium chloride (10 ml, 0.09%, Baxter, Lessines, Belgium) was manually injected in order to reduce bowel peristalsis. Afterwards, sagittal T₂ TSE images without fat suppression were obtained. All images were sent to a dedicated workstation.

Table 2: Overview of the MRI-scan parameters.

Parameters/Sequence	Localizer	T ₂ TSE	T ₂ TSE	T ₂ TSE	T ₂ TSE buscopan
Orientation	Sagittal	Transversal	Coronal	Sagittal	Sagittal
Repetition time (msec)	20	5100	5000	5000	4060
Time to echo (msec)	5	88	89	89	93
Field of view (mm)	400	370	320	340	360
Slice thickness (mm)	10	5	5	5	4
Flip angle (degrees)	40	180	180	180	180
Voxel size (mm x mm x mm)	3.1 x 1.6 x 10	1.1 x 0.8 x 5	0.8 x 0.6 x 5	0.9 x 0.7 x 5	0.9 x 0.7 x 4
Acquisition time (min.sec)	0.14	1.03	2.52	2.02	3.12
Fat suppression	-	-	-	-	-

T₂ TSE: T₂-weighted turbo spin echo sequences; T₂ TSE buscopan: T₂-weighted turbo spin echo sequences after manual injection of the antispasmodic agent buscopan.

3.3.4 MR image analysis

The measurements were performed on a specialized workstation (MMWP, Syngo MMWP VE36A) using the measuring cursor included in the workstation's software. All measurements were completed by two independent investigators, a radiologist with 13 years of experience in pelvic imaging and an intern in radiology with three years of pelvic MRI experience. Examinations were evaluated consecutively and both investigators were blinded for the clinical information of the women.

The T2 TSE images in transversal, coronal and sagittal plane before buscopan injection of the healthy nulliparous women were first analyzed by the radiologist in order to detect possible suspicious findings of congenital or acquired uterine abnormalities.

The corpus size latero-lateral (transverse or LL) was measured on the transversal T2 TSE image obtained before buscopan injection (figure 2A). The sagittal T2 TSE image after buscopan injection was used in order to measure the corpus length and the antero-posterior (AP) uterus size (figure 2B). The volume of the corpus uteri was subsequently calculated using the formula for an ellipsoid: length x height (AP) x width (LL) x 0.523 (16).

The sagittal T2 TSE image after buscopan injection was also used to measure the JZ and outer myometrial thickness at six different uterine wall locations. The six locations at which these thicknesses were measured are the anterior and posterior wall at the level of the isthmus, the middle (midcorpus) and the fundus (figure 2C and 2D). According to this method, both the anterior and posterior uterine wall were divided into three parts equally in length. Subsequently, the JZ and outer myometrial thickness were measured at the central point in each part. The ratio of JZ thickness versus total myometrial thickness was calculated as well. It was calculated by dividing the thickness of the JZ by the corresponding thickness of the total myometrium at the same location ($\text{ratio} = \text{JZ thickness} / (\text{JZ thickness} + \text{outer myometrial thickness})$). The average JZ thickness, outer myometrial thickness and ratio of JZ versus total myometrial thickness were calculated as the average of the six measurements of every women in the group.

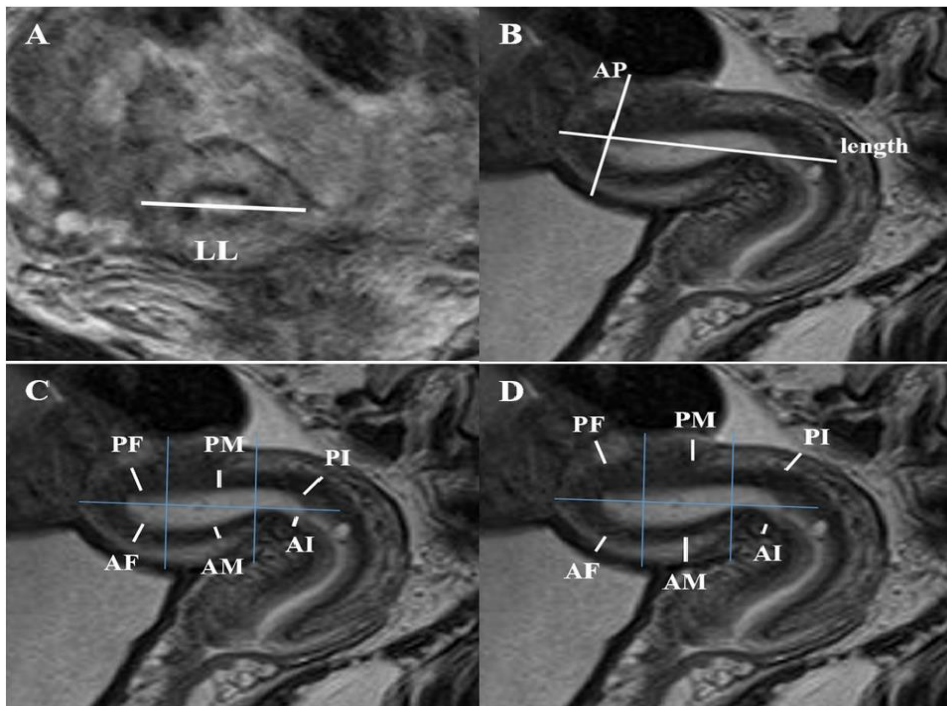


Figure 2: Measurements of the corpus uteri volume, the junctional zone thickness and outer myometrium thickness, assessed on T₂-weighted turbo spin echo magnetic resonance images. A: The transversal image obtained before buscopan injection was used to measure the corpus size latero-lateral (LL). B: On the sagittal image after

buscopan injection without fat suppression, the length and the antero-posterior (AP) uterus size were measured. C and D: The same sagittal image was also used to measure the junctional zone (C) and outer myometrium (D) thickness. According to the measuring method, the uterine walls were divided into three parts equally in length (blue lines), and the measurement was performed at a central point in each part. PF: posterior wall at the fundus; PM: posterior wall at the midcorpus; PI: posterior wall at the isthmus; AF: anterior wall at the fundus; AM: anterior wall at the midcorpus; AI: anterior wall at the isthmus.

3.3.5 Statistical analysis

All statistical analyses were performed by means of the computer program SAS version 9.4. A significance level of 5% was used. No correction for multiple testing was applied.

Cohen's kappa coefficient was calculated in order to evaluate the concordance between the two investigators. Moreover, we investigated using linear mixed models, whether the thickness of the JZ and outer myometrium were correlated with uterine volume, age at menarche, smoker/non-smoker and length and height of the women.

Linear mixed models were used in order to investigate the effect of infertility, the effect of the location in the uterine wall and the effect of menstrual phase (for the control group) on the JZ thickness, on the outer myometrium thickness and on the ratio of JZ versus total myometrial thickness. The first statistical model investigated the effect of the menstrual phase in the control group and included two fixed effects and their interaction. The fixed effects were the menstrual phase and the location in the uterine wall. The second statistical model also included two main fixed effects and their interaction. The first fixed effect comprised the effect of the group and the second fixed was the location in the uterine wall. The association between measurements of the same woman (e.g. JZ thickness measured in the three menstrual phases) was incorporated by means of a random intercept at woman level. A parsimonious model was obtained by backward elimination of the interaction terms not statistically significant at a 5% level of significance. In order to normalize the data, statistical analyses were performed on the natural log transformed outcome data.

3.4 Results

No congenital or acquired uterine abnormalities were found in the healthy nulliparous women. The JZ and outer myometrium thickness were identified and measured in each woman. Both investigators show high agreement, as Cohen's kappa equated 0.87. There were no correlations between the JZ and outer myometrial thickness with uterine volume, height and weight of the women, age at menarche and smoker/non-smoker ($p > 0.050$).

3.4.1 Junctional Zone Thickness

The JZ thickness measurements and the mean for the six uterine wall locations, for each group and per menstrual cycle phase, are displayed in figure 3.

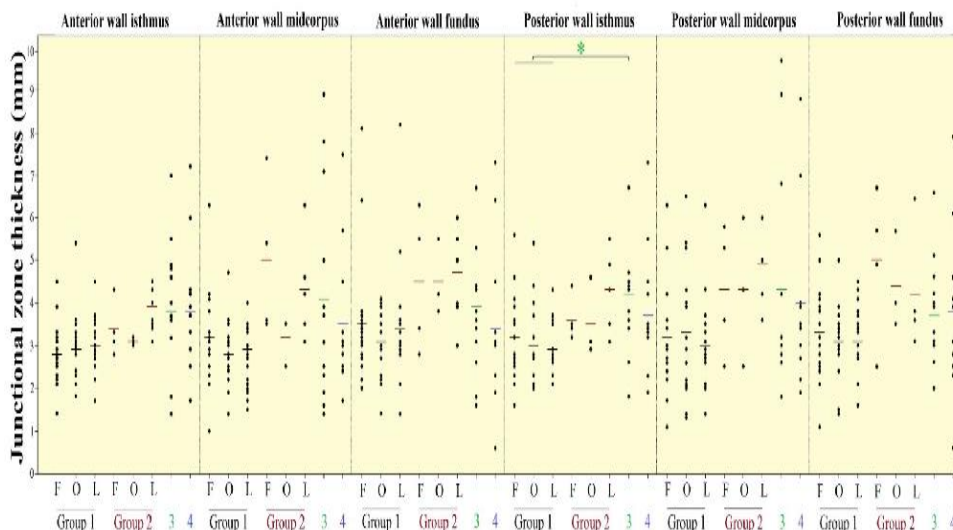


Figure 3: Junctional zone thickness measurements in the control group and in three groups of infertile women at six locations in the uterine wall during the menstrual cycle, assessed on T2-weighted turbo spin echo magnetic resonance images. The control group (group 1) consists of healthy nulliparous women without infertility history. The three groups of infertile women are women with unexplained infertility (group 2), anovulating women (group 3) and infertile women using ovarian stimulation therapy (group 4). Every dot represents the junctional zone thickness in one woman, the small line represents the average thickness for each group. Data analysis was performed on the natural log transformed data. F: follicular phase; O: ovulatory phase; L: luteal phase; *: $p < 0.050$ for group 3.

Table 3 shows the median, minimum and maximum JZ thickness per location and the average JZ for each group and menstrual phase.

Table 3: Junctional zone thickness (mm) in the control group consisting of healthy nulliparous women and in three groups of infertile women.

Group		Anterior wall isthmus	Anterior wall midcorpus	Anterior wall fundus	Posterior wall isthmus	Posterior wall midcorpus	Posterior wall fundus	Average	n	
Control group (healthy nulliparous women)	Follicular phase	0.14	0.10	0.20	0.16	0.11	0.11	3.2	17	
		0.28	0.29	0.33	0.32	0.29	0.30			
		0.45	0.63	0.81	0.56	0.63	0.56			
	Ovulatory phase	0.18	0.14	0.14	0.20	0.13	0.14	3.0	17	
		0.28	0.18	0.30	0.28	0.29	0.32			
		0.54	0.47	0.41	0.54	0.65	0.50			
	Luteal phase	0.17	0.15	0.14	0.21	0.14	0.16	3.1	16	
		0.30	0.29	0.31	0.28	0.30	0.32			
		0.45	0.40	0.82	0.43	0.63	0.45			
Women with unexplained infertility	Follicular phase	0.28	0.35	0.28	0.32	0.25	0.25	4.3	4	
		0.32	0.45	0.45	0.35	0.45	0.53			
		0.43	0.74	0.64	0.44	0.58	0.67			
	Ovulatory phase	0.30	0.25	0.38	0.29	0.25	0.35	3.8	3	
		0.31	0.35	0.42	0.31	0.43	0.40			
		0.32	0.35	0.55	0.46	0.60	0.56			
	Luteal phase	0.34	0.31	0.30	0.31	0.36	0.31	4.4	5	
		0.40	0.42	0.50	0.43	0.50	0.35			
		0.45	0.63	0.60	0.55	0.60	0.64			
Anovulating women	0.14	0.14	0.16	0.18	0.18	0.20	4.0	12		
	0.38	0.34	0.37	0.43	0.31	0.36				
	0.70	0.89	0.67	0.67	0.97	0.66				
	p (control)	0.162	0.177	0.453	0.027 *	0.165	0.395			
Infertile women on ovarian stimulation therapy		0.17	0.17	0.06	0.19	0.19	0.06	3.7	11	
		0.37	0.30	0.31	0.34	0.35	0.39			
		0.72	0.75	0.73	0.73	0.88	0.79			
		p (control)	0.121	0.493	0.473	0.278	0.200	0.710		
		p (anovulating women)	0.865	0.591	0.222	0.330	0.955	0.701		

The junctional zone thickness was measured during three menstrual phases: follicular, ovulatory and luteal phase; and at six locations in the uterine wall: anterior and posterior wall of the isthmus, midcorpus and fundus. The average represents the mean thickness over all locations. Data represents minimum, **median**, and maximum measurement. P (control): p-value concerning the group of interest and the control group by means of linear mixed model analysis; p (anovulating women): p-value concerning the group interest and the anovulating women by means of linear mixed model analysis; *: statistical significance at 5% significance level.

The average JZ in every group of infertile women was slightly thicker than in healthy nulliparous women (table 3). However, only the JZ in the anovulating women at the posterior wall of the isthmus was significantly thicker than the JZ at the corresponding location in the healthy nulliparous women ($p = 0.027$).

Furthermore, the different uterine wall locations show no significant differences in JZ thickness, in every group (anterior and posterior wall of the isthmus, midcorpus and fundus) ($p > 0.050$).

In the healthy nulliparous women, the JZ thickness was not significantly different between the three menstrual phases, for each measured location in the uterine wall ($p > 0.050$). In women with unexplained infertility, a decrease in JZ thickness can be observed in the ovulatory phase, followed by an increase in the luteal phase, especially at the anterior wall at the level of the isthmus and midcorpus. Statistical analysis of the significance of this difference was not possible due to the low number of subjects in this group.

3.4.2 Outer Myometrial Thickness

The outer myometrial thickness measurements for each group, menstrual phase and uterine wall location are shown in figure 4 and the median, minimum and maximum thickness and averaged over each assessed location are listed in table 4.

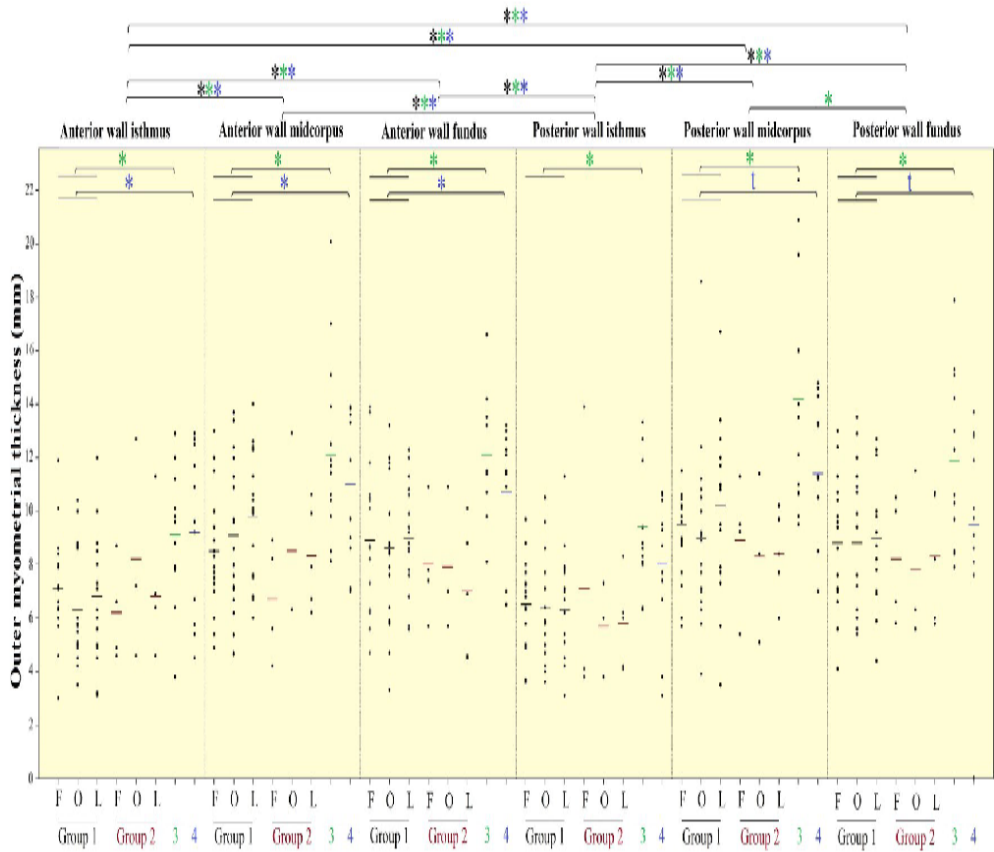


Figure 4: Outer myometrial thickness measurements in the control group and in three groups of infertile women at six locations in the uterine wall during the menstrual cycle, assessed on T2-weighted turbo spin echo magnetic resonance images. The control group (group 1) consists of healthy nulliparous women without infertility history. The three groups of infertile women are women with unexplained infertility (group 2), anovulating women (group 3) and infertile women using ovarian stimulation therapy (group 4). Every dot represents the outer myometrial thickness in one woman, the small line represents the average thickness for each group. Data analysis was performed on the natural log transformed data. F: follicular phase; O: ovulatory phase; L: luteal phase; *: $p < 0.050$ for group 1; *: $p < 0.050$ for group 3; *: $p < 0.050$ for group 4; t: $p < 0.100$ for group 4.

Table 4: Outer myometrial thickness (mm) in the control group consisting of healthy nulliparous women and in three groups of infertile women.

Group		Anterior wall isthmus	Anterior wall midcorpus	Anterior wall fundus	Posterior wall isthmus	Posterior wall midcorpus	Posterior wall fundus	Average	n	
Control group (healthy nulliparous women)	Follicular phase	0.30	0.49	0.47	0.36	0.57	0.41	8.1	17	
		0.66	0.83	0.86	0.64	0.90	0.86			
		1.19	1.30	1.39	0.97	1.15	1.30			
	Ovulatory phase	0.35	0.47	0.33	0.36	0.39	0.54	8.0	17	
		0.55	0.86	0.85	0.59	0.89	0.94			
		1.04	1.38	1.32	1.05	1.86	1.35			
	Luteal phase	0.31	0.60	0.56	0.31	0.35	0.44	8.5	16	
		0.67	1.01	0.90	0.65	1.09	0.90			
		1.20	1.40	1.23	1.13	1.67	1.27			
Women with unexplained infertility	Follicular phase	0.46	0.42	0.57	0.38	0.54	0.58	7.5	4	
		0.58	0.69	0.76	0.53	0.94	0.83			
		0.87	0.89	1.09	1.39	1.13	1.05			
	Ovulatory phase	0.46	0.63	0.57	0.38	0.51	0.56	7.7	3	
		0.72	0.63	0.70	0.60	0.84	0.63			
		1.27	1.29	1.09	0.73	1.14	1.15			
	Luteal phase	0.46	0.62	0.45	0.41	0.60	0.58	7.4	5	
		0.64	0.79	0.69	0.60	0.84	0.82			
		1.13	1.06	1.01	0.83	1.02	1.07			
Anovulating women	0.38	0.81	0.81	0.63	0.95	0.79	11.5	12		
	0.96	1.18	1.15	0.87	1.28	1.14				
	1.29	2.01	1.66	1.33	2.24	1.79				
	p (control)	0.005 *	0.002 *	0.001 *	0.001 *	0.001 *	0.002 *			
Infertile women on ovarian stimulation therapy		0.45	0.70	0.65	0.31	0.70	0.76	10.1	11	
		0.92	1.33	1.15	0.77	1.13	1.01			
		1.29	1.43	1.34	1.07	1.48	1.37			
		p (control)	0.015 *	0.012 *	0.047 *	0.128	0.061	0.052		
		p (anovulating women)	0.788	0.568	0.258	0.073	0.082	0.320		

The outer myometrial thickness was measured during three menstrual phases: follicular, ovulatory and luteal phase; and at six locations in the uterine wall: anterior and posterior wall of the isthmus, midcorpus and fundus. The average represents the mean thickness over all locations. Data represents minimum, **median**, and maximum measurement. P (control): p-value concerning the group of interest and the control group by means of linear mixed model analysis; p (anovulating women): p-value concerning the group of interest and the anovulating women by means of linear mixed model analysis; *: statistical significance at 5% significance level.

Statistical analysis revealed that the outer myometrium in anovulating women was significantly thicker than in healthy nulliparous women, at each measured uterine location ($p < 0.005$). The infertile women on ovarian stimulation therapy also demonstrated a thicker outer myometrium than healthy nulliparous women at the anterior wall at the level of the isthmus ($p = 0.015$), midcorpus ($p = 0.012$) and fundus ($p = 0.047$). Although the difference did not reach statistical significance, there was a trend towards a thicker outer myometrium in the infertile women on ovarian stimulation therapy compared to the healthy nulliparous women at the posterior wall of the midcorpus ($p = 0.061$) and fundus ($p = 0.052$). Observation of the data of the women with unexplained infertility showed that the average outer myometrium was thinner than in the other two infertile participant groups.

In each group, the outer myometrium at the level of the isthmus in both walls was significantly thinner than at the midcorpus and fundus in both walls ($p < 0.050$). In addition, in the group of the anovulating women, the outer myometrium at the posterior midcorpus was significantly thicker than at the posterior fundus ($p = 0.046$).

No differences in outer myometrial thickness were shown between the menstrual phases ($p > 0.050$) in healthy nulliparous women, for each uterine location, and empirically, this was also valid for women with unexplained infertility.

3.4.3 Ratio Of Junctional Zone Versus Total Myometrial Thickness

Figure 5 displays the individual ratios of JZ versus total myometrial thickness for each group at the six uterine wall locations. The median, minimum and maximum ratios per uterine wall location and the averaged ratio per group and

menstrual phase are listed in table 5. The ratios were not significantly different between the healthy nulliparous women and the infertile groups, for each location in the uterine wall. The ratio of women with unexplained infertility was notably higher than that of healthy nulliparous women and other infertile participating groups.

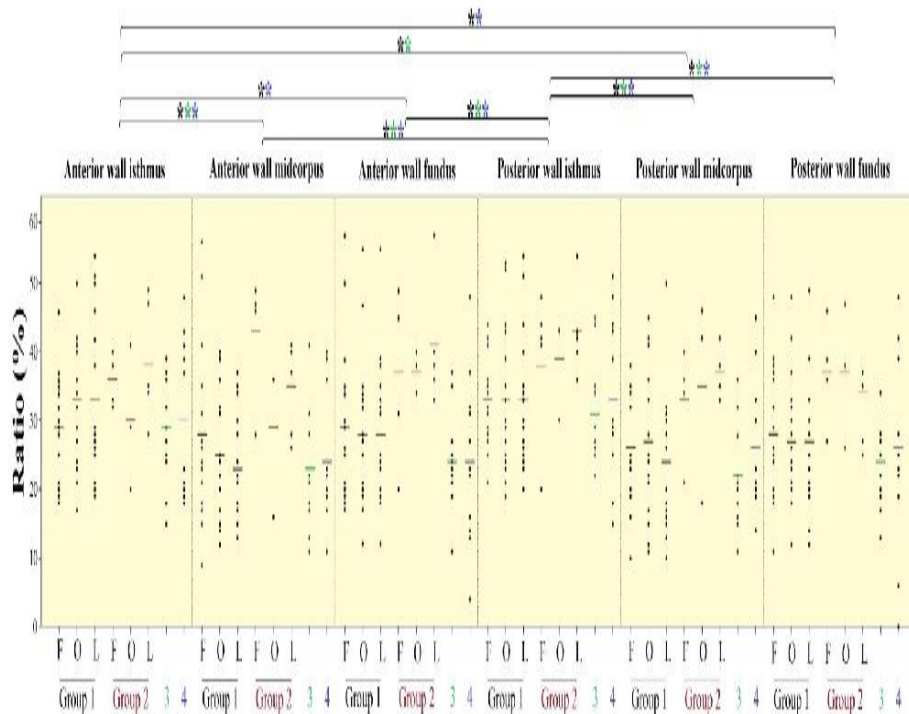


Figure 5: Outer myometrial thickness measurements in the control group and in three groups of infertile women at six locations in the uterine wall during the menstrual cycle, assessed on T2-weighted turbo spin echo magnetic resonance images. The control group (group 1) consists of healthy nulliparous women without infertility history. The three groups of infertile women are women with unexplained infertility (group 2), anovulating women (group 3) and infertile women using ovarian stimulation therapy (group 4). Every dot represents the outer myometrial thickness in one woman, the small line represents the average thickness for each group. Data analysis was performed on the natural log transformed data. F: follicular phase; O: ovulatory phase; L: luteal phase; *: $p < 0.050$ for group 1; *: $p < 0.050$ for group 3; *: $p < 0.050$ for group 4; t: $p < 0.100$ for group 4.

The ratios calculated at the six uterine wall locations were significantly different from each other. For healthy nulliparous women, the ratio calculated at the anterior and posterior wall of the isthmus was significantly higher than at the

anterior wall of the midcorpus ($p < 0.001$) and fundus ($p = 0.017$ and $p = 0.002$, respectively) and higher than at the posterior wall of the midcorpus ($p < 0.001$) and fundus ($p = 0.003$ and $p < 0.001$, respectively). For the anovulating women, the ratio assessed at the anterior and posterior wall of the isthmus was higher than at the anterior ($p = 0.014$ and $p = 0.003$) and posterior ($p = 0.006$ and $p = 0.001$) wall of the midcorpus and the ratio at the posterior wall of the isthmus was also significantly higher than the anterior ($p = 0.017$) and posterior ($p = 0.017$) wall of the fundus. For infertile women on ovarian stimulation therapy, the anterior wall of the isthmus had a significantly higher ratio than the anterior wall of the midcorpus ($p = 0.028$) and fundus ($p = 0.009$) and the posterior wall of the fundus ($p = 0.050$) and the posterior wall of the isthmus had a significantly higher ratio than the anterior and posterior wall of the midcorpus ($p = 0.006$ and $p = 0.038$, respectively) and fundus ($p = 0.002$ and $p = 0.012$, respectively)).

Table 5: Ratio of junctional zone versus total myometrial thickness (%) in the control group consisting of healthy nulliparous women and in three groups of infertile women.

Group		Anterior wall isthmus	Anterior wall midcorpus	Anterior wall fundus	Posterior wall isthmus	Posterior wall midcorpus	Posterior wall fundus	Average	n
Control group (healthy nulliparous women)	Follicular phase	18	9	17	21	10	11	29	17
		29	24	26	34	24	26		
		46	56	57	44	38	48		
	Ovulatory phase	17	12	12	19	11	12	29	17
		32	24	27	30	25	24		
		50	40	55	53	45	48		
	Luteal phase	19	13	12	20	10	12	28	16
		28	21	25	32	23	25		
		54	37	55	54	50	49		
Women with unexplained infertility	Follicular phase	32	28	20	20	21	27	37	4
		35	47	38	42	35	38		
		40	49	49	48	40	46		
	Ovulatory phase	20	16	34	30	18	26	35	3
		29	36	38	43	42	38		
		41	36	40	43	46	47		
	Luteal phase	28	26	33	36	33	25	38	5
		35	37	38	42	38	35		
		49	41	57	54	42	37		
Anovulating women		15	11	11	22	11	13	25	12
		31	21	23	28	21	23		
		39	41	37	45	36	34		
	p (control)	0.429	0.445	0.234	0.505	0.250	0.354		
Infertile women on ovarian stimulation therapy		19	11	4	15	14	6	27	11
		23	20	23	30	23	23		
		48	40	48	51	45	48		
	p (control)	0.493	0.592	0.071	0.605	0.945	0.301		
	p (anovulating women)	0.944	0.862	0.576	0.910	0.373	0.893		

The junctional zone and outer myometrial thicknesses were measured during three menstrual phases: follicular, ovulatory and luteal phase; and at six locations in the uterine wall: anterior and posterior wall of the isthmus, midcorpus and fundus. The ratio was calculated by dividing the junctional zone thickness by the total myometrial thickness (junctional zone thickness / (junctional zone thickness + outer myometrial thickness)). The average represents the mean thickness over all locations. Data represents minimum, **median**, and maximum measurement. P (control): p-value concerning the group of interest and the control group by means of linear mixed model analysis; p (anovulating women): p-value concerning the group of interest and the anovulating women by means of linear mixed model analysis.

During the menstrual cycle, no differences in the ratios were determined between the follicular, ovulatory and luteal phase in healthy nulliparous women ($p > 0.050$). Comparing the ratios of the different menstrual phases in women with unexplained infertility, no difference was noticed

3.5 Discussion

This study showed that the JZ thickness in anovulating women at the posterior wall of the isthmus is significantly thicker than in healthy nulliparous women.

The outer myometrial thickness is also thicker in several groups of infertile women: in anovulating women at each assessed location (anterior and posterior wall of the isthmus, midcorpus and fundus) and in infertile women taking ovarian stimulation therapy in the context of assisted reproductive therapy at the anterior uterine wall (at the level of the isthmus, the midcorpus and the fundus).

These findings imply that the thickness of the JZ and outer myometrium can best be measured at the anterior wall of the uterus in order to detect the largest differences between 'fertile' and each group of infertile women.

Our study found no differences in JZ thickness, in outer myometrial thickness or in ratio of JZ versus total myometrial thickness between the follicular, ovulatory and luteal phase in healthy nulliparous women. These results according the JZ thickness (17,18) and the outer myometrial thickness (18) were in concordance with previous studies. However, Haynor et al. (19) demonstrated significant changes in myometrial thickness throughout the menstrual cycle, with increasing thickness during the follicular phase followed by a significant decrease during the luteal phase. They investigated six healthy women twice a week during one

full menstrual cycle. This study is in contradiction with our findings. However, the healthy nulliparous women of our study were investigated only once during the follicular, ovulatory and luteal phase. Based on the results of our study, we conclude that the woman's menstrual phase during which the MRI investigation was executed, does not affect the thickness of the JZ and outer myometrium significantly.

A thickened JZ has generally been related to inner myometrium adenomyosis (15,20-22) and is considered a negative predictive factor for IVF implantation failure (8,9). Inner myometrium adenomyosis is a gynecological disorder characterized by benign invasion of basal endometrial stroma and glands into the underlying myometrium (15,21). Animal experiments and human studies have suggested that adenomyosis is associated with infertility (23,24). The diagnosis of adenomyosis remains difficult because of the lack of a definite consensus classification. Several studies suggested that adenomyosis is strongly suspected when the JZ measures at least 12 mm in thickness on MR images (15,20,21,25-27), whereas others concluded that a maximal thickness of 10 mm is considered as a cut-off value beyond which JZ adenomyosis is assumed (10,28). Hence, the maximum thickness of healthy JZ is still arguable.

Another parameter which can be considered in the diagnosis of adenomyosis is the ratio of JZ versus total myometrial thickness, representing the relationship between JZ and myometrial thickness, introduced by Reinhold et al. (27) and Bazot et al. (28). Reinhold et al. found a significant difference in this ratio between patients with adenomyosis (69%) and a control group (44%) and defined a maximum ratio of 40% in healthy women. Bazot et al. concluded similarly that a ratio higher than 40% allows diagnosis of adenomyosis with a sensitivity of 65% and a specificity of 92%.

The underlying association between adenomyosis and infertility is still not fully understood. The invasion of endometrial stroma and glands into the myometrium in adenomyosis results in surrounding smooth-muscle hyperplasia (10). It can be postulated that a thickened or an altered morphology of the JZ can reduce uterine peristaltic activity and decrease endometrial receptivity which affects respectively sperm transport and embryo implantation (29).

Furthermore, Maubon et al. (8) found a significantly lower rate of embryo implantation when the maximum JZ thickness was 10 mm or higher. The incidence of a thickened JZ (defined as an average JZ in anterior, posterior and fundal wall of at least 7 mm or a maximal JZ thickness of at least 10 mm) was significantly higher in the group of women with unexplained infertility in comparison with the incidence in other subtypes of infertility (male infertility, endometriosis, dysovulation or tubal abnormalities) (8). In addition, Youm et al. (30) concluded that a thickened myometrium (>2.5 cm) in infertile women assessed by transvaginal ultrasonography also exerts overall adverse effects on IVF and embryo transfer outcomes.

The infertile women in our study who had no ovulation demonstrated a significantly thicker JZ than the healthy nulliparous women at the posterior wall of the isthmus. This data suggest that the JZ can possibly play a role in the underlying cause of infertility in these women. A thickened JZ could possibly affect the contractility and therefore impede sperm transport or could interfere with embryo implantation. In addition, a significantly thicker outer myometrium was shown at the anterior and posterior uterine wall of the anovulating women and at the anterior wall of the infertile women on ovarian stimulation therapy. This implies that it is likely that the outer myometrium plays a role in the underlying cause of their infertility. A thicker JZ or outer myometrium was not noticed in the women with unexplained infertility, which was not as expected, but no definite conclusions can be made for this group due to the low number of subjects. Future research could go deeper in the underlying role of the JZ or outer myometrial thickness in infertile women or could focus on other characteristics of the JZ in reproduction such as contractility and perfusion characteristics.

A limitation of this study is the low number of infertile women, especially those with unexplained infertility. The number of this group of women was too low to perform statistical analysis on. This data is included in order to give an overview of all types of infertile women. Another limitation is that not all women underwent three MRI investigations per menstrual cycle.

In conclusion, infertile anovulating women demonstrated a significantly thickened JZ at the posterior wall of the isthmus and a significantly thickened outer myometrium at both the anterior and posterior uterine wall. In infertile women on ovarian stimulation therapy, a thickened outer myometrium was also demonstrated at the anterior uterine wall. These findings suggest that the thickness of the JZ, and more likely the outer myometrium, could possibly be associated with infertility. These results could be used in the context of assisted reproductive therapy in order to attempt to augment the implantation rate. The results need to be confirmed in further studies on larger series.

3.6 References

1. Benagiano G, Bastianelli C, Farris M. Infertility: a global perspective. *Minerva Ginecol* 2006;58(6):445-457.
2. Gelbaya TA, Potdar N, Jevic YB, Nardo LG. Definition and epidemiology of unexplained infertility. *Obstet Gynecol Surv* 2014;69(2):109-115.
3. Fusi L, Cloke B, Brosens JJ. The uterine junctional zone. *Best Pract Res Clin Obstet Gynaecol* 2006;20(4):479-491.
4. Noe M, Kunz G, Herberich M, Mall G, Leyendecker G. The cyclic pattern of the immunocytochemical expression of oestrogen and progesterone receptors in human myometrial and endometrial layers: characterization of the endometrial-subendometrial unit. *Hum Reprod* 1999;14(1):190-197.
5. Kunz G, Beil D, Deininger H, Wildt L, Leyendecker G. The dynamics of rapid sperm transport through the female genital tract: evidence from vaginal sonography of uterine peristalsis and hysterosalpingoscintigraphy. *Hum Reprod* 1996;11(3):627-632.
6. Kunz G, Kissler S, Wildt L. Uterine peristalsis: directed sperm transport and fundal implantation of the blastocyst. In Felicori M (ed.) *Endocrine Basis of Reproductive Function*; Bologna, Italy; 409-422. 2000.
7. Lyons EA, Taylor PJ, Zheng XH, Ballard G, Levi CS, Kredentser JV. Characterization of subendometrial myometrial contractions throughout the menstrual cycle in normal fertile women. *Fertil Steril* 1991;55(4):771-774.
8. Maubon A, Faury A, Kapella M, Pouquet M, Piver P. Uterine junctional zone at magnetic resonance imaging: a predictor of in vitro fertilization implantation failure. *J Obstet Gynaecol Res* 2010;36(3):611-618.

9. Piver P. Uterine factors limiting ART coverage. *J Gynecol Obstet Biol Reprod (Paris)* 2005;34(7 Pt 2):5S30-35S33.
10. Kunz G, Beil D, Huppert P, Noe M, Kissler S, Leyendecker G. Adenomyosis in endometriosis--prevalence and impact on fertility. Evidence from magnetic resonance imaging. *Hum Reprod* 2005;20(8):2309-2316.
11. Tocci A, Greco E, Ubaldi FM. Adenomyosis and 'endometrial-subendometrial myometrium unit disruption disease' are two different entities. *Reprod Biomed Online* 2008;17(2):281-291.
12. Campo S, Campo V, Benagiano G. Adenomyosis and infertility. *Reprod Biomed Online* 2012;24(1):35-46.
13. Hricak H, Alpers C, Crooks LE, Sheldon PE. Magnetic resonance imaging of the female pelvis: initial experience. *AJR Am J Roentgenol* 1983;141(6):1119-1128.
14. Togashi K, Nakai A, Sugimura K. Anatomy and physiology of the female pelvis: MR imaging revisited. *J Magn Reson Imaging* 2001;13(6):842-849.
15. Novellas S, Chassang M, Delotte J, et al. MRI characteristics of the uterine junctional zone: from normal to the diagnosis of adenomyosis. *AJR Am J Roentgenol* 2011;196(5):1206-1213.
16. Goldstein SR, Horii SC, Snyder JR, Raghavendra BN, Subramanyam B. Estimation of nongravid uterine volume based on a normogram of gravid uterine volume: its value in gynecologic uterine abnormalities. *Obstet Gynecol* 1988;72(1):86-90.

17. McCarthy S, Tauber C, Gore J. Female pelvic anatomy: MR assessment of variations during the menstrual cycle and with use of oral contraceptives. *Radiology* 1986;160(1):119-123.
18. Hauth EA, Jaeger HJ, Libera H, Lange S, Forsting M. MR imaging of the uterus and cervix in healthy women: determination of normal values. *Eur Radiol* 2007;17(3):734-742.
19. Haynor DR, Mack LA, Soules MR, Shuman WP, Montana MA, Moss AA. Changing appearance of the normal uterus during the menstrual cycle: MR studies. *Radiology* 1986;161(2):459-462.
20. Reinhold C, Tafazoli F, Wang L. Imaging features of adenomyosis. *Hum Reprod Update* 1998;4(4):337-349.
21. Reinhold C, Tafazoli F, Mehio A, et al. Uterine adenomyosis: endovaginal US and MR imaging features with histopathologic correlation. *Radiographics* 1999;19 Spec No:S147-160.
22. Brosens I, Derwig I, Brosens J, Fusi L, Benagiano G, Pijnenborg R. The enigmatic uterine junctional zone: the missing link between reproductive disorders and major obstetrical disorders? *Hum Reprod* 2010;25(3):569-574.
23. Barrier BF, Malinowski MJ, Dick EJ, Hubbard GB, Bates GW. Adenomyosis in the baboon is associated with primary infertility. *Fertil Steril* 2004;82 Suppl 3:1091-1094.
24. Zangos S, Kissler S, Mueller A, et al. Uterine adenomyosis in infertile patients: MR imaging findings and clinical conclusions. *Rofo* 2004;176(11):1641-1647.

25. Kang S, Turner DA, Foster GS, Rapoport MI, Spencer SA, Wang JZ. Adenomyosis: specificity of 5 mm as the maximum normal uterine junctional zone thickness in MR images. *AJR Am J Roentgenol* 1996;166(5):1145-1150.
26. Kissler S, Zangos S, Kohl J, et al. Duration of dysmenorrhoea and extent of adenomyosis visualised by magnetic resonance imaging. *Eur J Obstet Gynecol Reprod Biol* 2008;137(2):204-209.
27. Reinhold C, McCarthy S, Bret PM, et al. Diffuse adenomyosis: comparison of endovaginal US and MR imaging with histopathologic correlation. *Radiology* 1996;199(1):151-158.
28. Bazot M, Cortez A, Darai E, et al. Ultrasonography compared with magnetic resonance imaging for the diagnosis of adenomyosis: correlation with histopathology. *Hum Reprod* 2001;16(11):2427-2433.
29. Kido A, Togashi K, Nishino M, et al. Cine MR imaging of uterine peristalsis in patients with endometriosis. *Eur Radiol* 2007;17(7):1813-1819.
30. Youm HS, Choi YS, Han HD. In vitro fertilization and embryo transfer outcomes in relation to myometrial thickness. *J Assist Reprod Genet* 2011;28(11):1135-1140.

4. CHAPTER IV: PERFUSION OF THE UTERINE JUNCTIONAL ZONE IN NULLIPAROUS AND PRIMIPAROUS WOMEN ASSESSED BY DCE-MRI, AS A FUNCTION OF MENSTRUAL CYCLE AND HORMONAL CONTRACEPTION

Magn Reson Imaging. 2017 May;38:101-111

4.1 Abstract

Purpose: To evaluate the perfusion parameters of inner and outer myometrium in healthy nulliparous and primiparous women who are and who are not currently using hormonal contraceptives by means of dynamic contrast-enhanced magnetic resonance imaging (DCE-MRI).

Material and methods: We performed pelvic 1.5T DCE-MRI on 98 women: 18 nulliparous non-users, 30 nulliparous users, 12 primiparous non-users and 38 primiparous users of hormonal contraception (mean age respectively 26.4, 25.8, 30.23 and 28.18 years). The nulliparous non-users underwent DCE-MRI investigations during their follicular, ovulatory and luteal phase. Perfusion parameters (iAUC/volume, K^{trans} , K_{ep} and Ve) were assessed in the anterior and posterior wall of the junctional zone (JZ) and outer myometrium.

Results: In nulliparous non-users, the mean K^{trans} and iAUC/volume showed a decrease from follicular to luteal phase (0.82 vs 0.55 min^{-1} for K^{trans} , $p = 0/027$ and 1.28 vs 0.68 for iAUC/volume, $p < 0.001$). The anterior JZ demonstrated lower K^{trans} ($p = 0.050$) and higher K_{ep} ($p = 0.012$) in nulliparous non-users, lower K^{trans} in nulliparous users ($p < 0.001$) and lower Ve in primiparous users ($p = 0.012$) than the anterior outer myometrium. K^{trans} in the anterior and posterior JZ wall in nulliparous users was lower than in non-users ($p = 0.001$ and $p = 0.013$) and Ve at the anterior JZ wall in primiparous users was lower than in non-users ($p = 0.044$).

Conclusion: This study provides data on normal perfusion parameters of inner and outer myometrium, which may be potentially useful in assisted reproductive therapy.

KEYWORDS: DCE-MRI - Perfusion - Junctional Zone - Outer Myometrium - Nulliparous - Primiparous

4.2 Introduction

The female reproductive system is characterized by rapid cyclic changes in blood flow throughout the menstrual cycle. During the female reproductive period, arteries present in the inner myometrium or junctional zone (JZ), supply the endometrium with oxygen and nutrients to contribute to endometrial growth. These arteries subsequently constrict in order to cause ischemia resulting in endometrial shedding during menstruation (1).

Recent ultrasonographic studies have demonstrated that inner myometrium perfusion is impaired in women with unexplained infertility (2). Other conditions of the reproductive system such as tumoral lesions, endometriosis, adenomyosis, abnormal severe menstrual bleeding and breakthrough bleeding are also associated with disturbances of the uterine angiogenic process and the vascular network (2-8). Microvascular parameter assessment could potentially be used to detect pathogenic conditions or in assisted reproductive therapy. This requires profound knowledge of the normal myometrial vasculature.

Dynamic contrast-enhanced magnetic resonance imaging (DCE-MRI) provides semi-quantitative assessment of perfusion kinetics, including perfusion assessment in myometrium (9). This non-invasive technique obtains repeated T1-weighted MR images before, during and after a bolus injection of a contrast agent. Analysis of these images requires post-imaging processing with specialized software and physiological models. The software evaluates the signal enhancement resulting in the conversion of a signal intensity-time curve (10). Analysis of this curve, based on the model of Tofts (11) (figure 1), provides quantitative information about the perfusion parameters of the organ of interest.

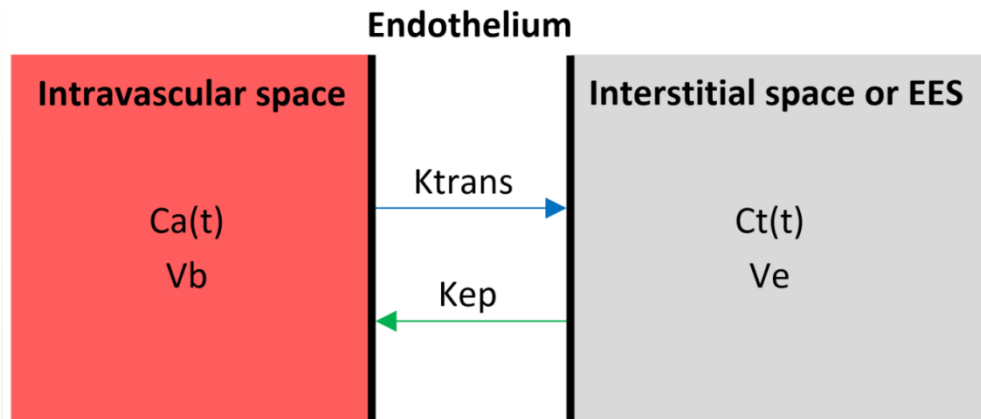


Figure 1: The assumptions used by dynamic contrast-enhanced magnetic resonance imaging (DCE-MRI) are based on the two compartment model of Tofts. Two compartments are assumed in this model: the intravascular space and the extracellular extravascular space (EES or interstitial space). The model provides information about the distribution of contrast agent across these compartments. C_a : arterial contrast agent concentration in function of time; C_t : tissue contrast agent concentration in function of time; V_b : whole blood volume per unit of tissue; V_e : total EES volume; K^{trans} : transfer constant; K_{ep} : reflux constant.

The purpose of this prospective study is to investigate perfusion characteristics of normal JZ and outer myometrium throughout the menstrual cycle in a population of healthy nulliparous and primiparous women between 18 and 35 years old, by means of DCE-MRI. In addition, this study aims to detect whether or not the perfusion parameters are influenced by the menstrual cycle status, the use of hormonal contraceptives and the location in the uterine wall.

4.3 Material and Methods

The study protocol was approved by the hospital ethics committee in order to perform this longitudinal study on volunteers (registration number 056). All included women provided a written informed consent and filled out an epidemiological questionnaire in order to obtain information regarding their birth date, height, weight, age at menarche, gestity and parity status and whether or not they currently smoke.

4.3.1 Study population

We included 48 volunteer nulliparous and 50 volunteer primiparous women at 6 to 12 months post-partum from December 2007 to January 2012. Recruitment was achieved by emailing and writing co-workers in our hospital, students and PhD students at the local university, personal contacts and cooperation with external physicians. Exclusion criteria were age less than 18 years or more than 35 years, non-Caucasian origin, pregnancy, medical history of infertility or a gynecological history such as heavy, prolonged or irregular menstrual periods, previous unknown uterine morphologic abnormality found on the first MRI examination, diminished renal function (assessed by creatinine levels collected prior to MRI investigation) and women with a pacemaker, clips or other MRI-incompatible implanted devices.

Both the nulliparous and primiparous women were subdivided based on their use of hormonal contraception. Among the nulliparous women, 18 women were non-users (mean age 26.4 years) and 30 women were users (mean age 25.8 years) of contraception therapy, and the group of primiparous women comprised 12 non-users (mean age 30.23 years) and 38 users (mean age 28.18 years) of contraception therapy (figure 2). The different types of contraception therapy included oral contraceptive pills, progesterone-only implants, hormonal vaginal rings and intrauterine devices (table 1).

			98 women			
48 nulliparous				50 primiparous (6-12 months post-partum)		
18 non-users of hormonal contraception		30 users sampled randomly		12 non-users of hormonal contraception	38 users sampled randomly	
16 women during follicular phase	17 women during ovulatory phase	17 women during luteal phase		7 women during follicular phase	5 women during luteal phase	

Figure 2: Overview of the study population and the menstrual phases during which MRI examination was performed.

4.3.2 Blood laboratory tests

Blood samples were taken prior to each MRI examination in order to assess human chorionic gonadotrophin (hCG), creatinine, follicle-stimulating hormone (FSH), luteinizing hormone (LH), estradiol and progesterone levels. The follicular phase was considered around day 6-13 of the menstrual cycle, the ovulatory phase around day 14-16 and the luteal phase around day 17-28. The exact phase of the menstrual cycle was determined based on the hormone levels in all participants who did not use hormonal contraception.

4.3.3 Magnetic Resonance Imaging

DCE-MRI investigations were obtained with a 1.5T magnet unit (Siemens Magnetom Symphony Tim (4G-Dot upgraded), Erlangen, Germany; Software Syngo MR B15). The women were inserted with an intravenous catheter in the elbow crease. They were positioned on the table of the scanner in head-first supine position and an eight-channel receiver body array was placed on the pelvis. The MRI examination started with a localizer sequence followed by T2-weighted turbo spin echo (T2 TSE) sequences without fat-suppression in transversal, coronal oblique in the long axis of uterine corpus and sagittal plane (repetition time/echo time: 5000-5100/88-89; flip angle: 180°; field of view: 320 x 370 mm; slice thickness: 5 mm with 1 mm intersection gap; and voxel

size: 0.8-1.1 x 0.6-0.8 x 4-5 mm). In mutual agreement with the women, an intravenous injection of the abdominal-specific antispasmodic hyoscine butylbromide (buscopan, 1 ml, 20 mg/ml, Boehringer Ingelheim, Germany), diluted in sodium chloride (10 ml, 0.09%, Baxter, Lessines, Belgium) was administered in order to reduce bowel movements. Then, another sagittal T2 TSE image without fat suppression was obtained (repetition time/echo time: 4060-5610/89-93; flip angle: 180°; field of view: 360 mm; slice thickness: 4 mm with 1 mm intersection gap; and voxel size: 0.9 x 0.7 x 4 mm).

For DCE-MRI, perfusion acquisition consisted of a pre-contrast T₁ mapping at different flip angle (three acquisitions pre-contrast). Subsequently, intravenous-contrast Gadoterate acid (Gd-DOTA, Dotarem) was administered at a rate of 3 ml/sec followed by a flush of 10 ml sodium chloride at an equal rate with an automatic injector (MEDRAD) (6). Then, dynamic series were acquired in the mid-sagittal plane of the uterus (in 2D FLASH or 3D FLASH). The scan parameters for 2D FLASH were: repetition time/echo time: 230/1.1 ms; time of acquisition: 3:04 min; flip angle: 15°; field of view: 400 mm; 5 slices/slab; distance factor: 25%; slice thickness: 10 mm; number of measurements: 160; bandwidth: 1130 (Hz/Px); and voxel size: 2.6 x 2.1 x 10 mm. The scan parameters for 3D FLASH were: repetition time/echo time: 3.66/1.23 ms; time of acquisition: 5:53 min; flip angle: 20°; field of view: 360 mm; 1 slab; distance factor: 20%; slice thickness: 1.5 mm; number of measurements: 29; bandwidth: 360 (Hz/Px); and voxel size: 1.3 x 0.9 x 1.5 mm.

All images were sent to a dedicated workstation.

The 18 nulliparous non-users of contraception were scheduled to undergo DCE-MRI investigation during three phases of their menstrual cycle: follicular (n = 17), ovulatory (n = 17) and luteal (n = 16) phase. Due to practical considerations, three women underwent DCE-MRI, respectively, only during the follicular phase, follicular and ovulatory phase and ovulatory and luteal phase. This resulted in a total number of 50 examinations for the 18 nulliparous non-users of hormonal contraception. The 30 nulliparous users of contraception also underwent three DCE-MRI examinations during their cycle, which were not

divided into the different phases because of the suppression by the contraceptive hormones. Two women underwent only two MRI investigations during their cycle, and one woman underwent only one MRI investigation. This resulted in a total number of 86 examinations for this group. The primiparous women acquired one DCE-MRI examination during their cycle on a random day (because of practical considerations concerning their newborn). Seven of the 12 primiparous women not using contraception were in their follicular phase at the time of DCE-MRI investigation and 5 women were in the luteal phase of their cycle.

4.3.4 MR image analysis

All measurements were performed on a specialized workstation (MMWP, Syngo MMWP VE36A) using the measuring cursor included in the workstation's software. The measurements were carried out consecutively by two independent investigators, a radiologist with 13 years of experience in pelvic imaging and a resident in radiology with three years of pelvic MRI experience. Both observers were blinded for the clinical information of the women (whether or not they were nulliparous or primiparous and non-users or users of hormonal contraception). The T₂ TSE images obtained in the three anatomical planes before hyoscine butylbromide injection were first analyzed by the radiologist in order to detect possible suspicious findings of congenital or acquired uterine abnormalities. The corpus and cervix sizes latero-lateral (LL, transverse) were measured on the coronal T₂ TSE image obtained before hyoscine butylbromide injection. The T₂ TSE sagittal image after hyoscine butylbromide injection without fat suppression was used to measure the length and antero-posterior (AP) size of the corpus (figure 3). The volume of corpus uteri was calculated using the formula for an ellipsoid: length x height (AP) x width (LL) x 0.523 (12).

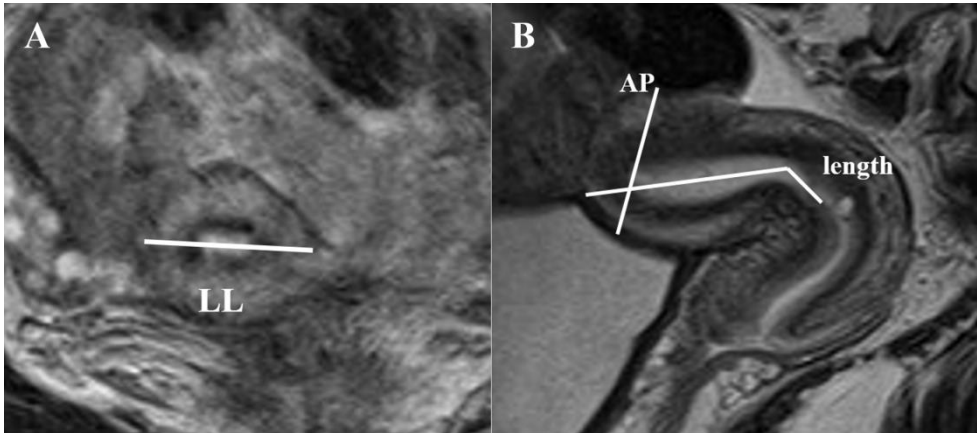


Figure 3: Dimensions measurements of the corpus uteri on sagittal and transversal magnetic resonance imaging (MRI). The sagittal T2-weighted MR image (B) was used to measure the antero-posterior (AP) uterine size and the length of the uterus, and the transversal T2 weighted image (A) was used to measure the latero-lateral (LL) uterine size.

The perfusion acquisitions were evaluated on Syngo Tissue 4D of Siemens. Two methods of evaluation were used: a quantitative method following the two compartment model of Tofts and a semi-quantitative evaluation method. The model of Tofts (11) comprises the following parameters: transfer constant (K^{trans}), interstitial volume fraction (V_e) and reflux constant (K_{ep}) (figure 1). The semi-quantitative evaluation method retrieves the following parameters: Time-to-Peak (TTP), Arrival Time (AT) and initial Area Under the Curve in 60 seconds (iAUC). The perfusion parameters analyzed in this study are: iAUC (in correlation with the uterus/cervix volume), K^{trans} , K_{ep} and V_e (9,10,13) (table 2).

Table 2: Description of the assessed perfusion parameters. EES: extravascular extracellular space.

Parameter	Description	Unit
iAUC/volume	Initial (first 60 seconds) area under the contrast agent concentration - time curve after contrast administration. It is an indicator for the amount of blood volume during the initial minute after the contrast agent enters the blood per unit mass of tissue. IAUC is evaluated in correlation with the volume of respectively the corpus or cervix uteri.	
K^{trans}	Transfer constant, the influx of contrast agent from the blood plasma into the EES, depends on capillary permeability, surface area and blood flow per unit mass of tissue.	min^{-1}
K_{ep}	Reflux constant, the efflux of contrast agent from the EES back into the blood plasma.	min^{-1}
V_e	EES volume fraction (K^{trans}/K_{ep}).	

In order to measure these parameters, Regions Of Interest (ROIs), with a diameter of 1 mm were placed in post-processing software at different places: the anterior and posterior wall of the JZ and outer myometrium (fundal and corpus region) (figure 4).

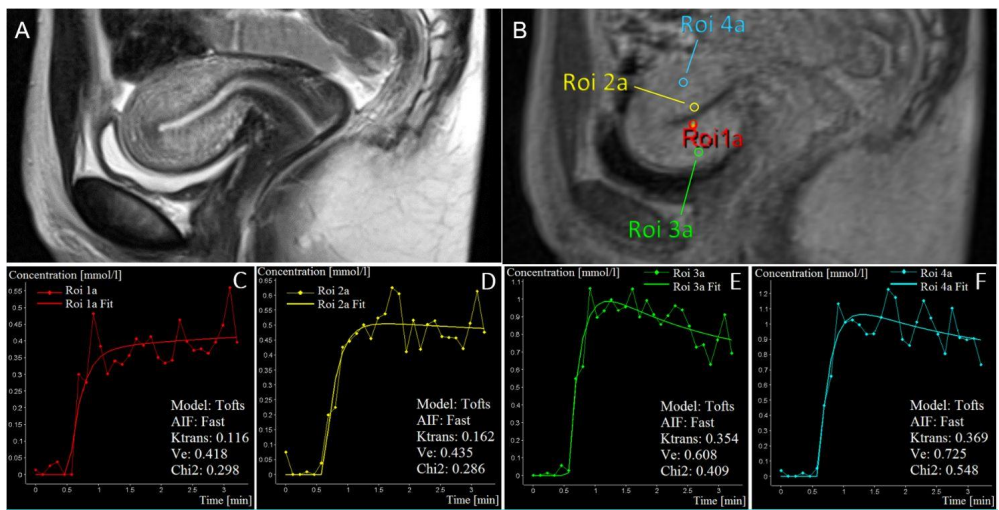


Figure 4: Example of perfusion assessment by dynamic contrast-enhanced magnetic resonance imaging (DCE-MRI) in the corpus and cervix uteri. A: Sagittal T_2 -weighted pelvic MRI-scan. B: Dynamic MRI-scan in order to assess perfusion Tissue 4D Calculations in different locations. The Regions of Interest (ROI) were placed at the anterior wall of the junctional zone (JZ) (ROI 1a), at the posterior wall of the JZ (ROI 2a), at the anterior wall of the outer myometrium (ROI 3a), at the posterior wall of the outer myometrium (ROI 4a), at the anterior wall of the inner third of the cervical stroma (ROI 1b), at the posterior wall of the inner third of the cervical stroma (ROI 2b), at the anterior wall of the outer two-thirds of the cervical stroma (ROI 3b) and at the posterior wall of the outer two-thirds of the cervical stroma (ROI 4b). C-J: Examples of concentration-time curves for respectively each ROI.

4.3.5 Statistical analysis

Mann-Whitney U-tests were performed in order to compare the uterine volumes between groups by means of IBM SPSS Statistics (version 23.0). All other statistical analyses were performed by means of the computer program SAS version 9.4. A significance level of 5% was used and no correction for multiple testing was applied.

Cohen's kappa coefficient was calculated in order to evaluate the concordance between the two readers for assessing the four perfusion parameters. Linear mixed models were used in order to investigate the effect of menstrual phase (for women not using hormonal contraception), the effect of parity and the effect of the location in uterine wall on the perfusion parameters iAUC/volume, K^{trans} , K_{ep} and V_e . The statistical model investigating the effect of phase in the nulliparous and primiparous non-users of hormonal contraception, included two main fixed effects and their interaction. The fixed effects were menstrual phase and the uterine location. In order to detect differences between groups, separate statistical models were constructed for nulliparous and primiparous women for each location including the fixed effect of hormonal contraception. The statistical models investigating the effect of uterine location, constructed for each group, contained the fixed effect of uterine location. The association between measurements of the same woman (e.g. measurements in different menstrual phases) was incorporated by means of a random intercept at woman level. A parsimonious model was obtained by backward elimination of interaction terms not statistically significant at a 5% level of significance. In order to normalize the data, statistical analyses were performed on the natural log transformed outcome data.

4.4 Results

The acquisition of the perfusion characteristics was accomplished successfully in 12 nulliparous non-users during the follicular phase, in 8 nulliparous non-users during the ovulatory and luteal phase, in 23 nulliparous users, in 5 primiparous non-users during the follicular phase, in 4 primiparous non-users during the luteal phase and in 33 primiparous users of contraception therapy. There was a

high concordance between the two observers regarding the perfusion parameter assessment, as Cohen’s kappa equated 0.87 for iAUC/volume, K^{trans} , K_{ep} and V_e together. No correlations were found between the perfusion parameters and the women’s height and weight, age at menarche, gestity and parity status and smoker/non-smoker ($p > 0.050$).

4.4.1 Uterine volumes

The uterine volume in the nulliparous contraceptive users was significantly lower compared to the nulliparous non-users during the ovulatory ($p = 0.002$) and luteal ($p = 0.002$) phase (table 3). The uterine volume of these groups during the follicular phase was not significantly different ($p = 0.101$). No statistically significant differences were noticed in the uterine volumes between both groups of primiparous women or between the nulliparous and primiparous non-users of contraceptives ($p > 0.050$).

Table 3: Volumes of corpus uteri in nulliparous and primiparous non-users and users of hormonal contraception therapy during three menstrual phases. Data represents median (minimum – maximum). Data analysis was carried out on the natural log transformed outcome data. [□]: significantly different from the volume of nulliparous users of hormonal contraception.

		Volume corpus uteri (cm ³)	n
Nulliparous non-users	Follicular phase	100.27 (49.02 - 183.24)	17
	Ovulatory phase	107.81 (58.86 - 197.48) [□]	14
	Luteal phase	105.91 (55.40 - 212.20) [□]	14
Nulliparous users		70.34 (27.36 - 156.05)	30
Primiparous non-users	Follicular phase	81.69 (54.05 - 150.06)	5
	Luteal phase	137.57 (35.71 - 204.83)	4
Primiparous users		91.99 (30.29 - 187.51)	37

4.4.2 Perfusion parameters throughout the menstrual cycle

The perfusion parameters assessed during the three menstrual phases in the nulliparous non-users of hormonal contraception were compared. K^{trans} and $iAUC/volume$ were significantly different between the menstrual phases, whereas K_{ep} and Ve were not ($p > 0.050$). K^{trans} and $iAUC/volume$ decreased over the menstrual cycle, from follicular to ovulatory to luteal phase (table 4).

Table 4: DCE-MRI perfusion parameters ($iAUC/volume$, K^{trans} , K_{ep} and Ve) assessed in nulliparous and primiparous non-users of hormonal contraception during different menstrual phases. Data represents mean values over all measured locations. Data analysis was carried out on the natural log transformed outcome data. *: significantly different from the luteal phase of the same group; Δ : significantly different from the ovulatory phase of the same group; \square : significantly different from the same phase of the other group.

		$iAUC/volume$	K^{trans} (min^{-1})	K_{ep} (min^{-1})	Ve
Nulliparous non-users	Follicular phase	1.28 *	0.82 Δ *	0.43 \square	1.13
	Ovulatory phase	1.23 *	0.42	0.35	0.96
	Luteal phase	0.68	0.55	0.59	1.12
Primiparous non-users	Follicular phase	1.27	0.52	0.38	1.46
	Luteal phase	1.28	0.38	0.36	0.78

K^{trans} significantly decreased during the ovulatory ($p = 0.008$) and luteal ($p = 0.027$) phase compared to the follicular phase. Furthermore, $iAUC/volume$ decreased during the luteal phase in comparison to the follicular ($p < 0.001$) and ovulatory ($p = 0.001$) phase. In the primiparous non-users, the perfusion parameters of the women in the follicular phase were not significantly different from those in the women in the luteal phase ($p > 0.050$).

Furthermore, the perfusion parameters during the follicular and luteal phases in the nulliparous and primiparous women were also compared. This revealed that K_{ep} was significantly higher in the nulliparous women than in the primiparous women during the follicular phase ($p = 0.041$), but not during the luteal phase ($p > 0.050$). The other perfusion parameters showed no significant differences between the nulliparous and the primiparous non-users.

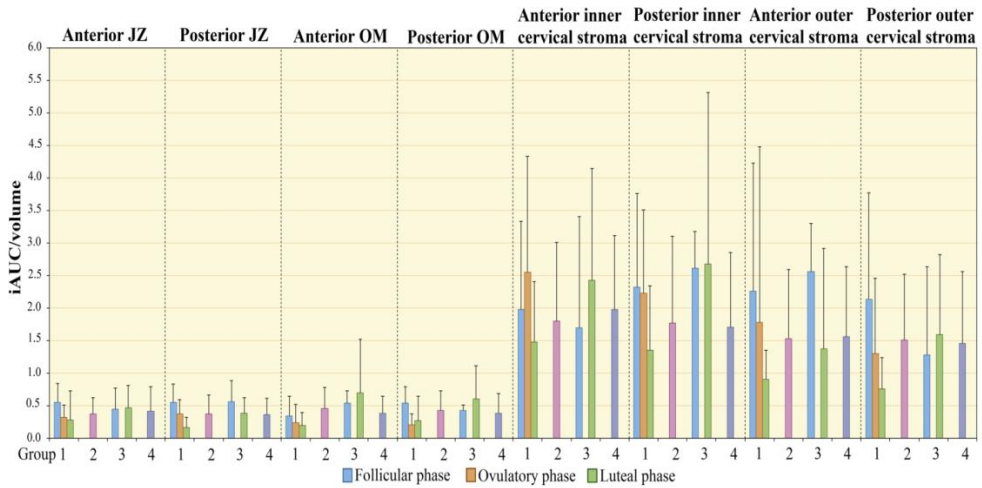


Figure 5: Mean (and SD) initial blood volumes (iAUC/volume) values of the junctional zone (JZ), outer myometrium (OM) and cervical inner third and outer two-thirds stroma. Initial blood volume was assessed in nulliparous non-users (group 1), nulliparous users (group 2), primiparous non-users (group 3) and primiparous users (group 4) of hormonal contraception during the menstrual cycle at different locations in the uterus and cervix.

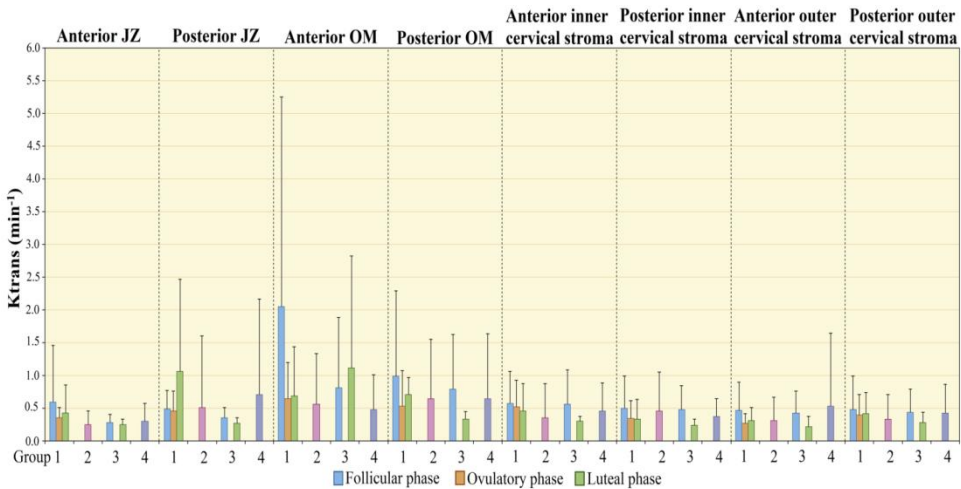


Figure 6: Mean (and SD) transfer constant (Ktrans) in the junctional zone (JZ), outer myometrium (OM) and cervical inner third and outer two-thirds stroma. The transfer constant was assessed in nulliparous non-users (group 1), nulliparous users (group 2), primiparous non-users (group 3) and primiparous users (group 4) of hormonal contraception during the menstrual cycle at different locations in the uterus and cervix.

4.4.3 Perfusion Parameters In Junctional Zone and Outer Myometrium

The median, minimum and maximum of iAUC/volume, K^{trans} , K_{ep} and V_e measurements are shown in respectively table 5, 6, 7 and 8. There were no significant differences between the anterior and posterior uterine wall in either perfusion parameter for each group ($p > 0.050$), except for the nulliparous users of hormonal contraception. In this group, a significantly higher K^{trans} was noticed in the posterior wall of the JZ compared to the anterior wall of the JZ ($p = 0.041$).

Table 5: Initial blood volume (iAUC/volume) measurements in nulliparous and primiparous non-users and users of hormonal contraception in the anterior and posterior junctional zone (JZ) and outer myometrium (OM). 5A: Data represents median values(minimum - maximum). Data analysis was carried out on the natural log transformed outcome data. ^Δ: significantly different from anterior and posterior JZ and outer myometrium of the same group; *: significantly different from nulliparous users in the same location; •: significantly different from primiparous users in the same location. **5B** an overview of the standard deviation for each location in every group.

5A

iAUC/volume		Anterior wall JZ ^Δ	Posterior wall JZ ^Δ	Anterior wall OM ^Δ	Posterior wall OM ^Δ
Nulliparous non-users	Follicular phase	0.56 (0.14 - 1.33)	0.48 (0.22 - 1.08)	0.23 (0.00 - 0.99)	0.53 (0.16 - 0.92)
	Ovulatory phase	0.39 (0.09 - 0.61)	0.39 (0.10 - 0.77)	0.15 (0.00 - 0.82)	
	Luteal phase	0.14 (0.00 - 1.28)	0.14 (0.00 - 0.42)	0.14 (0.00 - 0.56)	
Nulliparous users *		0.29 (0.03 - 1.17)	0.29 (0.00 - 1.64)	0.44 (0.01 - 1.50)	0.35 (0.00 - 1.14)
Primiparous non-users	Follicular phase	0.59 (0.08 - 0.67)	0.66 (0.20 - 0.82)	0.59 (0.33 - 0.70)	0.39 (0.36 - 0.52)
	Luteal phase	0.36 (0.17 - 0.86)	0.33 (0.17 - 0.64)	0.36 (0.11 - 1.64)	
Primiparous users •		0.29 (0.09 - 2.14)	0.29 (0.00 - 1.07)	0.36 (0.00 - 0.87)	0.35 (0.00 - 1.19)

5B

iAUC/volume		Anterior wall JZ Δ	Posterior wall JZ Δ	Anterior wall OM Δ	Posterior wall OM Δ
Nulliparous non-users	Follicular phase	0,557 (\pm 0,293)	0,552 (\pm 0,279)	0,342 (\pm 0,300)	0,540 (\pm 0,252)
	Ovulatory phase	0,326 (\pm 0,181)	0,371 (\pm 0,228)	0,241 (\pm 0,283)	* 0,213 (\pm 0,161)
	Luteal phase	0,278 (\pm 0,449)	0,168 (\pm 0,156)	0,196 (\pm 0,205)	0,275 (\pm 0,375)
Nulliparous users *		0,371 (\pm 0,260)	0,374 (\pm 0,299)	0,463 (\pm 0,324)	0,429 (\pm 0,302)
Primiparous non-users	Follicular phase	0,449 (\pm 0,319)	0,563 (\pm 0,323)	0,540 (\pm 0,187)	0,427 (\pm 0,084)
	Luteal phase	0,465 (\pm 0,355)	0,382 (\pm 0,240)	0,702 (\pm 0,819)	• 0,601 (\pm 0,521)
Primiparous users •		0,415 (\pm 0,382)	0,364 (\pm 0,254)	0,391 (\pm 0,253)	0,391 (\pm 0,295)

Comparison of the perfusion parameters of the JZ with those of the outer myometrium demonstrated several differences. These differences were noticed only in the anterior uterine wall. In the nulliparous non-users, the K_{ep} was significantly higher and K^{trans} significantly lower in the anterior JZ compared to the anterior outer myometrium ($p = 0.012$ and $p = 0.050$, respectively). Furthermore, there was a trend towards a higher iAUC/volume in the anterior JZ wall compared to the anterior outer myometrium wall in this group ($p = 0.060$). In the nulliparous users, K^{trans} in the anterior wall of the JZ was significantly lower than in the anterior outer myometrium wall ($p < 0.001$). V_e in the anterior JZ wall in the primiparous users was significantly lower compared to the anterior wall of the outer myometrium ($p = 0.012$).

Table 6: Transfer constant (K^{trans}) measurements in nulliparous and primiparous non-users and users of hormonal contraception in the anterior and posterior junctional zone (JZ) and outer myometrium (OM). 6A: Data represents median values (minimum – maximum). Data analysis was carried out on the natural log transformed outcome data. □: significantly different from posterior JZ of the same group, Δ: significantly different from anterior OM of the same group; *: significantly different from nulliparous non-users in the same location. **6B** an overview of the standard deviation for each location in every group.

6A

Ktrans (min-1)		Anterior wall JZ	Posterior wall JZ _□	Anterior wall OM _Δ	Posterior wall OM
Nulliparous non-users	Follicular phase	0,593 (± 0,865)	0,484 (± 0,285)	^Δ 2,051 (± 3,203)	0,990 (± 1,297)
	Ovulatory phase	0,351 (± 0,164)	^Δ 0,454 (± 0,306) *	0,641 (± 0,555)	0,528 (± 0,545)
	Luteal phase	0,430 (± 0,424)	1,061 (± 1,406)	0,683 ± (0,754)	0,710 ± (0,253)
Nulliparous users *		0,247 (± 0,214)	_□ 0,509 (± 1,090) _Δ	0,558 (± 0,774)	0,641 (± 0,907)
Primiparous non-users	Follicular phase	0,276 (± 0,133)	0,357 (± 0,149)	0,812 (± 1,075)	0,793 (± 0,834)
	Luteal phase	0,247 (± 0,091)	0,269 (± 0,082)	1,119 (± 1,699)	0,337 (± 0,110)
Primiparous users		0,303 (± 0,271)	0,703 (± 1,462)	0,481 (± 0,529)	0,647 (± 0,984)

6B

K^{trans} (min^{-1})		Anterior wall JZ	Posterior wall JZ \square	Anterior wall OM Δ	Posterior wall OM
Nulliparous non-users	Follicular phase	0.34 (0.20 - 3.30)	0.46 (0.19 - 1.12)	0.43 (0.20 - 8.72)	0.47 (0.08 - 4.10)
	Ovulatory phase	0.24 (0.16 - 0.58)	Δ 0.27 (0.14 - 0.97)	* 0.45 (0.11 - 1.72)	0.36 (0.10 - 1.79)
	Luteal phase	0.19 (0.14 - 1.32)	0.63 (0.16 - 4.40)	0.36 (0.10 - 2.17)	0.74 (0.32 - 1.12)
Nulliparous users *		0.17 (0.03 - 1.05)	\square 0.20 (0.03 - 7.18)	0.31 (0.02 - 5.40)	0.33 (0.06 - 5.60)
Primiparous non-users	Follicular phase	0.28 (0.13 - 0.45)	0.35 (0.16 - 0.54)	0.42 (0.14 - 2.72)	0.46 (0.11 - 2.20)
	Luteal phase	0.24 (0.15 - 0.36)	0.29 (0.15 - 0.35)	0.33 (0.14 - 3.66)	0.34 (0.21 - 0.45)
Primiparous users		0.19 (0.06 - 1.10)	0.33 (0.08 - 2.91)	0.25 (0.07 - 6.89)	0.31 (0.08 - 3.69)

4.4.4 *Perfusion Parameters in Nulliparous And Primiparous Non-users And Users Of Hormonal Contraception*

In the nulliparous women on hormonal contraception, K^{trans} was lower in the anterior and posterior wall of the JZ than in the non-users of hormonal contraception ($p = 0.001$ and $p = 0.013$, respectively) (table 6). K_{ep} and iAUC/volume in the anterior wall of the outer myometrium was higher in the nulliparous users of hormonal contraception compared to the non-users ($p = 0.049$ and $p = 0.001$) (table 7 and 5).

Table 7: Reflux constant (K_{ep}) measurements in nulliparous and primiparous non-users and users of hormonal contraception in the anterior and posterior junctional zone (JZ) and outer myometrium (OM). Data represents median values(minimum – maximum). Data analysis was carried out on the natural log transformed outcome data. ^A: significantly different from anterior OM of the same group; * significantly different from nulliparous users in the same location. **7B**: an overview of the standard deviation for each location in every group.

ZA

K_{ep} (min^{-1})		Anterior wall JZ	Posterior wall JZ	Anterior wall OM Δ	Posterior wall OM
Nulliparous non-users	Follicular phase	0.49 (0.00 - 3.49)	0.40 (0.00 - 1.77)	0.00 (0.00 - 0.64)	0.30 (0.00 - 1.17)
	Ovulatory phase	0.37 (0.00 - 0.62)	0.29 (0.00 - 1.15)	0.17 (0.00 - 0.70)	0.24 (0.00 - 0.61)
	Luteal phase	0.25 (0.00 - 2.69)	0.34 (0.00 - 1.52)	0.31 (0.00 - 0.67)	0.42 (0.00 - 10.73)
Nulliparous users *		0.25 (0.00 - 1.99)	0.28 (0.00 - 1.06)	0.33 (0.00 - 1.63)	0.30 (0.00 - 2.34)
Primiparous non-users	Follicular phase	0.26 (0.00 - 0.38)	0.42 (0.32 - 0.55)	0.22 (0.00 - 2.91)	0.48 (0.16 - 2.40)
	Luteal phase	0.30 (0.21 - 0.41)	0.51 (0.17 - 0.55)	0.24 (0.00 - 0.45)	0.40 (0.28 - 0.71)
Primiparous users		0.28 (0.00 - 2.44)	0.35 (0.00 - 2.59)	0.31 (0.00 - 2.91)	0.25 (0.00 - 4.93)

7B

K_{ep} (min-1)		Anterior wall JZ	Posterior wall JZ	Anterior wall OM ^Δ	Posterior wall OM
Nulliparous non-users	Follicular phase	0,719 (± 0,895)	0,462 (± 0,475)	0,213 (± 0,251)	0,350 (± 0,380)
	Ovulatory phase	0,327 (± 0,238)	^Δ 0,375 (± 0,371)	0,226 (± 0,287)	* 0,218 (± 0,226)
	Luteal phase	0,490 (± 0,904)	0,480 (± 0,546)	0,288 (± 0,272)	1,681 (± 3,678)
Nulliparous users *		0,325 (± 0,317)	0,309 (± 0,244)	0,398 (± 0,358)	0,419 (± 0,463)
Primiparous non-users	Follicular phase	0,190 (± 0,178)	0,422 (± 0,092)	0,726 (± 1,238)	0,890 (± 0,909)
	Luteal phase	0,305 (± 0,089)	0,434 (± 0,180)	0,236 (± 0,189)	0,449 (± 0,201)
Primiparous users		0,358 (± 0,421)	0,479 (± 0,491)	0,437 (± 0,560)	0,444 (± 0,859)

In the primiparous women, V_e in the anterior wall of the JZ was significantly lower in the users than in the non-users of hormonal contraception ($p = 0.044$) (table 8). iAUC/volume in the anterior wall of the outer myometrium decreased in the primiparous users of hormonal contraception compared to the non-users ($p = 0.036$).

Table 8: Interstitial volume (V_e) measurements in nulliparous and primiparous non-users and users of hormonal contraception in the anterior and posterior junctional zone (JZ) and outer myometrium (OM). Data represents median values (minimum – maximum). Data analysis was carried out on the natural log transformed outcome data. ^Δ: significantly different from anterior wall outer myometrium of the same group; •: significantly different from primiparous users in the same location. **8B**: an overview of the standard deviation for each location in every group.

8A

Ve		Anterior wall JZ	Posterior wall JZ	Anterior wall OM ^Δ	Posterior wall OM
Nulliparous non-users	Follicular phase	0.70 (0.48 - 1.78)	0.81 (0.47 - 5.43)	0.88 (0.00 - 1.63)	0.88 (0.55 - 1.90)
	Ovulatory phase	0.79 (0.42 - 1.59)	0.85 (0.46 - 2.10)	0.89 (0.09 - 3.04)	0.79 (0.53 - 3.99)
	Luteal phase	0.69 (0.05 - 1.89)	0.76 (0.00 - 2.22)	0.79 (0.00 - 2.40)	0.93 (0.08 - 2.00)
Nulliparous users		0.68 (0.00 - 82.66)	0.66 (0.00 - 1.76)	0.76 (0.00 - 4.08)	0.79 (0.00 - 4.31)
Primiparous non-users	Follicular phase	0.92 (0.48 - 14.13)	0.85 (0.52 - 0.99) •	0.94 (0.69 - 2.28)	0.91 (0.70 - 1.04)
	Luteal phase	0.83 (0.63 - 0.98)		0.91 (0.70 - 1.22)	0.80 (0.63 - 0.92)
Primiparous users •		0.68 (0.31 - 2.01) ^Δ	0.66 (0.33 - 2.24)	0.80 (0.40 - 1.84)	0.80 (0.00 - 4.37)

8B

Ve		Anterior wall JZ	Posterior wall JZ	Anterior wall OM _Δ	Posterior wall OM
Nulliparous non-users	Follicular phase	0,783 (± 0,347)	1,213 (± 1,385)	0,918 (± 0,444)	0,940 (± 0,378)
	Ovulatory phase	0,900 (± 0,444)	0,977 (± 0,534)	1,149 (± 0,945)	1,446 (± 1,247)
	Luteal phase	0,890 (± 0,630)	0,883 (± 0,657)	0,903 (± 0,701)	1,090 (± 0,618)
Nulliparous users		2,142 (± 10,376)	0,680 (± 0,381)	0,880 (± 0,617)	0,933 (± 0,787)
Primiparous non-users	Follicular phase	3,497 (± 5,946)	0,822 (± 0,188)	1,321 (± 0,677)	0,882 (± 0,133)
	Luteal phase	0,818 (± 0,150)	0,668 (± 0,190)	0,936 (± 0,213)	0,786 (± 0,119)
Primiparous users ●		0,776 (± 0,389) Δ	0,724 (± 0,348)	0,898 (± 0,407)	1,000 (± 0,875)

4.5 Discussion

To our knowledge, this study is the first in literature comparing DCE-MRI perfusion characteristics of the JZ and the outer myometrium in young healthy nulliparous and primiparous women, subdivided by their use of contraception therapy. Moreover, we used acquisition parameters with 1.5 mm slice thickness (3D FLASH) and DCE within three seconds per measurement over a time period of more than three minutes on a 1.5T MRI, most commonly used in daily clinical practice. These data could be useful in future attempts in assisted reproductive treatments or in detecting pathological uterine conditions.

The first description of healthy myometrial enhancement by 1.5T DCE-MRI was reported by Yamashita et al. in 1993, who investigated 27 healthy women (14). Another study assessed physiological microvascular perfusion of normal myometrium in 62 women of reproductive age using DCE-MRI, in which a 1.5T MRI scanner and a slice thickness of 5 mm was used (9). However, this study made no distinction based on the parity or the use of hormonal contraception and the women were investigated only once during their menstrual cycle.

In our study, nulliparous women who used hormonal contraceptives had a smaller uterine volume than nulliparous women who did not use hormonal contraceptives, during the ovulatory and luteal phase. Merz et al. investigated uterine volumes on transvaginal ultrasound in a group consisting of 52 nulliparous, 52 primiparous and 53 multiparous women, and detected a parity-related enlargement in uterine size (15). This result could not be derived from the measurements of our study.

We focused on investigating the perfusion of the JZ and outer myometrium by assessing the following physiological parameters: initial blood volume ($iAUC/volume$), transfer constant (K^{trans}), efflux constant (K_{ep}) and interstitial volume (V_e). Previously it is demonstrated that the uterine myometrial wall contains a discontinuity and that the inner third contains a different morphology than the outer two-thirds. This inner third is known as the junctional zone. Investigations on uterine specimens revealed a higher vascular perfusion rate in the JZ compared to the outer myometrium (16). This finding correlates with the

results of our study which show a higher reflux constant (K_{ep}) in nullipara non-users at the anterior JZ compared to the anterior outer myometrium. Furthermore, histological analysis studies on myometrial tissue found a threefold increase in percentage of nuclear area and cellular density, a decrease in extracellular matrix and a lower water content in the inner myometrium in comparison with the outer myometrium (17-19). These findings are also in concordance with our results, which indicate a lower transfer constant (K^{trans}) in nulliparous users of hormonal contraception and a lower interstitial volume (V_e) in primiparous users of hormonal contraception at the anterior JZ than at the anterior outer myometrium. Our results confirm the physiological differences between the inner third and the outer two-thirds of the myometrium, with dissimilar microvascular characteristics in both layers. These findings are as expected as a high JZ perfusion (due to higher transfer constant, lower efflux constant and higher initial blood volume than in the outer myometrium) in nulliparous non-users of contraceptives is believed to be involved in uterine contraction and subsequent transfer of spermatozoa and in embryo implantation (20,21).

It is known that, in women of reproductive age, the JZ demonstrated cyclic variations in blood flow throughout the menstrual cycle. This is already demonstrated by means of 3D power Doppler angiography and more recently also by means of DCE-MRI (9). In our study, the highest initial blood volume in the JZ was also found during the follicular phase, followed by a decrease in initial blood volume during the luteal phase. These findings can be explained by the development of small vessels, such as spiral arteries, in the inner myometrium during the follicular phase (1,22). In addition, just before ovulation, estradiol serum levels and a transient increase in myometrial basal tone and uterine contractility could also explain the higher blood volume (23,24). Doppler ultrasound differences in internal myometrial perfusion during the menstrual cycle are well described and are believed to be involved in migration of spermatozoa (contraction) and in embryo implantation. Raine-Fenning et al. characterized, based on Doppler ultrasound findings, an increased vascularisation in the JZ during the proliferative (follicular) phase, peaking

approximately three days prior to ovulation before decreasing to a nadir 5 days post-ovulation (20).

The study by Thomassin-Naggara et al. examined perfusion of the inner (JZ) and outer myometrium in 62 women of reproductive age (31 women in the proliferative phase and 31 women in the luteal phase) by DCE-MRI (used MRI acquisition characteristics: repetition time/echo time: 27/2.24 ms; flip angle: 80°; slice thickness: 5 mm; number of slices: 3; excitations: 1; field of view: 400–200 mm; interpolated matrix 256 × 134; bandwidth (BW): 300) and they found behavioral differences in inner myometrium in the different menstrual phases, whereas no differences in the outer myometrium were demonstrated (9). In the JZ, they noticed a higher tissue blood flow (F) and blood volume fraction (Vb) during the follicular phase than during the luteal phase. Nevertheless, they did not observe differences between those phases for permeability-surface area product (PS, which is correlated with K^{trans} , V_e and K_{ep}) and interstitial volume (V_e) in the JZ (9). Thomassin-Naggara and colleagues performed the study on women of all ages (whereas in our study the age limits were between 18 and 35 years), made no distinction between nulliparous and multipara women and between women who used contraception therapy and those who did not, and MRI examination was performed once in a woman's menstrual cycle.

The findings obtained with Doppler ultrasound and DCE-MRI, including our study and the study by Thomassin-Naggara et al., are thus consistent. However, DCE-MRI is more sensitive than Doppler ultrasound in the evaluation of myometrial flow, especially at the edges of the uterus and for retroverted uteri (2,25). In addition, DCE-MRI allows quantification of perfusion parameters, which is not obvious in Doppler ultrasound.

A limitation of our study is the low number of participating women, especially in the group of primiparous non-users of contraception therapy. Another limitation is that not all women underwent three MRI investigations per menstrual cycle, the nulliparous women were scanned three times during the menstrual cycle, whereas the primiparous women were investigated once. In addition, although this study included healthy nulliparous women, it is unknown if they are to have any reproductive challenges in the future.

In conclusion, this study provides DCE-MRI perfusion parameters (iAUC/volume, K^{trans} , K_{ep} and V_e) of the JZ and outer myometrium in a healthy population of nulliparous and primiparous women who use and did not use hormonal contraception. Our data showed that in nulliparous non-users of contraception therapy, especially the transfer constant (K^{trans}) and the initial uterine blood volume (iAUC/volume), demonstrated cyclic changes according to the menstrual cycle. In addition, the use of hormonal contraceptives led often to a reduction in transfer constant (K^{trans}) in the JZ. These perfusion characteristics of healthy JZ and outer myometrium can be expected to aid the diagnosis and/or therapeutic intervention of conditions of the female reproductive system and to characterize the myometrium, especially the JZ, in the context of assisted reproductive therapy in infertile patients.

4.6 References

1. Chard T, Grudzinskas JG. The Uterus - Anatomy of the Uterus - Nutrition; p. 29-39: 1994.
2. Raine-Fenning NJ, Campbell BK, Kendall NR, Clewes JS, Johnson IR. Endometrial and subendometrial perfusion are impaired in women with unexplained subfertility. *Hum Reprod* 2004;19(11):2605-2614.
3. Girling JE, Rogers PA. Recent advances in endometrial angiogenesis research. *Angiogenesis* 2005;8(2):89-99.
4. Benagiano G, Brosens I, Carrara S. Adenomyosis: new knowledge is generating new treatment strategies. *Womens Health (Lond Engl)* 2009;5(3):297-311.
5. Schreinemacher MH, Backes WH, Slenter JM, et al. Towards endometriosis diagnosis by gadofosveset-trisodium enhanced magnetic resonance imaging. *PLoS One* 2012;7(3):e33241.
6. Sala E, Rockall A, Rangarajan D, Kubik-Huch RA. The role of dynamic contrast-enhanced and diffusion weighted magnetic resonance imaging in the female pelvis. *Eur J Radiol* 2010;76(3):367-385.
7. Steer CV, Tan SL, Mason BA, Campbell S. Midluteal-phase vaginal color Doppler assessment of uterine artery impedance in a subfertile population. *Fertil Steril* 1994;61(1):53-58.
8. Reynolds LP, Grazul-Bilska AT, Redmer DA. Angiogenesis in the female reproductive organs: pathological implications. *Int J Exp Pathol* 2002;83(4):151-163.

9. Thomassin-Naggara I, Balvay D, Cuenod CA, Daraï E, Marsault C, Bazot M. Dynamic contrast-enhanced MR imaging to assess physiologic variations of myometrial perfusion. *Eur Radiol* 2010;20(4):984-994.
10. Heye T, Boll DT, Reiner CS, Bashir MR, Dale BM, Merkle EM. Impact of precontrast T1 relaxation times on dynamic contrast-enhanced MRI pharmacokinetic parameters: T1 mapping versus a fixed T1 reference value. *J Magn Reson Imaging* 2014;39(5):1136-1145.
11. Tofts PS. Modeling tracer kinetics in dynamic Gd-DTPA MR imaging. *J Magn Reson Imaging* 1997;7(1):91-101.
12. Goldstein SR, Horii SC, Snyder JR, Raghavendra BN, Subramanyam B. Estimation of nongravid uterine volume based on a nomogram of gravid uterine volume: its value in gynecologic uterine abnormalities. *Obstet Gynecol* 1988;72(1):86-90.
13. Thomassin-Naggara I, Siles P, Balvay D, Cuenod CA, Carette MF, Bazot M. MR perfusion for pelvic female imaging. *Diagn Interv Imaging* 2013;94(12):1291-1298.
14. Yamashita Y, Harada M, Sawada T, Takahashi M, Miyazaki K, Okamura H. Normal uterus and FIGO stage I endometrial carcinoma: dynamic gadolinium-enhanced MR imaging. *Radiology* 1993;186(2):495-501.
15. Merz E, Miric-Tesanic D, Bahlmann F, Weber G, Wellek S. Sonographic size of uterus and ovaries in pre- and postmenopausal women. *Ultrasound Obstet Gynecol* 1996;7(1):38-42.
16. Lee JK, Gersell DJ, Balfe DM, Worthington JL, Picus D, Gapp G. The uterus: in vitro MR-anatomic correlation of normal and abnormal specimens. *Radiology* 1985;157(1):175-179.

17. Scoutt LM, Flynn SD, Luthringer DJ, McCauley TR, McCarthy SM. Junctional zone of the uterus: correlation of MR imaging and histologic examination of hysterectomy specimens. *Radiology* 1991;179(2):403-407.
18. McCarthy S, Scott G, Majumdar S, et al. Uterine junctional zone: MR study of water content and relaxation properties. *Radiology* 1989;171(1):241-243.
19. Brown HK, Stoll BS, Nicosia SV, et al. Uterine junctional zone: correlation between histologic findings and MR imaging. *Radiology* 1991;179(2):409-413.
20. Raine-Fenning NJ, Campbell BK, Kendall NR, Clewes JS, Johnson IR. Quantifying the changes in endometrial vascularity throughout the normal menstrual cycle with three-dimensional power Doppler angiography. *Hum Reprod* 2004;19(2):330-338.
21. Kido A, Togashi K, Nakai A, Kataoka ML, Koyama T, Fujii S. Oral contraceptives and uterine peristalsis: evaluation with MRI. *J Magn Reson Imaging* 2005;22(2):265-270.
22. Blackwell PM, Fraser IS. A morphometric and ultrastructural study of the microvessels of the functional zone of normal human endometrium with some notions on possible secretory functions of the endothelial cells. *Asia Oceania J Obstet Gynaecol* 1988;14(2):233-250.
23. Ijland MM, Evers JL, Dunselman GA, van Katwijk C, Lo CR, Hoogland HJ. Endometrial wavelike movements during the menstrual cycle. *Fertil Steril* 1996;65(4):746-749.
24. Kunz G, Beil D, Deininger H, Wildt L, Leyendecker G. The dynamics of rapid sperm transport through the female genital tract: evidence from vaginal sonography of uterine peristalsis and hysterosalpingoscintigraphy. *Hum Reprod* 1996;11(3):627-632.

25. Steer CV, Campbell S, Pampiglione JS, Kingsland CR, Mason BA, Collins WP. Transvaginal colour flow imaging of the uterine arteries during the ovarian and menstrual cycles. *Hum Reprod* 1990;5(4):391-395.

5. CHAPTER V: PERFUSION OF THE UTERINE WALL IN INFERTILE WOMEN ASSESSED BY DCE-MRI: A PILOT STUDY

Paper in progress

5.1 Abstract

Objectives: To prospectively assess the perfusion characteristics of the inner and outer myometrium by dynamic contrast-enhanced magnetic resonance imaging (DCE-MRI) in five infertile women during the menstrual cycle and to compare them with those in healthy nullipara women.

Methods: We performed pelvic DCE-MRI on five women with unexplained infertility (34, 26, 26, 24 and 27 years old) and 18 healthy nullipara women (mean age 26.4 years) during three menstrual phases. Perfusion parameters (K^{trans} and iAUC/volume) were analyzed for the anterior and posterior wall of junctional zone (JZ) and outer myometrium.

Results: Multiple K^{trans} and iAUC/volume measurements in the infertile women were beyond the range of measurements of the control group, meaning that these measurements were lower than the minimum assessment or higher than the maximum assessment in the control group.

Conclusions: The results suggest that the uterine perfusion could be disturbed in women with unexplained infertility, but this needs to be confirmed in studies on a larger series. DCE- MRI assessment of the inner and outer myometrium could potentially be useful to characterize the perfusion characteristics in the context of assisted reproductive therapy.

KEYWORDS: Uterus – Perfusion magnetic resonance imaging – Perfusion – Myometrium – Unexplained infertility

KEY POINTS:

1. Dynamic contrast-enhanced MRI enables assessment of myometrial perfusion in infertile women
2. DCE-MRI investigation in five infertile women suggest that myometrial perfusion is disturbed
3. Could potentially be useful in assisted reproductive therapy

5.2 Introduction

Infertility is a worldwide condition that affects about 14% of the couples in the general population (1, 2). The underlying cause is unknown in 15-30% of these couples (1). Diagnosis of unexplained infertility is made when the underlying reason is not identified after completion of standard fertility tests, such as tests to investigate whether the infertility is attributed to ovulatory disorders, tubal damage, uterine or peritoneal problems or male factors (1, 2).

Although the standard infertility tests investigate a broad spectrum of possibilities, the optimal requirements for uterine receptivity are not included. Uterine receptivity is influenced by the endometrium and the inner third of the myometrium, also called junctional zone (JZ) or stratum subvasculare. Both layers of the uterine wall are likely to be key determinants in successful embryo implantation (3,4). Until now, assessment of the JZ in the context of assisted reproductive therapy is mostly restricted to determination of its appearance and measurement of its thickness. Several studies revealed that the JZ thickness can be used in order to predict implantation failure after *in vitro* fertilization (IVF) since conception is less likely to occur if the JZ is thicker than in normal women without infertility history (5-7).

However, besides the thickness of the JZ, adequate JZ blood supply (perfusion) is generally considered a crucial necessity for embryo implantation (3, 4, 8). According to recent studies, JZ perfusion is suggested to be impaired in women with unexplained subfertility based on findings by ultrasonic Doppler angiography (4, 9, 10).

The specific myometrial vascularization is composed of branches of the uterine arteries that form an arcuate wreath. Radial arteries branch of the wreath and after passage in the JZ, these vessels are known as spiral arteries. These spiral arteries play an important part in both the non-pregnant and the pregnant uterus. Their contribution in the non-pregnant uterus is to supply the superficial layers of the endometrium with nutrients and to constrict in order to cause ischemia and necrosis of these layers resulting in endometrial shedding during menstruation (11). These arteries also demonstrate a pregnancy related remodeling occurring between week 8 and 18 of gestation (3, 8, 12). This process reflects the contribution of adequate blood supply in the JZ to a

successful pregnancy.

Dynamic contrast-enhanced magnetic resonance imaging (DCE-MRI) is often used to diagnose female pelvic diseases because it enables (semi-)quantitative assessment of physiological parameters of the microvasculature. With this technique, repeated T1-weighted MR images are acquired during and after a bolus injection of contrast agent. Afterwards, the leakage of the contrast agent from capillaries into the extravascular extracellular space (EES or interstitium) is evaluated by software assessing signal enhancement over time (13, 14).

This study aims to investigate the perfusion characteristics of the JZ and outer myometrium by means of DCE-MRI in five women with unexplained infertility and compares these measurements with those in healthy nulliparous women. The study hypothesized that the JZ and/or outer myometrial perfusion characteristics are altered in women with unexplained infertility.

5.3 Material and Methods

The study protocol and informed consent were approved by the local hospital ethics committee in order to perform this pilot study on healthy volunteers and infertile women (registration number 056).

5.3.1 Study population

We included five women with unexplained infertility and 18 healthy nulliparous women not using hormonal contraception (control group) in this pilot study from December 2007 to January 2012.

The infertile patients were referred for participation in our study by our hospital infertility center. The control women were recruited by contacting co-workers from our hospital, students and PhD students from the local university, personal contacts and by cooperation with external physicians. Exclusion criteria were age less than 18 years or more than 35 years, non-Caucasian origin, pregnancy, medical history of infertility or a gynecological history such as heavy, prolonged or irregular menstrual periods (for the control group), previous unknown uterine morphologic abnormality found on the first MRI examination, diminished renal function (assessed by creatinine levels collected prior to MRI investigation) and women with a pacemaker, clips or other MRI-incompatible implanted devices.

The age of the infertile women was 34, 26 and 26 and 24 and 27 years (mean: 27.4 years). The first three infertile women were not using ovarian stimulation therapy, whereas the latter two were on ovarian stimulation therapy. The mean age of the control group was 26.4 years (+/-SD).

All included women provided a written informed consent and filled out an epidemiological questionnaire in order to obtain information concerning their birth date, height, weight, age at menarche, parity status and smoking habits.

5.3.2 Blood laboratory tests

Blood samples were taken prior to each MRI examination in order to assess human chorionic gonadotrophin (hCG), creatinine, follicle-stimulating hormone (FSH), luteinizing hormone (LH), estradiol and progesterone levels. The follicular phase was considered around day 6-13 of the menstrual cycle, the ovulatory phase around day 14-16 and the luteal phase around day 17-28. The exact phase of the menstrual cycle was determined based on the FSH, LH, estradiol and progesterone levels.

5.3.3 Magnetic Resonance Imaging

DCE-MRI investigations were obtained with a 1.5T magnet unit (Siemens Magnetom Symphony Tim (4G-Dot upgraded), Erlangen, Germany; Software Syngo MR B15). The women were inserted with an intravenous catheter in the elbow crease. They were positioned on the table of the scanner in head-first supine position and an eight-channel receive only body array was placed on the pelvis.

The MRI examination started with a localizer sequence followed by T₂- weighted turbo spin echo(T₂TSE) sequences without fat-suppression in transversal, coronal and sagittal plane (repetition time/echo time: 5000-5100/88-89; flip angle: 180°; field of view: 320 x 370 mm; slice thickness: 5 mm with 1 mm intersection gap; and voxel size: 0.8-1.1 x 0.6-0.8 x 4-5 mm). In mutual agreement with the women, an intravenous injection of the abdominal -specific antispasmodic hyoscine butylbromide (buscopan, 1 ml, 20 mg/ml, Boehringer Ingelheim, Germany), diluted in sodium chloride (10 ml, 0.09%, Baxter, Lessines, Belgium) was administered in order to reduce bowel movements.

Then, another sagittal T_2 TSE image without fat suppression was obtained (repetition time/echo time: 4060-5610/89-93; flip angle: 180°; field of view: 360 mm; slice thickness: 4 mm with 1 mm intersection gap; and voxel size: 0.9 x 0.7 x 4 mm).

Perfusion acquisition consisted of a pre-contrast T_1 mapping at different flip angle (three acquisitions pre-contrast). IV-contrast Gadoterate acid (Gd-DOTA, Dotarem) was administered at a rate of 3 ml/sec followed by a flush of 10 ml sodium chloride at an equal rate with an automatic injector (MEDRAD) (15). Subsequently, dynamic series were acquired in the mid-sagittal plane of the uterus. The scan parameters for 2D FLASH were: repetition time/echo time: 230/1.1 ms; time of acquisition: 3:04 min; flip angle: 15°; field of view: 400 mm; 5 slices/slab; distance factor: 25%; slice thickness: 10 mm; number of measurements: 160; bandwidth: 1130 (Hz/Px); and voxel size: 2.6 x 2.1 x 10 mm. The scan parameters for 3D FLASH were: repetition time/echo time: 3.66/1.23 ms; time of acquisition: 5:53 min; flip angle: 20°; field of view: 360 mm; 1 slab; distance factor: 20%; slice thickness: 1.5 mm; number of measurements: 29; bandwidth: 360 (Hz/Px); and voxel size: 1.3 x 0.9 x 1.5 mm.

All images were sent to a dedicated workstation.

The first three women with unexplained infertility, not on ovarian stimulation therapy, underwent DCE-MRI examinations during the follicular ($n = 3$), ovulatory ($n = 3$) and luteal ($n = 2$) phase, but one of these women only had investigations during the follicular and ovulatory phase. The fourth infertile woman, on ovarian stimulation therapy, underwent DCE-MRI examination during the follicular phase, whereas the other woman on ovarian stimulation therapy, the fifth woman, underwent DCE-MRI examination during the ovulatory and luteal phase.

The 18 control women were also scheduled to undergo DCE-MRI investigation during three phases of their menstrual cycle: the follicular ($n = 17$), ovulatory ($n = 17$) and luteal ($n = 16$) phase. Due to practical considerations, one woman underwent MRI only during the follicular phase, one woman during the follicular and ovulatory phase and one woman during the ovulatory and luteal phase.

5.3.4 MR image analysis

The measurements were performed on a specialized workstation (MMWP, Syngo MMWP VE36A) using the measuring cursor included in the workstation's software. All measurements were carried out consecutively by two independent investigators, a radiologist with 13 years of experience in pelvic imaging and an intern in radiology with three years of pelvic MRI experience. Both observers were blinded for the clinical information of the women.

The T₂TSE images obtained in the three anatomical planes before buscopan injection were first analyzed by the radiologists in order to detect possible suspicious findings of congenital or acquired uterine abnormalities. The corpus and cervix sizes latero-lateral (LL, transverse) were measured on

the coronal T₂ TSE image obtained before hyoscine butylbromide injection. The T₂ TSE sagittal image after hyoscine butylbromide injection without fat suppression was used to measure the length and antero-posterior (AP) size of corpus and cervix uteri (figure 1). The volumes of corpus and cervix uteri were calculated using the formula for an ellipsoid: length x height (AP) x width (LL) x 0.523 (16).

The perfusion acquisitions were evaluated on Syngo Tissue 4D of Siemens, an advanced post-processing software for pharmacokinetic modeling of DCE-MRI datasets (17). Two methods of evaluation were used, a quantitative method according to the pharmacokinetic Tofts' model and a semi-quantitative evaluation method. The model of Tofts [18] comprises the following parameters: contrast transfer coefficient (K^{trans}), interstitial volume fraction (Ve) and interstitial coefficient transfer (Kep). The semi-quantitative evaluation method retrieves the following parameters: Time-to-Peak (TTP), Arrival Time (AT) and initial Area Under Curve in 60 seconds (iAUC).

The perfusion parameters obtained in this study are K^{trans} and $iAUC$ (incorrelation with corpus/cervix uteri volume)(figure 1and table 1) (19, 20).

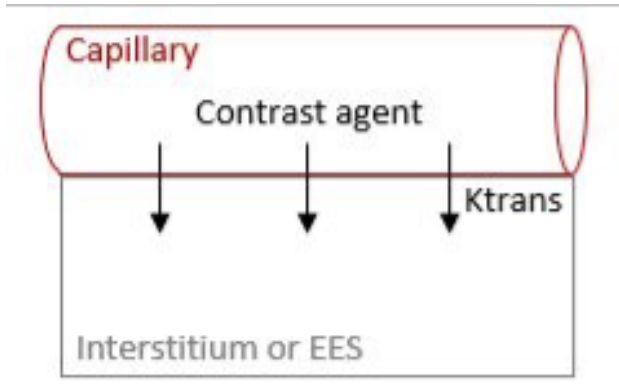


Figure 1: Representation of the two-compartment model of Tofts depicting the transfer constant. The transfer constant represents the influx of contrast agent from the blood plasma in the capillary into the interstitium or extravascular-extracellular space (EES).

Table 1: Description of the assessed perfusion parameters K^{trans} and $iAUC/volume$.

Parameter	Description	Unit
K^{trans}	Transfer constant, the influx of contrast agent from the blood plasma into the EES, depends on capillary permeability, surface area and blood flow per unit mass of tissue.	min^{-1}
$iAUC/volume$	Initial (first 60 seconds) area under the contrast agent concentration - time curve after contrast administration. It is an indicator for the amount of blood volume during the initial minute after the contrast agent enters the blood per unit mass of tissue. $iAUC$ is evaluated in correlation with the volume of respectively the corpus or cervix uteri.	

In order to measure these parameters, four regions of interest (ROIs) with a diameter of 1 mm were placed at different places: the anterior and posterior wall of the JZ and outer myometrium (fundal and corpus region) (figure 2).

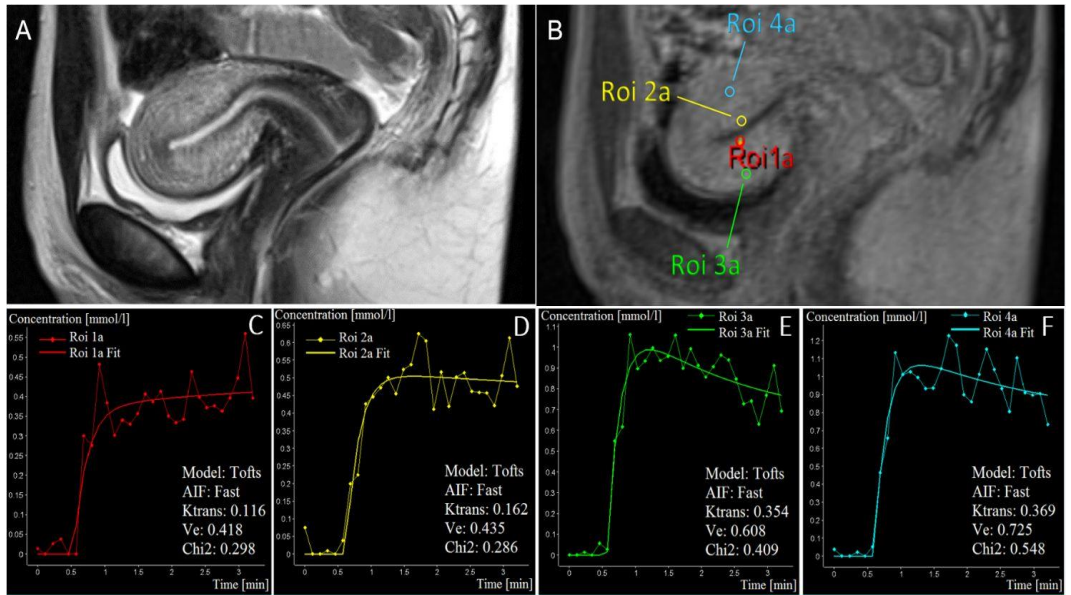


Figure 2: Example of perfusion assessment by dynamic contrast-enhanced magnetic resonance imaging (DCE-MRI) in the corpus and cervix uteri. A: Sagittal T₂-weighted pelvic MRI-scan. B: Dynamic MRI-scan in order to assess perfusion Tissue 4D Calculations in different locations. The Regions of Interests (ROI's) were placed at the anterior wall of the junctional zone (ROI 1a), at the posterior wall of the junctional zone (ROI 2a), at the anterior wall of the outer myometrium (ROI 3a), at the posterior wall of the outer myometrium (ROI 4a), at the anterior wall of the inner third of the cervical stroma (ROI 1b), at the posterior wall of the inner third of the cervical stroma (ROI 2b), at the anterior wall of the outer two-thirds of the cervical stroma (ROI 3b) and at the posterior wall of the outer two-thirds of the cervical stroma (ROI 4b). C-J: Examples of concentration-time curves for respectively each ROI.

5.3.5 Statistical analysis

All statistical analyses were performed by means of the computer program SAS version 9.4. No correction for multiple testing was applied. Cohen's kappa coefficient was calculated in order to evaluate the concordance between the two investigators.

The number of infertile women was too low to perform statistics. Therefore, we discussed the data purely by observation. For the control group, linear mixed models were fitted in order to compare the perfusion parameters throughout the menstrual cycle. This linear mixed model contained two main fixed effects, the menstrual phase and location in the uterine wall, and their interaction. The association between measurements of the same woman (e.g. measurements in different menstrual phases) was incorporated by means of a random intercept at woman level. A parsimonious model was obtained by backward elimination of interaction terms not statistically significant at a 5% level of significance. In order to normalize the data, statistical analyses were performed on the natural log transformed outcome data.

5.4 Results

K^{trans} and iAUC/volume measurements through out the menstrual cycle are discussed for the JZ and outer myometrium separately. The measurements are represented in tables 2 and 3.

5.4.1 Transfer Constant Of The Junctional Zone

In the first infertile woman, the anterior and posterior wall of the JZ demonstrated an increase in K^{trans} from the follicular phase (0.26 and 0.39 min^{-1} , respectively) to the ovulatory phase (0.59 and 0.85 min^{-1} , respectively), followed by a decrease during the luteal phase (0.29 and 0.25 min^{-1} , respectively). The second woman showed a slight decrease in K^{trans} throughout the menstrual cycle, from follicular (0.22 min^{-1}) to ovulatory (0.20 min^{-1}) to luteal (0.13 min^{-1}) phase at the anterior wall of the JZ, whereas a strong increase in K^{trans} was noticed at the posterior JZ (from 0.18 to 1.68 to 2.42 min^{-1}). The third woman of this group, on whom DCE-MRI was performed only during her follicular and ovulatory phase, showed an increase in K^{trans} at the anterior and posterior wall of the JZ from follicular (0.10 and 0.23 min^{-1} , respectively) to ovulatory (0.30 and 0.33 min^{-1} , respectively) phase.

The fourth infertile woman had a K^{trans} of 0.12 and 0.10 min^{-1} at respectively the anterior and posterior wall of the JZ during her follicular phase. The fifth infertile woman showed a K^{trans} of respectively 0.30 and 0.26 min^{-1} during the ovulatory phase and 0.12 and 0.39 min^{-1} during the luteal phase.

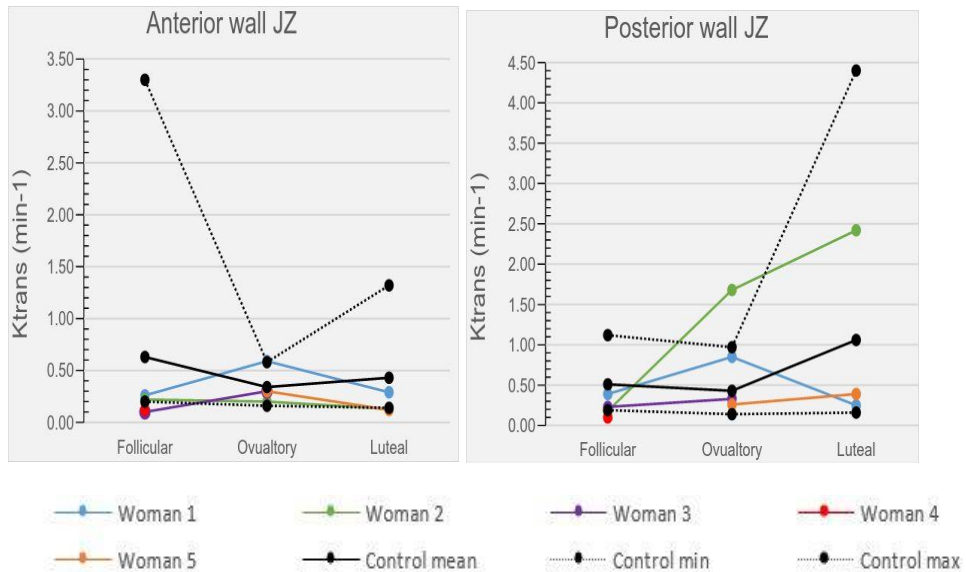


Figure 3: Transfer constant (K^{trans}) measurements at the anterior and posterior wall of the junctional zone (JZ) in five infertile women and in a control group during the follicular, ovulatory and luteal menstrual phases. The control group consists of 18 healthy nulliparous women and the minimum and maximum measurement in this group was indicated as well for each menstrual phase.

In comparison to the findings in the infertile women, the anterior wall of the JZ in the control group showed a drop in the mean K^{trans} during the ovulatory phase compared to the other two phases. The mean K^{trans} equated 0.63min^{-1} (range $0.20\text{--}3.30\text{min}^{-1}$) during the follicular phase, 0.34min^{-1} (range $0.16\text{--}0.58\text{min}^{-1}$) during the ovulatory phase and 0.43min^{-1} (range $0.14\text{--}1.32\text{min}^{-1}$) during the luteal phase. At the posterior wall of the JZ, an increase in K^{trans} was established during the luteal phase (1.06min^{-1} (range $0.16\text{--}4.40\text{min}^{-1}$)) compared to the follicular (0.51min^{-1} (range $0.19\text{--}1.12\text{min}^{-1}$)) and ovulatory (0.43min^{-1} (range $0.14\text{--}0.97\text{min}^{-1}$)) phases.

It was notable that multiple K^{trans} measurements in the infertile women were beyond the range of measurements in the control group. This means that those measurements in the infertile women were smaller than the lowest measurement assessed in the control group, whereas others were higher than the maximum measurement in the control group (table 2).

Table 2: Transfer constant measurements of myometrium in the nulliparous and in infertile women. Transfer constant (K^{trans}) was assessed in a control group consisting of 18 healthy nulliparous women and in women with unexplained infertility not using (n = 3: women 1-3) and using (n = 2: women 4-5) ovarian stimulation therapy at the anterior and posterior wall of the junctional zone (JZ) and outer myometrium (OM) during the follicular phase (F), ovulatory phase (O) and luteal phase (L). ↑: measurement higher than the maximum assessment in the control group; ↓: measurement lower than the minimum assessment in the control group.

K^{trans} (min^{-1})	Phase	Nulliparous women (n = 18)				Infertile women not on therapy			Infertile women on therapy	
		mean	SD	min	max	woman 1	woman 2	woman 3	woman 4	woman 5
Anterior JZ	F	0.63	0.90	0.20	3.30	0.26	0.22	0.10 ↓	0.12 ↓	
	O	0.34	0.16	0.16	0.58	0.59 ↑	0.20	0.30	0.30	
	L	0.43	0.42	0.14	1.32	0.29	0.13 ↓		0.12 ↓	
Posterior JZ	F	0.51	0.29	0.19	1.12	0.39	0.18 ↓	0.23	0.10 ↓	
	O	0.43	0.30	0.14	0.97	0.85	1.68 ↑	0.33	0.26	
	L	1.06	1.41	0.16	4.40	0.25	2.42		0.39	
Anterior OM	F	2.22	3.30	0.20	8.72	0.53	0.32	0.14 ↓	0.24	
	O	0.59	0.53	0.11	1.72	0.76	1.28	0.52	0.16 ↓	
	L	0.68	0.75	0.10	2.17	0.54	1.38		0.43	
Posterior OM	F	1.06	1.34	0.08	4.10	1.08	0.38	0.16	0.17	
	O	0.49	0.52	0.10	1.79	0.28	0.42	0.38	0.54	
	L	0.71	0.25	0.32	1.12	0.69	0.41		0.22	

5.4.2 Initial Blood Volume Of The Junctional Zone

The first woman with unexplained infertility demonstrated a slight increase in iAUC/volume over the menstrual cycle at the anterior and posterior wall of the JZ: from 0.13 to 0.16 and 0.35 during respectively the three menstrual phases at the anterior wall of the JZ, and respectively 0.22, 0.23 and 0.32 at the posterior JZ wall. The second woman had a slight decrease in iAUC/volume at the anterior wall of the JZ during the luteal phase (0.19) in comparison to the follicular (0.34) and ovulatory (0.41) phases. For the posterior wall of the JZ, software analysis indicated an iAUC of 0.00 for the follicular and ovulatory phase. iAUC/volume during the luteal phase equated 0.56. Furthermore, the JZ of the third woman showed an increase in iAUC/volume from follicular phase

(0.18 and 0.21 in respectively the anterior and posterior wall) to ovulatory phase (0.55 and 0.70, respectively).

The fourth woman revealed an iAUC/volume at the anterior and posterior wall of the JZ of respectively 0.20 and 0.14 during the follicular phase. iAUC/volume in the fifth woman was respectively 0.72 and 0.30 during the ovulatory phase, and 0.93 and 1.76 during the luteal phase.

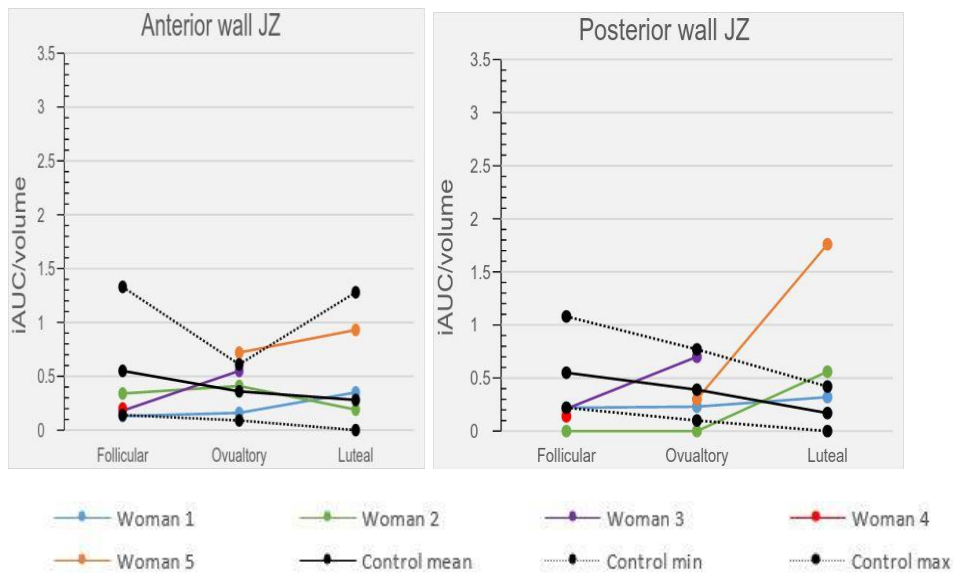


Figure 4: Initial blood volume (iAUC/volume) measurements at the anterior and posterior wall of the junctional zone (JZ) in five infertile women and in a control group during the follicular, ovulatory and luteal menstrual phases. The control group consists of 18 healthy nulliparous women and the minimum and maximum measurement in this group was indicated as well for each menstrual phase.

The following data represent the mean iAUC/volume of the control group at respectively the anterior and posterior JZ, which recognized a decrease throughout the menstrual cycle: 0.55 (range 0.14 – 1.33) and 0.55 (range 0.22 – 1.08) during the follicular phase, 0.36 (range 0.09 – 0.61) and 0.39 (range 0.10 – 0.77) during the ovulatory phase and 0.28 (range 0.00 – 1.28) and 0.17 (range 0.00 – 0.42) during the luteal phase.

Similarly as for K^{trans} , iAUC/volume in the infertile women also demonstrated

measurements beyond the range of the control group (table 3).

Table 3: Initial blood volume measurements of myometrium in the nulliparous and in infertile women. Initial blood volume (iAUC/volume) was assessed in a control group consisting of 18 healthy nulliparous women and in women with unexplained infertility not using (n = 3: women 1-3) an using (n = 2: women 4-5) ovarian stimulation therapy at the anterior and posterior wall of the junctional zone (JZ) and outer myometrium (OM) during the follicular phase (F), ovulatory phase (O) and luteal phase (L). ↑: measurement higher than the maximum assessment in the control group; ↓: measurement lower than the minimum assessment in the control group.

iAUC/ volume	Phase	Nulliparous women (n = 18)				Infertile women not on therapy			Infertile women on therapy	
		mean	SD	min	max	woman 1	woman 2	woman 3	woman 4	woman 5
Anterior JZ	F	0.55	0.31	0.14	1.33	0.13 ↓	0.34	0.18	0.20	
	O	0.36	0.19	0.09	0.61	0.16	0.41	0.55	0.72	
	L	0.28	0.45	0.00	1.28	0.35	0.19		0.93	
Posterior JZ	F	0.55	0.29	0.22	1.08	0.22	0.00 ↓	0.21 ↓	0.14 ↓	
	O	0.39	0.22	0.10	0.77	0.23	0.00 ↓	0.70	0.30	
	L	0.17	0.16	0.00	0.42	0.32	0.56 ↑		1.76 ↑	
Anterior OM	F	0.32	0.31	0.00	0.99	0.11	0.34	0.14	0.22	
	O	0.28	0.29	0.00	0.82	0.10	0.98 ↑	0.31	0.41	
	L	0.20	0.20	0.00	0.56	0.33	0.73 ↑		2.19 ↑	
Posterior OM	F	0.54	0.27	0.16	0.92	0.34	0.40	0.13 ↓	0.21	
	O	0.25	0.19	0.00	0.56	0.05	0.89 ↑	0.13	0.42	
	L	0.27	0.37	0.00	1.17	0.10	0.49		1.61 ↑	

5.4.3 Transfer Constant Of The Outer Myometrium

The anterior wall of the outer myometrium of the first woman with unexplained infertility showed a peak in K^{trans} during the ovulatory phase (0.76 min^{-1}) in comparison to the follicular (0.53 min^{-1}) and luteal (0.54 min^{-1}) phases. In contrast, the posterior wall showed a drop in K^{trans} during the ovulatory phase (0.28 min^{-1}) compared to the follicular (1.08 min^{-1}) and luteal (0.69 min^{-1}) phases. In the second woman, K^{trans} at the anterior wall of the outer myometrium equated 0.32 min^{-1} during the follicular phase, which strongly increased to 1.28 min^{-1} during the ovulatory phase, followed by a slower

increase during the luteal phase to 1.38 min^{-1} . The posterior wall displayed K^{trans} measurements of 0.38, 0.42 and 0.41 min^{-1} during respectively the three menstrual phases. Finally, the outer myometrium of the third infertile woman showed an increase in K^{trans} from follicular phase (0.14 and 0.16 min^{-1} at respectively the anterior and posterior wall) to ovulatory phase (0.52 and 0.38 min^{-1} , respectively).

Furthermore, K^{trans} assessed at the outer myometrium of the fourth infertile woman equaled in respectively the anterior and posterior uterine wall 0.24 and 0.17 min^{-1} during her follicular phase. In the fifth infertile woman, K^{trans} equaled 0.16 and 0.54 min^{-1} during the ovulatory and 0.43 and 0.22 min^{-1} during the luteal phase.

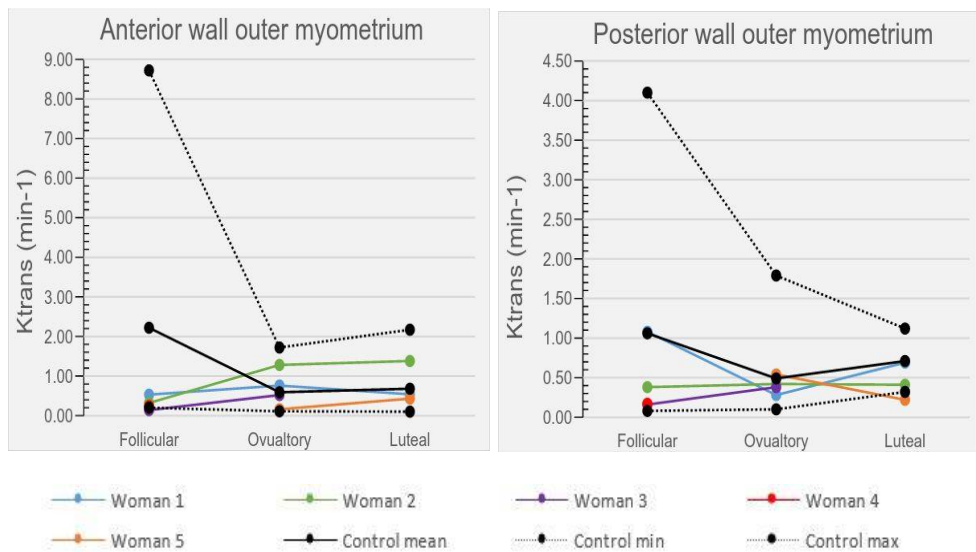


Figure 5: Transfer constant (K^{trans}) measurements at the anterior and posterior wall of the outer myometrium in five infertile women and in a control group during the follicular, ovulatory and luteal menstrual phases. The control group consists of 18 healthy nulliparous women and the minimum and maximum measurement in this group was indicated as well for each menstrual phase.

The control group demonstrated that the mean K^{trans} decreased over the menstrual cycle. At the anterior wall of the outer myometrium these values equaled 2.22 min^{-1} (range $0.20\text{--}8.72 \text{ min}^{-1}$), 0.59 min^{-1} (range 0.11--

1.72min⁻¹) and 0.68min⁻¹(range 0.10–2.17 min⁻¹), in respectively the follicular, ovulatory and luteal phases, and these values at the posterior wall were respectively 1.06min⁻¹(range 0.08–4.10min⁻¹), 0.49min⁻¹(range 0.10–1.79 min⁻¹) and 0.71 min⁻¹ (range 0.32 – 1.12 min⁻¹).

Generally, no substantial differences were noticed between the infertile women who were using and not using ovarian stimulation therapy and the control group. Although, one woman not on and one woman on ovarian stimulation therapy showed a K^{trans} lower than the lowest measured K^{trans} in the control group at the anterior wall of the outer myometrium (table 2).

5.4.4 Initial Blood Volume Of The Outer Myometrium

The outer myometrium in the first infertile woman showed an increase in iAUC/volume during the luteal phase (0.33) in comparison with the follicular (0.11) and ovulatory (0.10) phase at the anterior wall, whereas at the posterior wall, the follicular phase (0.34) demonstrated a higher iAUC/volume than the ovulatory (0.05) and luteal (0.10) phases. iAUC/volume at the outer myometrium of the second woman was 0.34 and 0.40 during the follicular phase at respectively the anterior and posterior wall which increased during the ovulatory phase (0.98 vs 0.89), followed by a subsequent decrease during the luteal phase (0.73 vs 0.49). The third woman revealed an iAUC/volume of 0.14 during the follicular phase and 0.31 during the ovulatory phase at the anterior wall of the outer myometrium. These values at the posterior wall equaled respectively 0.13 and 0.13.

Furthermore, the outer myometrium in the fourth infertile woman had iAUC/volumes of respectively 0.22 and 0.21 at the anterior and posterior outer myometrial wall during her follicular phase. The iAUC/volume of the fifth woman at the outer myometrium was 0.41 and 0.42 during the ovulatory phase, and

2.19 and 1.61 during the luteal phase at respectively the anterior and posterior wall.

The mean iAUC/volumes for the anterior wall of the outer myometrium in the control group were 0.32 (range 0.00 – 0.99) during the follicular phase, 0.28 (range 0.00 – 0.82) during the ovulatory phase and 0.20 (range 0.00 – 0.56) during the luteal phase. The mean values at the posterior wall of the outer myometrium equated respectively 0.54 (range 0.16 – 0.92), 0.25 (range 0.00 – 0.56) and 0.27 (range 0.00 – 1.17).

Part of the measurements of the second infertile woman concerning the iAUC/volume of the outer myometrium were higher than the maximum measurement in the control group, whereas the iAUC/volume during the follicular phase in the third infertile woman was lower than the minimum control measurement (table 3).

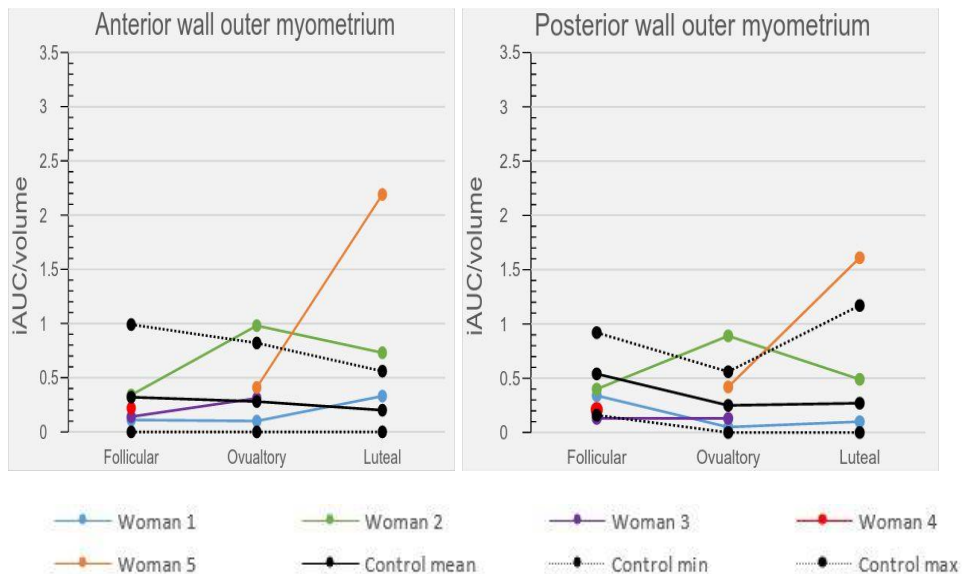


Figure 6: Initial blood volume (iAUC/volume) measurements at the anterior and posterior wall of the outer myometrium in five infertile women and in a control group during the follicular, ovulatory and luteal menstrual phases. The control group consists of 18 healthy nulliparous women and the minimum and maximum measurement in this group was indicated as well for each menstrual phase.

5.4.5 Transfer constant and initial blood volume in the control group

For the control group, a significantly higher K^{trans} (averaged over all measured locations) was noticed during the follicular phase in comparison to the ovulatory ($p = 0.008$) and luteal ($p = 0.027$) phase. iAUC/volume revealed to be significantly higher during the follicular and ovulatory phase than during the luteal phase ($p < 0.001$ for both comparisons).

5.4.6 Discussion

The present study offers the first DCE-MRI perfusion results in five women with unexplained infertility in the JZ and outer myometrium. This study compared these results with perfusion data in a control group consisting of 18 nulliparous women between the age of 18 and 35 years with no medical history of infertility and who were not taking hormonal contraception.

Myometrial perfusion was initially measured by invasive techniques (i.e. DSA). Later on, uterine perfusion measurements were also performed by assessing the vascularization index and vascular flow index by means of non-invasive 3D Doppler transvaginal ultrasound. Recently, some authors have demonstrated that DCE-MRI is able to quantify physiological variations in myometrial vascularization throughout the menstrual cycle and to differentiate reproductive age from post-menopausal state [21]. The DCE-MRI technique is more sensitive for perfusion evaluation of the complete uterus than Doppler transvaginal ultrasonography, due to the large distance that is created between the transvaginal probe and the edges of the uterus and for retroverted uteri in transvaginal ultrasonography [21].

The first suggestion that uterine perfusion was impaired in women with unexplained infertility came from a study by Goswamy et al. [22] who used Doppler ultrasound findings. In the ensuing years a variety of studies found

similar observations [4, 10, 23]. A study by Raine-Fenning et al. [4] used 3D power Doppler angiography in order to examine subendometrial (and endometrial) vascularity during the normal cycle in 29 women with unexplained infertility and in 19 controls. They demonstrated significant changes with time in the indices of vascularity within the subendometrium during the menstrual cycle in women with unexplained infertility. These changes were characterized by a pre-ovulatory peak followed by a fall reaching a nadir approximately five days after ovulation. Similar changes were noticed in the control group but with significantly higher values. However, the vascular indices were significantly reduced during the mid-late follicular phase and early luteal phase in the women with unexplained infertility. These results on power Doppler angiography were not completely in concordance with the results of our study using DCE-MRI. In the infertile women of our study, no remarkable differences were observed for both K^{trans} and iAUC/volume in the uterine wall throughout the menstrual cycle. These women demonstrated various patterns in K^{trans} and iAUC/volume throughout the menstrual cycle. However, the most surprising observation was that multiple measurements in the infertile women, both those on ovarian stimulation therapy and not, were generally lower or higher than the range of measurements in the control group. Besides reduced perfusion parameters (for both K^{trans} and iAUC/volume) in women with unexplained infertility, also increased measurements were observed in comparison to the control group. These findings refer not only to a reduced perfusion, but these indicate an impaired perfusion (K^{trans} and iAUC/volume) in the women with unexplained infertility of our study.

In our study, the control group showed that the mean K^{trans} was significantly higher during the follicular phase in comparison to the ovulatory and luteal phase and that iAUC/volume was significantly higher during the follicular and ovulatory phase than during the luteal phase. These findings could indicate an increase in perfusion over the menstrual cycle. The higher K^{trans} and iAUC/volume could be explained by a raise in blood volume right before ovulation

due to the transient increase in estradiol serum levels, myometrial basal tone and uterine contractility [24, 25].

Generally, it is accepted that an adequate uterine blood supply is required for successful embryo implantation as part of assisted reproductive therapy. However, contrary to this hypothesis, it is also believed that a period of relative ischemia and hypoxia during the peri-ovulatory period is beneficial for embryo implantation to occur. The second hypothesis is supported by evidence of a beneficial role for hypoxia during implantation in humans. It is demonstrated that relative low oxygen levels are present at the time the blastocyst implants. Less is known about the perfusion in the myometrium in the context of embryo implantation.

If an impaired perfusion will be identified in an infertile woman by DCE-MRI in future examinations, this woman may be offered treatments in order to normalize the uterine perfusion as an attempt to increase natural fertility before continuing to other, more invasive treatments in the context of assisted reproductive therapy.

In conclusion, based on the preliminary data of our study about perfusion parameters in the JZ and outer myometrium in women with unexplained infertility, it is demonstrated that DCE-MRI perfusion parameter assessment is possible in infertile women. Furthermore, it is suggested that the perfusion in the uterine wall is disturbed in comparison to control women. Studies in larger series are necessary in order to draw definite conclusions about the way the perfusion is disturbed.

5.5 References

1. Gelbaya TA, Potdar N, Jevic YB, Nardo LG (2014) Definition and epidemiology of unexplained infertility. *Obstet Gynecol Surv* 69:109-115.
2. Benagiano G, Bastianelli C, Farris M (2006) Infertility: a global perspective. *Minerva Ginecol* 58:445-457.
3. Brosens JJ, Pijnenborg R, Brosens IA (2002) The myometrial junctional zone spiral arteries in normal and abnormal pregnancies: a review of the literature. *Am J Obstet Gynecol* 187:1416-1423.
4. Raine-Fenning NJ, Campbell BK, Kendall NR, Clewes JS, Johnson IR (2004) Endometrial and subendometrial perfusion are impaired in women with unexplained subfertility. *Hum Reprod* 19:2605-2614.
5. Friedler S, Schenker JG, Herman A, Lewin A (1996) The role of ultrasonography in the evaluation of endometrial receptivity following assisted reproductive treatments: a critical review. *Hum Reprod Update* 2:323-335.
6. Piver P (2005) Uterine factors limiting ART coverage. *J Gynecol Obstet Biol Reprod (Paris)* 34:5S30-35S33.
7. Maubon A, Faury A, Kapella M, Pouquet M, Piver P (2010) Uterine junctional zone at magnetic resonance imaging: a predictor of in vitro fertilization implantation failure. *J Obstet Gynaecol Res* 36:611-618.
8. Pijnenborg R, Vercruyse L, Brosens I (2011) Deep placentation. *Best Pract Res Clin Obstet Gynaecol* 25:273-285.

9. Uysal S, Ozbay EP, Ekinçi T et al (2012) Endometrial spiral artery Doppler parameters in unexplained infertility patients: is endometrial perfusion an important factor in the etiopathogenesis? *J Turk Ger Gynecol Assoc* 13:169-171.
10. El-Mazny A, Abou-Salem N, Elshenoufy H (2013) Doppler study of uterine hemodynamics in women with unexplained infertility. *Eur J Obstet Gynecol Reprod Biol* 171:84-87.
11. Chard T, Grudzinskas JG (1994) *The Uterus - Anatomy of the Uterus - Nutrition*; p. 29-39.
12. Staff AC, Johnsen GM, Dechend R, Redman CW (2014) Preeclampsia and uteroplacental acute atherosclerosis: immune and inflammatory factors. *J Reprod Immunol* 101-102:120-126.
13. Hall GH, Atkin SL, Turnbull LW (2002) Use of dynamic contrast-enhanced MRI to assess the functional vascular pharmacokinetic parameters of normal human ovaries. *J Reprod Med* 47:107-114.
14. Medved M, Karczmar G, Yang C et al (2004) Semiquantitative analysis of dynamic contrast enhanced MRI in cancer patients: Variability and changes in tumor tissue over time. *J Magn Reson Imaging* 20:122-128.
15. Sala E, Rockall A, Rangarajan D, Kubik-Huch RA (2010) The role of dynamic contrast-enhanced and diffusion weighted magnetic resonance imaging in the female pelvis. *Eur J Radiol* 76:367-385.
16. Goldstein SR, Horii SC, Snyder JR, Raghavendra BN, Subramanyam B (1988) Estimation of nonpregnant uterine volume based on a normogram of gravid uterine volume: its value in gynecologic uterine abnormalities. *Obstet Gynecol* 72:86-90.

17. Carmona A, Chrastek R (2013) Tissue 4D on *syngo.via*How I do it. Siemens Healthcare, Erlangen, Germany.
18. Tofts PS (1997) Modeling tracer kinetics in dynamic Gd-DTPA MR imaging. *J Magn Reson Imaging* 7:91-101
19. Heye T, Boll DT, Reiner CS, Bashir MR, Dale BM, Merkle EM (2014) Impact of precontrast T1 relaxation times on dynamic contrast-enhanced MRI pharmacokinetic parameters: T10 mapping versus a fixed T1 reference value. *J Magn Reson Imaging* 39:1136-1145.
20. Thomassin-Naggara I, Siles P, Balvay D, Cuenod CA, Carette MF, Bazot M (2013) MR perfusion for pelvic female imaging. *Diagn Interv Imaging* 94:1291-1298.
21. Thomassin-Naggara I, Balvay D, Cuenod CA, Daraï E, Marsault C, Bazot M (2010) Dynamic contrast-enhanced MR imaging to assess physiologic variations of myometrial perfusion. *Eur Radiol* 20:984-994.
22. Goswamy RK, Williams G, Steptoe PC (1988) Decreased uterine perfusion-
-a cause of infertility. *Hum Reprod* 3:955-959.
23. Kurjak A, Kupesic-Urek S, Schulman H, Zalud I (1991) Transvaginal color flow Doppler in the assessment of ovarian and uterine blood flow in infertile women. *Fertil Steril* 56:870-873.
24. Ijland MM, Evers JL, Dunselman GA, van Katwijk C, Lo CR, Hoogland HJ (1996) Endometrial wavelike movements during the menstrual cycle. *Fertil Steril* 65:746-749.

25. Kunz G, Beil D, Deininger H, Wildt L, Leyendecker G (1996) The dynamics of rapid sperm transport through the female genital tract: evidence from vaginal sonography of uterine peristalsis and hysterosalpingoscintigraphy. *Hum Reprod* 11:627-632.

6. Discussion

This study is the first in literature to perform MRI examinations during three menstrual phases in the same woman in a group of women between the age of 19 and 35 years. The JZ thickness, outer myometrial thickness and the ratio of JZ versus total myometrial thickness is prospectively investigated in 47 healthy nulliparous women between the age of 19 and 35 years on T₂ weighted images acquired on a 1.5T MRI (a total of 133 MRI examinations). The women were subdivided based on the hormonal contraception status. The acquired data is subsequently used in evaluating (1) JZ and myometrial thickness, (2) the ratio of JZ versus total myometrial thickness on MRI, as in the control group and in infertile women. More specific 5 of unknown infertility origin, 12 anovulating women and 11 women on ovarian stimulation therapy in the context of assisted reproductive therapy (a total of 35 MRI examinations). The infertile women are, age matched with the control group (19 and 35 years).

As elaborated in the introduction not only the junctional zone thickness but the vascularity of the endometrial-myometrial junction or archimetrium aka junctional zone has a role in fertility.

This is the first report comparing DCE-MRI perfusion characteristics of the JZ and the outer myometrium in young healthy nulliparous (48 women, 133 MRI examinations) and primiparous women (50 women, 50 MRI examinations), subdivided by their use of contraception therapy.

The focus while investigating the perfusion of JZ and outer myometrium is on the assessment of the following physiological parameters: initial blood volume (iAUC/volume of the uterus), transfer constant (K^{trans}), efflux constant (K_{ep}) and interstitial volume (V_e).

Finally, a comparison of these perfusion parameters is made between 5 women of unexplained infertility (8 MRI examinations) and 18 women suspectedly healthy with no medical history (50 MRI examinations), not using hormonal contraception, both groups aged between 19 and 35 years.

6.1 JZ and Myometrial Thickness

In nullipara non-users, the menstrual phase nor the uterine wall location affected the JZ thickness significantly. This is consistent with previous studies, where no significant changes in JZ thickness between the follicular phase and luteal phase have been reported (Hauth et al, 2007; McCarthy et al, 1986). However, the outer myometrial thickness and the ratio of JZ versus total myometrial thickness are dependent on the location in the uterine wall. They are significantly lower at the midcorpus and fundus in both uterine walls. The thickest mean JZ was measured at the anterior fundal wall during the follicular phase. The mean JZ thickness in this phase and location equaled 3.5 mm, with a ratio of 29% to the total myometrial thickness. These findings concerning the JZ thicknesses are consistent with previous studies in which the normal JZ thickness is 5-8 mm (Hauth et al., 2007; Kunz et al., 2000a; Novellas et al., 2011). The group of Hauth et al. (2007) evaluated the normal thickness of different uterine wall layers (endometrium, JZ and outer myometrium) in 100 women (47 women with and 53 women without adenomyosis and/or myomas aged between 20 and 80 years) as a function of age and menstrual cycle phase. They noticed an increase in JZ thickness until the age of 41-50 years, followed by a decrease in thickness. The mean JZ thickness in a similar group as this study of 16 healthy women without adenomyosis and myomas between the age of 20 and 30 years was 5 mm and a mean thickness of the myometrium was 10 mm (McCarthy et al, 1986). They did not observe a significant difference in the JZ thickness between the women in the follicular nor the luteal phase. The main argument for the lack of difference in evaluating their data is the used slice thickness of 8mm in their MRI examinations in order to measure the JZ thickness and the absence of data of each menstrual phase in each participant. The nullipara users of contraception revealed a statistically significant thinner JZ than the non-users in both walls of the midcorpus and fundus. And the use of hormonal contraception significantly lowered the ratio at the midcorpus in both walls and at the fundus of the anterior wall. These findings are in line with previous results published by McCarthy et al. (1986) and Kido et al. (2005). McCarthy et al. indicated that the JZ thickness was significantly smaller in the pill-using group (9 subjects) than in the non-pill-using group (12 subjects) ($p <$

0.005). Kido et al. reported a significantly thinner JZ in the posterior uterine wall in women who use oral contraceptives (23 women) in comparison to women who did not use oral contraceptives (15 women) at mid-cycle. They observed a markedly suppressed uterine peristalsis in oral contraceptives users, which could contribute to the prevention of conception by disturbing the upward sperm transport. The thinner JZ in the users of hormonal contraception suggests that the thickness of the JZ at the midcorpus and fundus can be involved in the prevention of conception. This considers not only a maximum, but also a minimum JZ thickness to be fertile.

Anovulating women, included in this study, showed a JZ statistically significant thicker at the posterior wall of the isthmus than in healthy nulliparous women. The outer myometrium is in several groups of infertile women thicker. Namely, in anovulating women at each assessed location (anterior and posterior wall of the isthmus, midcorpus and fundus), in infertile women on ovarian stimulation therapy (in the context of assisted reproductive therapy) in the anterior uterine wall at the level of the isthmus, the midcorpus and the fundus. A thicker JZ or outer myometrium is not noticed in the women with unexplained infertility, which is not as expected, but no definite conclusions can be made for this group due to the low number of subjects.

Thus the thickness of the JZ and outer myometrium should be measured at the anterior wall of the uterus in order to detect differences between 'fertile' and each group of infertile women.

6.2 Perfusion characteristics and fertility

The second aim of this study is revealing the perfusion characteristics of the junctional zone and outer myometrium. While evaluating these perfusion parameters (i.e. iAUC), the volume of the investigated organ, namely the uterus needs to be determined in each women. During the ovulatory and luteal phase, nulliparous women who used hormonal contraceptives show a statistically significant smaller uterine volume than nulliparous women who did not use hormonal contraceptives. No statistically significant differences were noticed in the uterine volumes between both groups of primiparous women or between the

nulliparous and primiparous non-users of contraceptives. Merz et al. investigated uterine volumes on transvaginal ultrasound in nulliparous, primiparous and multiparous women, and detected a parity-related enlargement in uterine size (Merz et al, 1996). This relation was not found in this study.

It is known that, in women of reproductive age, the JZ demonstrates cyclic variations in blood flow throughout the menstrual cycle. This is demonstrated by means of 3D power Doppler angiography (Raine-Fenning et al, 2004) and more recently by means of DCE-MRI (Thomassin-Naggara et al, 2010). In this study, K^{trans} and iAUC/volume decreased over the menstrual cycle in nullipara non-users, from follicular to ovulatory to luteal phase (table 4 in Chapter 4). The highest initial blood volume in the JZ (iAUC/volume) is found during the follicular phase, followed by a decrease in initial blood volume during the luteal phase. K_{ep} and V_e were not significant different over the menstrual cycle.

These findings can be explained by the development of small vessels, such as spiral arteries, in the inner myometrium during the follicular phase (Chard et al, 1994; Blackwell et al, 1988). In addition, just before ovulation, increase of the estradiol serum levels and a transient increase in myometrial basal tone and uterine contractility could also explain the higher blood volume (Ijland et al, 1996; Kunz et al, 1996). The use of hormonal contraceptives leads in most of the investigated women to a reduction in transfer constant (K^{trans}) in the JZ.

Investigations on uterine specimens revealed a higher vascular perfusion rate in the JZ compared to the outer myometrium (Lee et al, 1985). This correlates with this study results, which show a higher reflux constant (K_{ep}) in nullipara non-users at the anterior JZ compared to the anterior outer myometrium. Furthermore, histological analysis studies on myometrial tissue found a threefold increase in percentage of nuclear area and cellular density, a decrease in extracellular matrix and a lower water content in the inner myometrium in comparison with the outer myometrium (Scoutt et al, 1991; Mc Carthy et al, 1989; Brown et al, 1991). This is also in concordance with this study results, which indicate a lower transfer constant (K^{trans}) in nulliparous users of hormonal contraception and a lower interstitial volume (V_e) in primiparous users of hormonal contraception at the anterior JZ than at the anterior outer

myometrium. This is a confirmation of the physiological differences between the inner third and the outer two-thirds of the myometrium, with dissimilar microvascular characteristics in both layers. These findings are as expected as a high JZ perfusion (due to higher transfer constant, lower efflux constant and higher initial blood volume than in the outer myometrium) in nulliparous non-users of contraceptives is believed to be involved in uterine contraction and subsequent transfer of spermatozoa and in embryo implantation (Raine-Fenning et al, 2004; Kido et al, 2005).

In the JZ, Thomassin-Naggara and colleagues noticed a higher tissue blood flow (F) and blood volume fraction (Vb) during the follicular phase than during the luteal phase. Nevertheless, they did not observe differences between those phases for permeability-surface area product (PS, which is correlated with K^{trans} , V_e and K_{ep}) and interstitial volume (V_e) in the JZ (Thomassin-Naggara et al, 2010). In their study women of all ages were included (whereas in our study the age limits were between 18 and 35 years), and there is no distinction made between nulliparous and multipara women and between women who used contraception therapy and those who did not. Furthermore MRI examination was performed only once in a woman's menstrual cycle.

Finally, the junctional zone and outer myometrium vascularity parameters were compared in 5 women of unexplained infertility and 18 women with no medical history, aged between 18 and 35 years and not using hormonal contraception.

These infertile women demonstrate various patterns in K^{trans} and iAUC/volume and no remarkable differences throughout the menstrual cycle for both K^{trans} and iAUC/volume in the uterine wall. The most surprising observation was that the measurements in the infertile women were generally lower or higher than in the control group. Besides reduced perfusion parameters (for both K^{trans} and iAUC/volume) in women with unexplained infertility, also increased parameters were observed in comparison to the control group. These findings refer not only to a reduced perfusion, but indicate an impaired perfusion (K^{trans} and iAUC/volume).

The first suggestion that uterine perfusion was impaired in women with unexplained infertility came from a study by Goswamy et al. (1988) who used

Doppler ultrasound findings. In the ensuing years a variety of studies found similar observations (Raine-Fenning et al, 2004; El Mazny et al, 2013 and Kurjak et al 1991). A study by Raine-Fenning et al (2004) used 3D power Doppler angiography in order to examine subendometrial (and endometrial) vascularity during the normal cycle in 29 women with unexplained infertility and in 19 controls. They demonstrated significant changes with time in the indices of vascularity within the subendometrium during the menstrual cycle in women with unexplained infertility. These changes were characterized by a pre-ovulatory peak followed by a fall reaching a nadir approximately five days after ovulation. Similar changes were noticed in their control group but with significantly higher values.

However, the vascular indices were significantly reduced during the mid-late follicular phase and early luteal phase in the women with unexplained infertility. If an impaired perfusion will be identified in an infertile woman by DCE-MRI according to the achieved features of the MRI vascularity parameters (iAUC, K trans, ...), these women may be offered treatments to normalize their uterine perfusion as an attempt to increase natural fertility. This before continuing to other, more invasive treatments in the context of assisted reproductive therapy. In conclusion, DCE-MRI perfusion parameter assessment is possible in infertile women. Furthermore, these preliminary results reveal a disturbed perfusion in the uterine wall. Studies in larger series of infertile women are necessary in order to draw definite conclusions.

Important to notice are the recent findings in literature regarding GBCAs (gadolinium based contrast agents). GBCAs have been injected in hundreds of millions of patients for MRI examinations. They are made of a gadolinium ion complexed with an organic ligand. Gadolinium is a rare earth heavy metal of the lanthanide series and is highly toxic, like other members of the lanthanide series. The atomic number is 64 and the Gd^{3+} ion radius (1.08 \AA) is close to that of Ca^{2+} (1.14 \AA) and can thus block the activity of some Ca dependent enzymes and block calcium channels leading to problems in muscle contractions or nerve conduction. The chemical stability or the propensity to release free gadolinium, depends on the structure of the ligand and on the ionicity of the complex (Port M et al, 2008). Gadolinium chelates were considered as very safe products until 2006 (Marckmann et al, 2006), when they first were associated

with the occurrence of nephrogenic systemic fibrosis (NSF), which has been observed exclusively in patients with severe or end-stage renal failure and most frequently after administration of low-stability linear GBCA (Thomson et al, 2013).

In 2007, the European Medicines Agency (EMA) contraindicated the use of the linear gadolinium agents (gadodiamide, gadoversetamide and gadopentetate dimeglumine) in patients with severe renal impairment.

Since 2009, NSF has almost disappeared thanks to the effective screening of patients with renal disease, to the avoidance of high-risk agents in patients with severe renal insufficiency, and to the use of more stable GBCAs (Huckle et al (2016); Edwards BJ et al (2014)).

However in 2014, after the MRI examinations of this study were performed, Kanda et al found on T1-weighted unenhanced brain scans of patients with normal renal function hyperintense zones in brain parenchyma after receiving multiple injections of a linear agent, resulting from a local accumulation of gadolinium in the cerebral vasculature and in the brain parenchyma (Mc Donald et al (2015), Kanda et al (2015)). This was not observed with the macrocyclic GBCAs (Kanda et al (2015), Radbruch et al (2015), Cao et al (2016)). Electron microscopic images of brain specimens showed the presence of gadolinium-rich hypointense spots, representing dissociated gadolinium from its complex (McDonald et al (2015)). It is now clear that intravenously injected Gd can slowly pass an intact BBB, with mechanisms possibly involving transmetallation, specific metal transporters or even a pathway through the CSF, perivascular spaces and the glymphatic system (Tedeschi et al (2017)). However, to date the exact chemical form of each GBCA accumulated in the central nervous system, the reversibility of this phenomenon, and the possible consequences for the brain tissue and/or functions remain unknown, as in human bone (Darrah et al,(2009)). These new findings have led the FDA and EMA to request additional information from GBCA marketing authorization holders about the potential long-term retention and long-term effects of their products, and adjusted GBCA protocols by the ESUR and ISMRM (Lancelot E (2016)).

This study has used macrocyclic ionic GBCA in all participants, and all participants had proven normal renal function. To our knowledge, no participant has reported symptoms related to GDD so far (Gadolinium Deposition Disease:

persistent symptoms that arise hours to 2 months after the administration of GBCAs with typical clinical features such as persistent headache, bone and joint pain, often clouded mentation and soft-tissue thickening, painful and thickened tendons and ligaments) (Semelka et al, 2016).

7. Conclusion

In daily practice, a MRI examination is recommended in the work-up of a woman consulting for possible in/subfertility. Next to evaluating hormonal status (menstrual cycle), a transvaginal ultrasound (presence and morphology of the ovaries and uterus, endometriomata..., tubal patency (transvaginal hydrosonography)), performing a MRI examination in a standard in/subfertility investigation is preferable before starting therapy. Compared to other techniques MRI is a non-invasive examination that depicts e.g. foci of endometriosis outside the internal gonades, is better in delineating the external contour of the uterus, depicting and defining congenital abnormalities in detail (uterus arcuate – septate (fibrous or muscular origin), ..., vaginal and cervical anomalies), evaluating the junctional zone (thickness and vascularity) and JZ-total myometrium ratio. The MRI examination should be performed in the follicular phase (if a menstrual cycle is present) and measurements should be done in the anterior wall of the fundus or/and midcorpus of the uterus. Normal JZ thickness is considered between 3.2 and 3.5mm (mean values of the presented results) in nullipara women non-users and between the age of 19 and 35 years, together with a ratio of JZ thickness versus total myometrial thickness of 28-29% (less than 40% (Bazot et al (2001))). The normal value considered for iAUC/volume in the follicular phase in the anterior wall in nullipara women non-users is 0,557 (\pm 0,293) and Ktrans (min-1) 0,593 (\pm 0,865).

8. References

1. Bazot M, Cortez A, Darai E, Rouger J, Chopier J, Antoine JM, Uzan S (2001) Ultrasonography compared with magnetic resonance imaging for the diagnosis of adenomyosis: correlation with histopathology. *Hum Reprod* 16:2427-2433.
2. Blackwell PM, Fraser IS. (1988) A morphometric and ultrastructural study of the microvessels of the functional zone of normal human endometrium with some notions on possible secretory functions of the endothelial cells. *Asia Oceania J Obstet Gynaecol* 14(2):233-250.
3. Brown HK, Stoll BS, Nicosia SV, et al. (1991) Uterine junctional zone: correlation between histologic findings and MR imaging. *Radiology* 179(2):409-413.
4. Cao Y, Huang DQ, Shih G, et al.(2016) Signal change in the dentate nucleus on T1-weighted MR images after multiple administrations of gadopentetate dimeglumine versus gadobutrol. *AJR Am J Roentgenol* 206:414-419.
5. Chard T, Grudzinskas JG. (1994) *The Uterus – Anatomy of the Uterus – Nutrition*;p.29-39.
6. Darrah TH, Prutsman-Pfeiffer JJ, Poreda RJ, et al. (2009) Incorporation of excess gadolinium into human bone from medical contrast agents. *Metallomics*. 1: 479-488.
7. Edwards BJ, Laumann AE, Nardone B, et al. (2014) Advancing pharmacovigilance through academic-legal collaboration: the case of gadolinium-based contrast agents and nephrogenic systemic fibrosis- a Research on Adverse Drug Events and Reports (RADAR) report. *Br J Radiol*.87:20140307.

8. El-Mazny A, Abou-Salem N, Elshenoufy H. (2013) Doppler study of uterine hemodynamics in women with unexplained infertility. *Eur J Obstet Gynecol Reprod Biol* 171:84-87.
9. Goswamy RK, Williams G, Steptoe PC. (1988) Decreased uterine perfusion-a cause of infertility. *Hum Reprod* 3:955-959.
10. Hauth EA, Jaeger HJ, Libera H, Lange S, Forsting M. (2007) MR imaging of the uterus and cervix in healthy women: determination of normal values. *Eur Radiol* 17:734-742.
11. Huckle JE, Altun E, Jay M, et al.(2016) Gadolinium deposition in humans: when did we learn that gadolinium was deposited in vivo? *Invest Radiol* 51:236-240.
12. Ijland MM, Evers JL, Dunselman GA, van Katwijk C, Lo CR, Hoogland HJ (1996) Endometrial wavelike movements during the menstrual cycle. *Fertil Steril* 65:746-749.
13. Kanda T, Ishii K, Kawaguchi H, et al (2014). High signal intensity in the dentate nucleus and globus pallidus on unenhanced T1-weighted MR images: relationship with increasing cumulative dose of a gadolinium-based contrast material. *Radiology*, 270:834-841.
14. Kanda T, Fukusato T, Matsuda M, et al.(2015) Gadolinium-based contrast agent accumulates in the brain even in subjects without severe renal dysfunction: evaluation of autopsy brain specimens with inductively coupled plasma mass spectroscopy. *Radiology* 276:228-232.
15. Kanda T, Osawa M, Oba H, et al. (2015) High signal intensity in dentate nucleus on unenhanced T1-weighted MR images: association with linear versus macrocyclic gadolinium chelate administration. *Radiology* 275:803-809.

16. Kido A, Togashi K, Nakai A, Kataoka ML, Koyama T, Fujii S (2005) Oral contraceptives and uterine peristalsis: evaluation with MRI. *J Magn Reson Imaging* 22:265-270.
17. Kunz G, Beil D, Huppert P, Leyendecker G (2000) Structural abnormalities of the uterine wall in women with endometriosis and infertility visualized by vaginal sonography and magnetic resonance imaging. *Hum Reprod* 15:76-82.
18. Kunz G, Beil D, Deininger H, Wildt L, Leyendecker G (1996) The dynamics of rapid sperm transport through the female genital tract: evidence from vaginal sonography of uterine peristalsis and hysterosalpingoscintigraphy. *Hum Reprod* 11:627-632.
19. Kurjak A, Kupesic-Urek S, Schulman H, Zalud I (1991) Transvaginal color flow Doppler in the assessment of ovarian and uterine blood flow in infertile women. *Fertil Steril* 56:870-873.
20. Lancelot E (2016). Revisiting the Pharmacokinetic Profiles of Gadolinium-Based Contrast Agents. *Invest Radiol* 51:691-700.
21. Lee JK, Gersell DJ, Balfe DM, Worthington JL, Picus D, Gapp G. (1985) The uterus: in vitro MR-anatomic correlation of normal and abnormal specimens. *Radiology* 157(1):175-179.
22. Marckmann P, Skov L, Rossen K, Dupont A, Damholt MB, Heaf JG, et al. (2006) Nephrogenic systemic fibrosis: suspected causative role of gadodiamide used for contrast-enhanced magnetic resonance imaging. *J Am Soc Nephrol* 17:2359-62.
23. McCarthy S, Tauber C, Gore J. (1986) Female pelvic anatomy: MR assessment of variations during the menstrual cycle and with use of oral contraceptives. *Radiology* 160(1):119-123.

24. McCarthy S, Scott G, Majumdar S, et al. (1989). Uterine junctional zone: MR study of water content and relaxation properties. *Radiology* 171(1):241-243.
25. McDonald RJ, McDonald JS, Kallmes DF, et al. (2015) Intracranial gadolinium deposition after contrast-enhanced MR imaging. *Radiology* 275:772-782.
26. Merz E, Miric-Tesanic D, Bahlmann F, Weber G, Wellek S. Sonographic size of uterus and ovaries in pre- and postmenopausal women. *Ultrasound Obstet Gynecol* 1996;7(1):38-42.
27. Novellas S, Chassang M, Delotte J, Toullalan O, Chevallier A, Bouaziz J, Chevallier P (2011) MRI characteristics of the uterine junctional zone: from normal to the diagnosis of adenomyosis. *AJR Am J Roentgenol* 196:1206-1213.
28. Port L, Idée JM, Medina C, et al. (2008) Efficiency, thermodynamic and kinetic stability of marketed gadolinium chelates and their possible clinical consequences: a critical review. *Biometals* 21:469-490.
29. Radbruch A, Weberling LD, Kieslich PJ, et al.(2015) Gadolinium retention in the dentate nucleus and globus pallidus is dependent on the class of contrast agent. *Radiology*;275:783-791.
30. Radbruch A, Weberling LD, Kieslich PJ, et al. (2015) High-signal intensity in the dentate nucleus and globus pallidus on T1-weighted images: evaluation of the macrocyclic gadolinium-based contrast agent gadobutrol. *Invest RAdiol* 50:805-810.
31. Raine-Fenning NJ, Campbell BK, Kendall NR, Clewes JS, Johnson IR (2004) Endometrial and subendometrial perfusion are impaired in women with unexplained subfertility. *Hum Reprod* 19:2605-2614.

32. Scoutt LM, Flynn SD, Luthringer DJ, McCauley TR, McCarthy SM. (1991) Junctional zone of the uterus: correlation of MR imaging and histologic examination of hysterectomy specimens. *Radiology* 179(2):403-407.
33. Semelka RC, Ramalho M, AlObaidy M, Ramalho J. (2016) Gadolinium in Humans: A Family of Disorders. *AJR* 14:229-233.
34. Tedeschi E, Caranci F, Giordano F et al.(2017) Gadolinium retention in the body: what we know and what we can do. *Radiol med* 122:589-600.
35. Thomassin-Naggara I, Balvay D, Cuenod CA, Daraï E, Marsault C, Bazot M (2010) Dynamic contrast- enhanced MR imaging to assess physiologic variations of myometrial perfusion. *Eur Radiol* 20:984-994.
36. Thomson HS, Morcos SK, Almén T, et al (2013). Nephrogenic systemic fibrosis and gadolinium-based contrast media: updated ESUR Contrast Medium Safety Committee guidelines. *Eur Radiol*. 23:307-318.

9. Samenvatting

Deze studie gaat na of het interne 1/3 vd baarmoederwand, m.a.w. de junctionele zone bij vrouwen tussen 19 en 35 jaar oud gedurende menstruele cyclus significant verandert in dikte. De dikte wordt gemeten met behulp van een MRI onderzoek (magnetische resonantie beeldvorming). Tevens wordt er geëvalueerd of de locatie van meten (voorwand versus achterwand van de uterus en in de top of fundus, middenste 1/3 of corpus en of distale 1/3 of isthmus van de baarmoeder) significant verschilt in metingen in de verschillende fasen vd menstruele cyclus. Deze metingen werden uitgevoerd bij vrouwen onderverdeeld in 2 grote groepen. Namelijk bij vrouwen zonder een (gynaecologische) medische voorgeschiedenis en nog niet zwanger geweest. Deze eerste groep werd onderverdeeld in twee subgroepen naargelang ze wel of niet contraceptie gebruikten. De tweede grote groep zijn vrouwen die eenmaal een partus hebben doorgemaakt en dit minstens 6 maanden na hun eerste zwangerschap. Ook deze tweede groep werd onderverdeeld in een subgroep gebruiker en niet-gebruiker van contraceptie.

Vervolgens willen we de bekomen resultaten vergelijken met de waarden van junctionele zonedikte bij vrouwen met fertiliteitsproblemen en zo dichterbij tot een antwoord komen van de oorzaak van hun infertiliteit.

Naast de dikte van de junctionele zone speelt de vascularisatie ook een belangrijke rol in de fertiliteit. De vascularisatie wordt in onze studie geëvalueerd op een niet-invasieve manier met behulp van MRI onderzoek na dynamische contrastmiddel toediening. De bekomen parameters betreffende de vascularisatie die we in deze studie gebruikten waren het initiële bloedvolume ten op zichte van het uterusvolume ($iAUC/volume$), permeabiliteitsconstante (K_{trans}), interstitieel volume (V_e) en refluxconstante (K_{ep}).

Onze bevindingen tonen aan dat bij nullipara vrouwen de junctionele zone statistisch verschillend is van bij vrouwen die hormonale contraceptie nemen. Er is een statistisch significant dunnere junctionele zone waargenomen bij vrouwen welke contraceptie nemen in vergelijking met niet-gebruikers in de voorste en achterste wand van de uterus op niveau van de fundus en midcorpus. Niet zozeer de localisatie van meting in de uteruswand zelf of de fase in de

menstruele cyclus zijn van significant belang in het evalueren van de junctionele zone dikte.

Bij het evalueren van het buitenste 2/3 van het uteruswand, het myometrium evalueren, blijkt dat deze dikte wel varieert naargelang de localisatie in de uteruswand. Een dikker buitenste 2/3 myometrium is waargenomen op niveau van de fundus en midcorpus. Deze verschillen in dikte van de junctionele zone en buitenste myometrium worden weerspiegeld in de ratio van de junctionele zone versus totale myometrium dikte. De ratio toont verschillen tussen de nullipara niet gebruikers versus gebruikers van contraceptie en tussen de verschillende localisaties in de uteruswand. We verkiezen om de metingen van de junctionele zone dikte uit te voeren op niveau van de fundus en midcorpus.

Vervolgens werden deze gegevens vergeleken met die van infertiele anovulatoire vrouwen. Deze vertonen een significant dikkere junctionele zone in de achterste wand van de isthmus en een significant dikker buitenste myometrium in de voorste en achterste uteruswand. Infertiele vrouwen die ovariële stimulatie therapie ondergaan, vertonen ook een verdikt buitenste myometrium in de anterior uteruswand.

Deze bevindingen suggereren dat de dikte van de junctionele zone en buitenste myometrium mogelijk geassocieerd zijn met infertiliteit. Deze bevindingen kunnen toegepast worden in geassisteerde reproductiviteitsbehandeling om zo de succesratio na implantatie te verhogen.

De vascularisatie beoordeelt via de DCE (dynamic contrast enhancement) MRI perfusie parameters

($iAUC/volume$, K^{trans} , K_{ep} and Ve) van de junctionele zone en buitenste myometrium wordt vervolgens beoordeeld in een controle groep van nullipara en primipara vrouwen die geen en wel gebruik maken van contraceptie. Onze data tonen dat in nullipara niet-gebruikers van contraceptie hoofdzakelijk de transfer constante (K^{trans}) en initiële uterusbloedvolume ($iAUC/volume$) verandering tonen doorheen de menstruele cyclus. Hierbij wordt vastgesteld dat hormonale contraceptieven vaak een vermindering in K^{trans} in de junctionele zone teweeg brengen.

Deze perfusie karakteristieken van de gezonde junctionele zone en buitenste 2/3 van het myometrium kunnen weerom toegepast worden in diagnose en eventuele therapeutische interventie voor tot voorheen nog niet-geïdentificeerde pathologiën van het vrouwelijke reproductieve systeem, dit in de context van geassisteerde reproductieve therapie bij infertiele patiënten.

Tenslotte hebben we daarom deze data van de perfusie parameters toegepast bij een beperkt aantal vrouwen met onverklaarde infertiliteit. Onze bevindingen in deze kleine groep tonen enerzijds aan dat de techniek DCE-MRI uitvoerbaar is en anderzijds dat de bekomen gegevens toepasbaar zijn in de dagelijkse praktijk. Niemand van deze vijf patiënten toonde normale waarden, of waarden vergelijkbaar met onze controle groep. We hopen dit werk nog verder te kunnen uitbreiden in een grotere groep infertiele vrouwen van ongekende etiologie.

10. Summary

This study investigates whether the internal 1/3 of uterine wall, i.e. the junctional zone in women between 19 and 35 years of age, during menstrual cycle significantly changes in thickness. The thickness is measured using a MRI examination (magnetic resonance imaging). It is also evaluated whether the location of measurement (front wall versus back of the uterus and in the top or fundus, middle 1/3 or corpus and or distal 1/3 or isthmus of the uterus) is significantly different in measurements in the different phases of the menstrual cycle. These measurements were performed in women subdivided into 2 large groups. Namely in women without a (gynecological) medical history and not yet pregnant. This first group was subdivided into two subgroups depending on whether or not they used contraception. The second large group are women who have had one child and at least 6 months after their first pregnancy. This second group was also subdivided into a subset of users and non-users of contraception. Next, we want to compare the results obtained with the values of junctional zones in women with fertility problems, thus getting closer to the response to the cause of their infertility.

In addition to the thickness of the junctional zone, vascularization also plays an important role in fertility. Vascularization is evaluated in our study in a non-invasive way using MRI after dynamic contrast agent administration. The available vascularization parameters used in this study were the initial blood volume in vivo uterine volume (iAUC / volume), permeability constant (K_{trans}), interstitial volume (V_e) and reflux constant (K_{ep}).

Our findings show that in nullipara women the junctional zone is statistically different than in women taking hormonal contraception. There is a statistically significant thinner junctional zone observed in women taking contraception compared to non-users in the front and back wall of uterus at the level of fundus and midcorpus. Not so much the location of measurement in the uterine wall itself or the phase in the menstrual cycle are of significant importance in evaluating junction zone thickness.

When evaluating the outer 2/3 of the uterus wall, evaluating myometrium, it appears that this thickness varies according to the localization of the uterine wall. A thicker outer 2/3 myometrium has been observed at the fundus and midcorpus level. These differences in thickness of the junction zone and outer myometrium are reflected in the ratio of the junctional zone versus total myometrium thickness. The ratio shows differences between nullipara non-users versus contraception users and between the various uterine wall locations. We prefer to perform the measurements of the junctional zone thickness at the level of fundus and middle corpus.

Then, these data were compared to those of infertile anovulatory women. These exhibit a significantly thicker junctional region in the posterior wall of the isthmus and a significantly thicker outer myometrium in the anterior and posterior uterus wall. Infertile women undergoing ovarian stimulation therapy also exhibit a thickened outer myometrium in the anterior uterine wall.

These findings suggest that the thickness of the junctional zone and outer myometrium may be associated with infertility. These findings can be used in assisted reproduction treatment to increase the success rate after implantation.

Vascularization investigated by DCE (dynamic contrast enhancement) MRI perfusion parameters

(IAUC / volume, K_{trans}, K_{ep} and V_e) of the junctional zone and outer myometrium is then evaluated in a control group of nullipara and primipara women who do not use contraceptive. Our data show that in nullipara non-contraceptive users primarily change the transfer constant (K_{trans}) and initial uterine blood volume (iAUC / volume) throughout the menstrual cycle. It is found that hormonal contraceptives often cause a reduction in K_{trans} in the junctional zone.

These perfusion characteristics for healthy junctional zone and outer 2/3 of myometrium can be used again in diagnosis and possible therapeutic intervention for previously unidentified pathologies of female reproductive system. This in the context of assisted reproductive therapy in infertile patients.

Finally, we have used these perfusion parameters data in a limited number of women with unexplained infertility. Our findings in this small group show, on the

one hand, that the technique DCE-MRI is feasible and on the other hand that the data obtained is applicable in the daily practice. None of these five patients showed normal values, or values similar to our control group. We hope to expand this work even further to a larger group of infertile women of unknown etiology.

11. Curriculum Vitae

Name: Meylaerts
First name: Liesbeth Johannes
Date of birth: 16/09/1976
Place of birth: Leuven
Nationality: Belgian
Address: Molenblookstraat 1, 3600 Genk
Contact: 0485-879990 or 089-324546

Education

- Bachelor in Medicine from 1994-1997 at UHasselt Diepenbeek, Belgium
- Master in Medicine from 1997-2001 at Catholic University of Leuven, Belgium
- Residency in Radiology 2001-2003 at Imelda Ziekenhuis, Bonheiden and 2003-2006 at Universital Hospital of Leuven, Belgium
- Fellowship Abdominal Imaging January – February 2006 at Bringham and Womens Hospital, Boston, USA
- Fellowship pediatric neuro-imaging January-February 2011 at Gaslini Hospital, Genua, Italy
- Fellowship Head and Neck Imaging January 2012 at Emory Hospital, Atlanta, USA
- Postgraduate master in Hospital Management at Catholic University of Leuven
2001-2003

Books

Chapter 7 PELVIS in CT an MRI of the Abdomen and Pelvis: A Teaching File. Ros P.R.,
Mortele K.J. 2007 by Lippincott Williams & Wilkins 2007.ISBN13 978-0-7817-7237-2

Papers

1. Perfusion of the uterine junctional zone in nulliparous and primiparous women assessed by DCE-MRI, as a function of menstrual cycle and hormonal contraception. Meylaerts LJ, Wijnen L, Bazot M, Grieten M, Ombelet W, Vandersteen M. Magn Reson Imaging. 2017 May; 38:101-111.
2. Junctional zone thickness in young nulliparous women according to menstrual cycle and hormonal contraception use. Meylaerts LJ, Wijnen L, Grieten M, Palmers Y, Ombelet W, Vandersteen M. Reprod Biomed Online. 2017 Feb;34(2):212-220.
3. Uterine junctional zone thickness in infertile women evaluated by MRI. Meylaerts LJ, Wijnen L, Ombelet W, Bazot M, Vandersteen M. J Magn Reson Imaging. 2016 Aug 18. doi: 10.1002/jmri.25422.
4. Sulfite oxidase deficiency in a newborn. Westerlinck H, Meylaerts L, Van Hoestenbergh MR, Rossi A. JBR-BTR. 2014 Mar-Apr;97(2):113-4.
5. Incarceration of the gravid uterus: diagnosis and preoperative evaluation by magnetic resonance imaging. Dierickx I, Meylaerts LJ, Van Holsbeke CD, de Jonge ET, Martens IF, Mesens T, Gyselaers WJ. Eur J Obstet Gynecol Reprod Biol. 2014 Aug;179:191-7. doi: 10.1016/j.ejogrb.2014.05.037. Epub 2014 Jun 4. Review.

6. Macrocephaly in an 8-month-old infant. Ramakers K, Siemons W, Meylaerts L. *JBR-BTR*. 2013 Nov-Dec;96(6):392. No abstract available.
7. An unusual complication after renal biopsy. Westerlinck H, Meylaerts L, Verresen L, Willems E, Stockx L. *JBR-BTR*. 2013 Sep-Oct;96(5):328. No abstract available.
8. Fetal hydrometrocolpos, uterus didelphys with low vaginal and anal atresia: difficulties in differentiation from a complex cloacal malformation: a case report. Witters I, Meylaerts L, Peeters H, Coumans A, Wirjosoekarto S, Fryns JP. *Genet Couns*. 2012;23(4):513-7.
9. Validation of 3D power Doppler and VOCAL software in the sonographic assessment of hepatic venous flow. Claeskens J, Tomsin K, Molenberghs G, Van Holsbeke C, Mesens T, Meylaerts L, Gyselaers W. *Facts Views Vis Obgyn*. 2013;5(1):7-12.
10. Magnetic resonance imaging: value of diffusion-weighted imaging in differentiating benign from malignant breast lesions. Stijven S, Gielen E, Bevernage C, Horvath M, Meylaerts L. *Eur J Obstet Gynecol Reprod Biol*. 2013 Feb;166(2):215-20. doi: 10.1016/j.ejogrb.2012.10.029. Epub 2012 Dec 7.
11. MRI features of ovarian fibroma and fibrothecoma with histopathologic correlation. Shinagare AB, Meylaerts LJ, Laury AR, Morteale KJ. *AJR Am J Roentgenol*. 2012 Mar;198(3):W296-303. doi: 10.2214/AJR.11.7221.
12. MRI features of ovarian fibroma and fibrothecoma with histopathologic correlation. Shinagare AB, Meylaerts LJ, Laury AR, Morteale KJ. *AJR Am J Roentgenol*. 2012 Mar;198(3):W296-303. doi: 10.2214/AJR.11.7221.

13. Peroneal neuropathy after weight loss: a high-resolution ultrasonographic characterization of the common peroneal nerve. Meylaerts L, Cardinaels E, Vandevenne J, Velghe B, Gelin G, Vanormelingen L, Weyns F. *Skeletal Radiol.* 2011 Dec;40(12):1557-62. doi: 10.1007/s00256-011-1177-4. Epub 2011 May 3.
14. Recurrent incarceration and/or sacculation of the gravid uterus: a review. Dierickx I, Mesens T, Van Holsbeke C, Meylaerts L, Voets W, Gyselaers W. *J Matern Fetal Neonatal Med.* 2010 Aug;23(8):776-80. doi: 10.3109/14767050903410680.Review.
15. Alobar holoprosencephaly. Meylaerts L. *JBR-BTR.* 2008 Nov-Dec;91(6):269. No abstract available.
16. Hypoplasia of L5 and wedging and pseudospondylolisthesis in patients with spondylolysis: study with MR imaging. Wilms G, Maldague B, Parizel P, Meylaerts L, Vanneste D, Peluso J. *AJNR Am J Neuroradiol.* 2009 Apr;30(4):674-80. doi: 10.3174/ajnr.A1450. Epub 2009 Jan 15.
17. Adenomatoid leiomyoma of the epididymis. Meylaerts P, Pennings J, Meylaerts L. *JBR-BTR.* 2008 Sep-Oct;91(5):220.
18. Additional value of integrated PET-CT in the detection and characterization of lung metastases: correlation with CT alone and PET alone. De Wever W, Meylaerts L, De Ceuninck L, Stroobants S, Verschakelen JA. *Eur Radiol.* 2007 Feb;17(2):467-73.
19. Hypertensive brain stem encephalopathy in a patient with chronic renal failure. Meylaerts L, Ooms V, Lyra S, Claes K, Vanrenterghem Y, Demaerel P. *Clin Nephrol.* 2006 Feb;65(2):138-40.

Posters

2005 ESGAR, Firenze, Italy: Anal fistula on MRI: modified scoring system.

2010 ESHRE, Rome, Italy: MRI of the junctional zone in nulli and primipara women.

2013 NeuPSIG, Toronto, Canada: Correlation of n.fibularis communis and BMI on ultrasound.

Scientific Presentations

2003 Titulariate Belgian Society of Radiology: PET/CT of thorax in staging lungtumor.

2005 ESGAR, Firenze, Italy: Anal fistula on MRI: modified scoring system.

2006 ESSR, Bruges, Belgium: Dermoid cyst on MRI: pictoral essay – won second prize

2015 BIT, Barcelona, Spain: Perfusion of the Junctional zone in nullipara women on MRI

2016 ESGE, Brussels, Belgium: MRI of the uterus – anatomy

Reviewer

- British Journal of Radiology
- Journal of Magnetic Resonance Imaging
- European Radiology

Member of the Flemish board of licence in radiology since 2013.

Member of ESGAR, ESSR, ESR, BSR and RSNA

Dankwoord

Ik zou graag de Dienst Medische Beeldvorming van het ZOL en de UHasselt willen bedanken voor het ter beschikking stellen van onder meer hun infrastructuur.

Verder gaat mijn dank uit naar Mevr. M. Kelchtermans, Mej. L. Wijnen, Mej. L. Dreesen, Dhr. P. Hamaekers en het team ingenieurs van Siemens (met name Dhr J. Michiels en collega's).

Ook mijn welgemeende dank aan CENSTAT, met name Prof. L. Bruckers en Prof. Dr. M. Bazot voor de respectievelijke technische, methodologische en statistische ondersteuning.

Uiteraard was dit proefschrift niet tot stand gekomen zonder de medewerking van alle studiedeelnemers die het mogelijk gemaakt hebben om de informatie te vergaren en dit schrijven te kunnen verwezenlijken.

Tenslotte gaat mijn dank naar mijn familie voor hun niet aflatende steun tijdens het maken van dit proefschrift.